



JOHANNES GUTENBERG
UNIVERSITÄT MAINZ

Complement Receptor 1 mediated control of *Leishmania* infection in inflammatory human macrophages

Dissertation

Zur Erlangung des Grades

Doktor der Naturwissenschaften

Am Fachbereich Biologie

Der Johannes Gutenberg-Universität

Mainz

Stephan Alberto Machado de Oliveira

Geb. am 26.04.1984 in Berlin

Mainz, 2016

Diese Publikation ist urheberrechtlich geschützt. Vervielfältigungen jeder Art, zur Schau stellen oder andere Verwendungen sind nur nach Absprache mit der Abteilung Immunologie des Paul-Ehrlich-Instituts zulässig.

Dekan:

1. Gutachter:
2. Gutachter:

Tag der mündlichen Prüfung: 24.05.16

This PhD project was funded by the Brazilian funding agency Conselho Nacional de Desenvolvimento Científico e Tecnológico (CNPq).

During this time the obtained research data led to the following manuscripts:

Stephan A. M. de Oliveira, Sabine Förster, Elena Bank, Menberework Chanyalew, Peter Crauwels, Ger van Zandbergen. Distinct *Leishmania* species, causing cutaneous or visceral Leishmaniasis, interact differently with human primary macrophages. **PLoS ONE, submitted**

Stephan A. M. de Oliveira, Sabine Förster, Marie-Sophie Phillip, Peter Crauwels, Ger van Zandbergen. CR1 and the role with *Leishmania major* killing in pro-inflammatory human macrophages. **In preparation**

CONTENTS

| | | |
|--------|---|----|
| 1. | I. SUMMARY | 15 |
| 1. | II. ZUSAMMENFASSUNG | 16 |
| 1. | III. RESUMO | 17 |
| 2. | INTRODUCTION | 19 |
| 2.1 | LEISHMANIASIS..... | 19 |
| 2.2 | CUTANEOUS LEISHMANIASIS..... | 20 |
| 2.3 | MUCOCUTANEOUS LEISHMANIASIS | 21 |
| 2.4 | VISCERAL LEISHMANIASIS..... | 22 |
| 2.5 | <i>LEISHMANIA</i> LIFE CYCLE | 23 |
| 2.6 | HUMAN HOST MACROPHAGES | 25 |
| 2.7 | ENTRY MECHANISM..... | 26 |
| 2.8 | THE ROLE OF CR1 AND CR3 IN THE OUTCOME OF <i>LEISHMANIA</i> INFECTION IN MACROPHAGES..... | 28 |
| 3. | AIMS OF THE STUDY | 31 |
| 4. | MATERIAL AND METHODS | 33 |
| 4.1 | MATERIALS | 33 |
| 4.1.1 | <i>Chemicals And Compounds</i> | 33 |
| 4.1.2 | <i>Culture Medium And Buffers</i> | 34 |
| 4.1.3 | <i>Human Leukocytes</i> | 37 |
| 4.1.4 | <i>Leishmania Strains</i> | 37 |
| 4.1.5 | <i>Ready To Use Kits</i> | 38 |
| 4.1.6 | <i>Antibodies</i> | 38 |
| 4.1.7 | <i>Marker And Dyes</i> | 39 |
| 4.1.8 | <i>Oligonucleotides</i> | 39 |
| 4.1.9 | <i>Sirna</i> | 41 |
| 4.1.10 | <i>Enzymes</i> | 41 |
| 4.1.11 | <i>Laboratory Supplies</i> | 42 |
| 4.1.12 | <i>Instruments</i> | 43 |
| 4.1.13 | <i>Software</i> | 44 |
| 4.2 | METHODS | 45 |
| 4.2.1 | <i>Cell Culture</i> | 45 |
| 4.2.2 | <i>Cultivation Of Leishmania Promastigote Parasites</i> | 45 |
| 4.2.3 | <i>Generation And Cultivation Of Leishmania Amastigote Parasites In Vitro</i> | 46 |
| 4.2.4 | <i>Annexin-Binding</i> | 46 |
| 4.2.5 | <i>Amastigote Isolation</i> | 47 |
| 4.2.6 | <i>Promastigote Transformation From An Amastigote Culture</i> | 47 |
| 4.2.7 | <i>Isolation Of Human Peripheral Blood Mononuclear Cells (PBMC)</i> | 47 |
| 4.2.8 | <i>Generation Of Monocytes Derived Macrophages</i> | 48 |
| 4.2.9 | <i>Co-Incubation Of Macrophage With Leishmania Parasites</i> | 49 |
| 4.2.10 | <i>Co-Incubation In 96-Well Plate</i> | 49 |
| 4.2.11 | <i>Co-Incubation In Centrifuge Tubes</i> | 49 |
| 4.2.12 | <i>CR1 And CR3 Staining On HMDM I And HMDM II</i> | 50 |
| 4.2.13 | <i>Blocking Complement Receptor 1 And 3</i> | 50 |

| | | |
|------------|---|------------|
| 4.2.14 | Microscopy | 51 |
| 4.2.15 | Molecular Biology Methods | 52 |
| 5. | RESULTS | 61 |
| 5.1 | PHENOTYPICAL CHARACTERIZATION OF DIFFERENT HUMAN MACROPHAGE PHENOTYPES | 61 |
| 5.2 | COMPLEMENT RECEPTOR 1 AND 3 EXPRESSION ON PRO- AND ANTI-INFLAMMATORY HUMAN MACROPHAGES | 63 |
| 5.3 | CHARACTERIZATION OF DIFFERENT <i>LEISHMANIA</i> SPECIES BY RESTRICTION FRAGMENT LENGTH POLYMORPHISM ANALYSIS OF ITS1..... | 65 |
| 5.4 | GROWTH KINETICS AND MORPHOLOGICAL ASSESSMENT OF PROMASTIGOTE STAGE OF DIFFERENT <i>LEISHMANIA</i> SPECIES ... | 66 |
| 5.5 | GROWTH KINETICS AND MORPHOLOGICAL ANALYSIS OF AMASTIGOTE PARASITES..... | 68 |
| 5.6 | <i>LEISHMANIA</i> STAGE-SPECIFIC GENE EXPRESSION ANALYSES..... | 69 |
| 5.7 | PROMASTIGOTE AND AMASTIGOTE STAGE SPECIFIC GENE EXPRESSION IN INFECTED HMDM I. | 72 |
| 5.8 | <i>LEISHMANIA</i> PARASITE SPECIES AND PROMASTIGOTE SPECIFIC INFECTION OF HMDM I AND HMDM II..... | 74 |
| 5.9 | <i>LEISHMANIA</i> PARASITE SPECIES AND AMASTIGOTE SPECIFIC INFECTION OF HMDM I AND HMDM II | 77 |
| 5.10 | EXPRESSION OF CELL MARKERS ON HMDM I AND HMDM II AFTER <i>LM</i> AND <i>LD</i> PROMASTIGOTE INFECTION | 79 |
| 5.11 | INFECTION OF HMDM I AND HMDM II USING FLUORESCENT PROTEIN EXPRESSING <i>LM</i> AND <i>LAE</i> PROMASTIGOTES..... | 80 |
| 5.12 | INFECTION OF HMDM I AND HMDM II USING FLUORESCENT PROTEIN EXPRESSING <i>LM</i> AND <i>LAE</i> AMASTIGOTES..... | 81 |
| 5.13 | HIGH THROUGHPUT SCREENING IN PRIMARY HUMAN MACROPHAGES AND MODULATION OF PROTEINS, POTENTIALLY INVOLVED IN PARASITE UPTAKE AND/OR CONTROL | 84 |
| 5.14 | MODULATION OF CR1 AND CR3 USING SIRNA APPROACH..... | 87 |
| 5.15 | BLOCKING OF CR1 AND CR3 USING SPECIFIC BLOCKING ANTIBODIES | 91 |
| 5.16 | THE UPTAKE OF <i>LM</i> AND <i>LAE</i> IS HMDM PHENOTYPE, PARASITE-STAGE AND RECEPTOR DEPENDENT | 92 |
| 5.17 | UPTAKE OF FLUORESCENT PROTEIN EXPRESSING <i>LM</i> AND <i>LD</i> PROMASTIGOTE IS INHIBITED AFTER BLOCKING CR1 ON HMDM I | 94 |
| 5.18 | EFFECT OF CR1 INACTIVATION ON THE INTRACELLULAR SURVIVAL OF <i>LD</i> PARASITES IN HMDM I..... | 96 |
| 5.19 | ASSESSMENT OF <i>LM</i> SURVIVAL IN HMDM I BASED ON STAGE SPECIFIC GENE EXPRESSION | 97 |
| 5.20 | LYSOSOMAL RECRUITMENT IN PRO-INFLAMMATORY CELLS IS INCREASED AFTER CR1 BLOCKING | 99 |
| 5.21 | BLOCKING OF CR1 ON HMDM I AND ITS EFFECT ON THE GENE EXPRESSION OF MOLECULES INVOLVED IN PHAGOLYSOSOME MATURATION | 101 |
| 6. | DISCUSSION..... | 105 |
| 6.1 | <i>LEISHMANIA</i> AND MACROPHAGE INTERACTION..... | 105 |
| 6.2 | STAGE SPECIFIC GENE EXPRESSION IN <i>LM</i> PARASITES | 107 |
| 6.3 | THE ROLE OF CR1 IN <i>LEISHMANIA MAJOR</i> SURVIVAL INSIDE HUMAN INFLAMMATORY MACROPHAGES..... | 108 |
| 7. | CONCLUDING REMARKS | 113 |
| 8. | FIGURE AND TABLE LIST..... | 115 |
| 9. | REFERENCES | 119 |
| 10. | ACKNOWLEDGMENTS..... | 127 |
| 11. | DECLARATION OF AUTHORSHIP..... | 131 |
| 12. | CURRICULUM VITAE | 133 |
| 13. | PUBLICATIONS..... | 135 |

ABBREVIATIONS

| | |
|--------------|--|
| ABC | ABC-transporter homologue |
| bp | base pairs |
| BSA | bovine serum albumin |
| C3 | complement component 3 |
| C3b | complement subcomponent C3b |
| C3bi | inactive complement subcomponent C3b |
| cDNA | complementary DNA |
| CR1 | complement receptor 1 |
| CR3 | complement receptor 3 |
| DAPI | 4',6-diamidino-2-phenylindole |
| DNA | deoxyribonucleic acid |
| dNTPs | deoxyribonucleosidtriphosphate |
| dpi | days post infection |
| DsRed | red fluorescent protein |
| eGFP | enhanced green fluorescent protein |
| EEA1 | early endosome antigen 1 |
| FACS | fluorescence-activated cell sorting |
| FCS | fetal calf serum |
| GAPDH | glyceraldehyde 3-phosphate dehydrogenase |
| gDNA | genomic DNA |
| GM-CSF | granulocyte-macrophage colony-stimulating factor |
| GP63 | surface protease gp63 |
| hMDM | human monocyte derived macrophages |
| hpi | hours post infection |
| IFN γ | interferon γ |
| IL | interleukin |
| LAMP-1 | lysosomal-associated membrane protein 1 |

| | |
|---------------|---|
| LL-37 | cathelicidin |
| LPG | lipophosphoglycan |
| LSM | leukocyte separation medium |
| M-CSF | macrophage colony-stimulating factor |
| MFI | mean fluorescence intensity |
| MOI | multiplicity of infection |
| mRNA | messenger RNA |
| PBMC | peripheral blood mononuclear cells |
| PBS | phosphate buffered saline |
| PCR | polymerase chain reaction |
| PE | phycoerythrin |
| qRT-PCR | quantitative Realtime Polymerase Chain reaction |
| Rab | rabenosyn |
| rRNA45 | ribosomal RNA 45 |
| ULK1 | unc-51 like kinase 1 |
| α -CR1 | anti-CR1 |
| α -CR3 | anti-CR3 |

1. I. SUMMARY

In this study we focused on the interaction of *Leishmania* species causative for cutaneous and visceral Leishmaniasis with human pro- and anti-inflammatory macrophages. Furthermore, the role of complement receptor (CR) 1 and 3, in parasite uptake and survival, was assessed during infection of human primary macrophages. We hypothesize that *Leishmania* infectivity for its main host cell, is species dependent and that CR1-mediated phagocytosis plays a role in promoting *Leishmania* killing in pro-inflammatory human macrophages.

Upon infection with the *Leishmania* (*Lm*) infectious inoculum, we observed that *Lm* promastigotes were able to sustain infection over time, in both pro- and anti-inflammatory macrophages, whereas *Leishmania aethiopica* (*Lae*) and *Leishmania donovani* (*Ld*) showed a decreased infection rate over time. To elucidate on the differences in parasite survival, we investigated whether the entry route, hereby focusing on complement receptors in macrophages, influenced parasite survival. By modulating CR1, either by blocking antibodies or a siRNA approach, we demonstrated a significant reduction in parasite uptake followed by an increased intracellular survival. In parallel, we observed an increase in lysosomal recruitment and demonstrated a higher gene expression of cellular molecules responsible for cell maturation and acidification such Cathepsin D, Synaptotagmin XI, ULK1 and LL-37.

In conclusion, we found that *Lm* and *Lae*, causing cutaneous Leishmaniasis, infect human macrophages more efficiently as *Ld*, causative for visceral Leishmaniasis. Interestingly, we found CR1 working as a double-edged sword in innate immunity, enabling parasite survival at the same time playing a role in cell activation and acidification. These findings shed light on the interspecies differences, which may contribute in the understanding of *Leishmania* disease development in a human *in vitro* model, with regard to complement receptors.

1. II. ZUSAMMENFASSUNG

In der vorliegenden Arbeit haben wir uns mit der Interaktion von Leishmanien, die die Ursache für kutane und viszerale Leishmaniose sind, und humanen pro- und anti-inflammatorischen Makrophagen befasst. Weiterhin wurde die Rolle von Komplementrezeptor (KR) 1 und 3 für Parasitenaufnahme und -überleben während der Infektion von humanen primären Makrophagen im Detail analysiert. Wir vermuten, dass die Infektivität für die Hauptwirtszelle abhängig von Leishmanien Spezies ist und dass die Phagozytose durch KR1 eine unterstützende Rolle beim Abtöten der Leishmanien in pro-inflammatorischen Makrophagen spielt.

Nach Infektion mit dem infektiösen Inoculum haben wir beobachtet, dass Lm Promastigoten in der Lage sind die Infektion über Zeit aufrecht zu erhalten während sich bei Lae und Ld die Infektionsrate in pro- und anti-inflammatorischen Makrophagen über Zeit verringert. Um die Unterschiede im Parasitenüberleben zu analysieren haben wir den Aufnahmeweg in Makrophagen, fokussierend auf die Komplementrezeptoren, untersucht. Indem wir KR1 entweder durch blockierende Antikörper oder mit einem siRNA Ansatz moduliert haben, konnten wir eine signifikante Reduktion der Parasitenaufnahme gefolgt von einem erhöhten intrazellulären Überleben zeigen. Außerdem haben wir eine vermehrte Rekrutierung von Lysosomen beobachtet und konnten eine erhöhte Genexpression von Molekülen zum Zell-Ansäuern, wie Cathepsin D, Synaptotagmin XI, ULK1 und LL3, nachweisen.

Zusammenfassend haben wir gefunden, dass die kutane Leishmaniose auslösenden Lm und Lae humane Makrophagen effizienter infizieren, als *Ld*, welche viszerale Leishmaniose auslösen. Interessanterweise ist dabei KR1 ein zweischneidiges Schwert in der angeborenen Immunität, da sowohl Parasitenüberleben als auch Zellaktivierung und Ansäuern vermittelt wird. Diese Ergebnisse werfen Licht auf die Unterschiede zwischen Spezies und tragen zum besseren Verstehen der Krankheitsentwicklung von Leishmaniose in Bezug auf Komplementrezeptoren im humanen *in vitro* Model bei.

1. III. RESUMO

O presente trabalho centrou-se na interação de diferentes espécies de *Leishmania* responsáveis por causar Leishmaniose Cutânea e Visceral com macrófagos humanos pró e anti-inflamatórios. Além disso, a função dos Receptores do Complemento (RC) 1 e 3 na internalização e desenvolvimento do parasita foi investigada durante a infecção em macrófagos humanos primários. Hipotetizamos que a infectividade do parasita *Leishmania* em sua principal célula hospedeira é espécie dependente e que a fagocitose mediada pelo RC1 tem a função de promover a morte do parasita em macrófagos humanos pró-inflamatórios.

Depois da infecção com o inóculo infectivo de *Leishmania* (*Lm*), foi observado que *Lm* promastigotas foram capazes de sustentar a infecção ao longo do tempo, em ambos macrófagos pró e anti-inflamatórios, enquanto que *Leishmania aethiopica* (*Lae*) e *Leishmania donovani* (*Ld*) mostraram um decréscimo na infecção com o passar do tempo. Para elucidar as diferenças no desenvolvimento do parasita, foi investigado se a rota de entrada, com foco nos receptores do complemento dos macrófagos, influencia a sobrevivência do parasita. Modulando o RC1 por meio de anticorpos bloqueadores ou por abordagem usando siRNA, verificamos uma significativa redução na internalização do parasita seguido por um crescimento no desenvolvimento intracelular. Em paralelo, observou-se um crescimento no recrutamento de lisossomos e verificou-se uma alta expressão gênica de moléculas responsáveis pela maturação e acidificação celular tal como Catapsina D, Synaptotagmin XI, ULK1 e LL-37.

Em conclusão, *Lm* e *Lae*, causadoras da Leishmaniose Cutânea, infectam macrófagos humanos mais eficientemente quando comparadas a *Ld*, responsável por causar Leishmaniose Visceral. Interessantemente, encontramos que o RC1 funciona como uma “faca de dois gumes” na imunidade inata, permitindo a sobrevivência do parasita e ao mesmo tempo desempenhando uma função na acidificação celular. Estes resultados esclarecem as diferenças inter-espécies, as quais podem contribuir no entendimento do desenvolvimento da doença Leishmaniose em um modelo humano *in vitro*, em relação aos Receptores do Complemento.

2. INTRODUCTION

2.1 Leishmaniasis

Leishmaniasis is a vector born disease caused by the intracellular protozoan parasite of the genus *Leishmania*. It is a neglected disease prevalent in 98 countries with 1.3 million new cases of individuals infected and 50,000 deaths annually (WHO, 2015). Leishmaniasis disease severity in humans is dependent on the parasite species and the host's immunological status and can vary from a self-healing skin disease to a lethal organ infiltrating form. Three main clinical forms of human Leishmaniasis have been described: cutaneous, mucocutaneous and visceral Leishmaniasis (Piscopo and Mallia, 2006). The protozoan is transmitted by the bite of a sandfly of the Phlebotominae family, present in different areas around the world (Lewis, 1971). The clinical manifestations of Leishmaniasis disease are different spread around the globe, since the distribution of the vector is strongly dependent on the climate. With the constant climate changes and urbanization of areas where the vector inhabits, it has been foreseen that a majority of the European population can come in contact with Leishmaniasis disease by the end of 21th century (Lainson, 1988; Attila Trájer et al., 2013).

2.2 Cutaneous Leishmaniasis

Cutaneous Leishmaniasis is caused by *Leishmania major* (*Lm*) and *Leishmania aethiopica* (*Lae*) species and is characterized by local skin ulcers. This skin disease is normally self-healing without any medical treatment, but is accompanied by severe scar tissue. Cutaneous Leishmaniasis is mainly found in areas of the Old World (Lewis, 1971), such as Algeria, Pakistan, Saudi Arabia and South America, where the habitat is optimal for the development and reproduction of the sandfly *Phlebotomus*, the main vector of *Lm* parasites (WHO, 2015) (**Figure 1**).

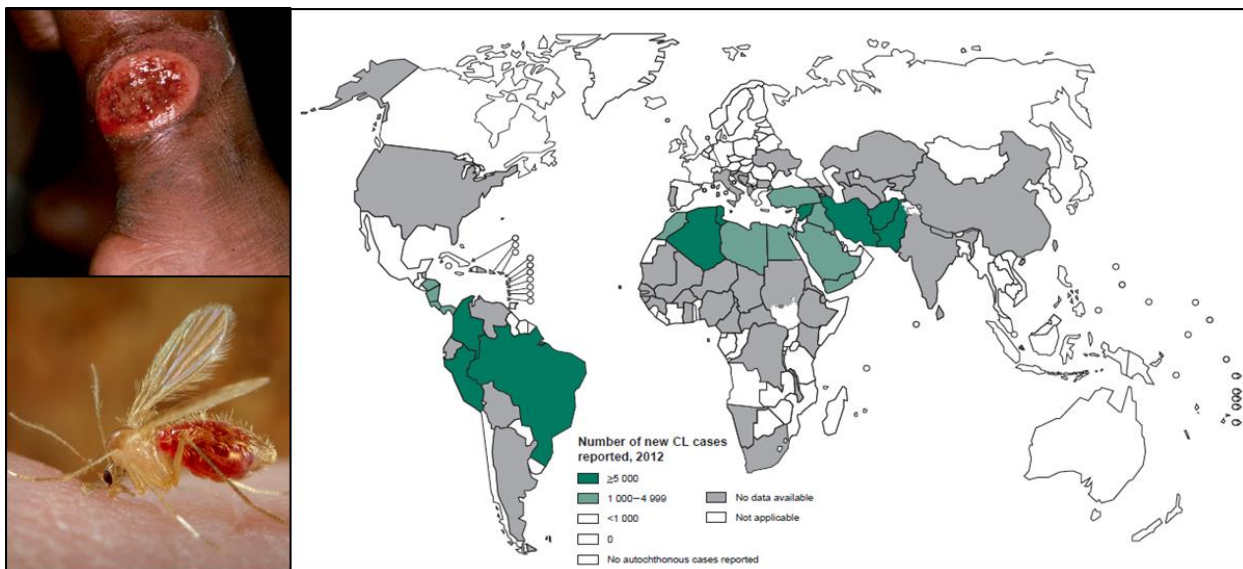


Figure 1: Distribution of cutaneous Leishmaniasis worldwide according to WHO report of 2015. The disease manifestation is characterized by a papule on the site of sandfly bite, which increases in size with the presence of crusts and eventually ulcers. The most common vectors in the Old World are sandflies of the genus *Phlebotomus*. These sandflies belongs to the Psychodidae family and are hallmarked by a yellowish color, black eyes and hairy bodies. The lanceolate wings are carried erected on the humped thorax (Killick-Kendrick R., 1999).

2.3 Mucocutaneous Leishmaniasis

Classical mucocutaneous Leishmaniasis, also known as *espundia*, is caused by *Leishmania braziliensis* and is most described in South America. The parasite is transmitted by the sandfly of the genus *Lutzomyia*. Initially, the disease is presented as localized self-healing ulcers. After the apparent resolution of the oriental sore, years later, recurrences of metastatic lesions involving the nasal, oral, pharyngeal and laryngeal mucosa are typical (Ramírez and Guevara, 1997; Ashford, 2000). Usually, this recurrent disease is progressive and resistant to the common treatments (Castes et al., 1983) (Figure 2).



Figure 2: Distribution of mucocutaneous Leishmaniasis in the New World according to WHO report. The disease is characterized by initial localized ulcer. The recurrent disease appears years later and affects mainly the oral and nasal mucosa causing anatomical and functional disruption. The most common vectors are the sandfly of the genus *Lutzomyia*. These sandflies are small with a body length of up to 3mm with a hairy body, which color ranges from a near-white to near-black (Killick-Kendrick R., 1999).

2.4 Visceral Leishmaniasis

The most severe form of Leishmaniasis is the visceral form caused by *Leishmania donovani* (*Ld*). This manifestation includes hepatosplenomegaly as well as lymphadenopathy and is lethal if untreated. The disease is present in areas such as Ethiopia, India and Nepal. The transmission of *Ld* has been extensively reported in the New World, such as in Brazil, in temperatures around 21-24°C and has been associated with the sandfly vector of the genus *Lutzomyia* (Oliveira et al., 2013) (Figure 3).

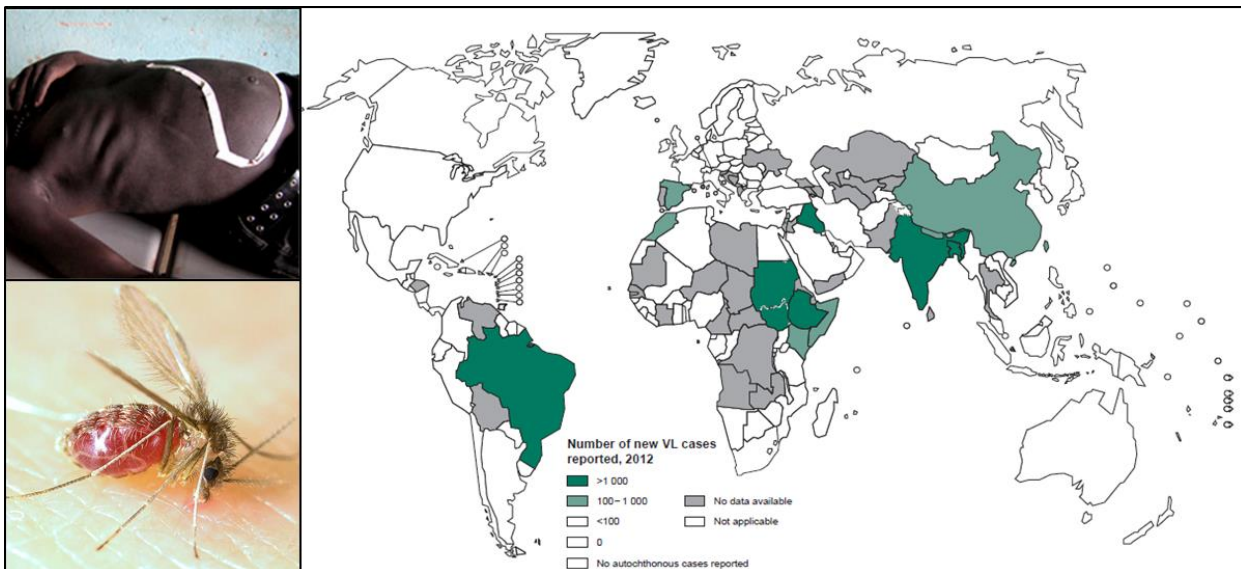


Figure 3: Distribution of visceral Leishmaniasis worldwide according to WHO report of 2015. The disease is characterized by fever, hepatosplenomegaly, lymphadenopathy, and pancytopenia. Skin pigmentation may occur. The vector is the sandfly of the genus *Lutzomyia*. This sandfly is small with a body length of up to 3mm. Is an insect with hairy body and color ranging from a near-white to near-black (Killick-Kendrick R., 1999).

An important public health issue has been raised in Africa in the past years due to HIV and *Leishmania* co-infection. Since there is an overlap of the endemic areas of both pathogens and the fact that HIV and *Leishmania* can infect the same host cell, the macrophage, a more complex disease image occurs upon co-infection. In addition, there is an increase in disease development, especially of visceral Leishmaniasis in HIV-positive individuals. Moreover, Leishmaniasis disease

increases the serum HIV load, leading to a rapid progression of AIDS development (Alvar et al., 2008; Garg et al., 2008; Garg et al., 2009).

2.5 *Leishmania* life cycle

Leishmania is a protozoan parasite belonging to the order Kinetoplastida. It is characterized by a dimorphic life cycle including an extracellular promastigote replicative form in the midgut of *Phlebotomus* and *Lutzomyia* sandflies. In the sandfly, procyclic *Leishmania* parasites differentiate into an infective metacyclic promastigote form through a process called metacyclogenesis (Kaye and Scott, 2011). Metacyclic parasites are accumulated in the anterior gut of the sandfly and are regurgitated in the skin of a mammalian host during the blood meal (Bates, 2007). The infective metacyclic inoculum consists of a mixture of viable and apoptotic *Leishmania* parasites, a mixture which is important for disease development (van Zandbergen et al., 2006) (**Figure 4**). Once in the skin, *Leishmania* encounter resident skin macrophages and neutrophils. The latter ones are recruited to the site of infection by the *Leishmania* chemotactic factor (LCF) and are able to phagocytize the parasite. After the silent entry into the neutrophils, *Leishmania* parasites are able to delay the death program of these cells up to two days. In addition, secretion of MIP-1 β is enhanced which in turn leads to the recruitment of monocytes. Upon differentiation of monocytes into macrophages, infected apoptotic neutrophils are cleared at the site of infection (Ritter et al., 2009). Inside macrophages, promastigote parasites transform into the amastigote form within phagolysosome compartments, a process influenced by the change of temperature and local pH (Sacks, 1989; Bates, 2007). Amastigotes have a droplet shape and are non-motile as the flagellum does not protrude the parasites body. Amastigotes are responsible for the propagation of Leishmaniasis disease by infecting neighboring macrophages (Bogdan and Röllinghoff, 1998). The life cycle is complete when the sandfly takes a blood meal of an infected mammalian host containing free amastigotes that will differentiate into the promastigote life stage inside the gut of the vector.

Introduction

During parasite stage transformation from procyclic to metacyclic promastigotes and subsequently into multiplying amastigotes, parasite stage specific genes and their corresponding proteins have been described. The small hydrophilic ER-associate protein (SHERP) is specifically expressed in the promastigote stage and is involved in the metacyclogenesis inside the vector (Sádlová et al., 2010). The ATP-binding cassette (ABC) is mainly found in the amastigote stage of *Leishmania* parasites and is involved in the transport of different molecules through the biological membranes of the parasite (Leprohon et al., 2006). Glycoprotein 63 (GP63), or Major Surface Protease, has been shown to be expressed on promastigote parasites. It has been shown that GP63 is able to cleave C3 and leads to *Leishmania* opsonization with either C3b or iC3b, enabling parasite binding to CR1 and CR3 respectively (Russell, 1987).

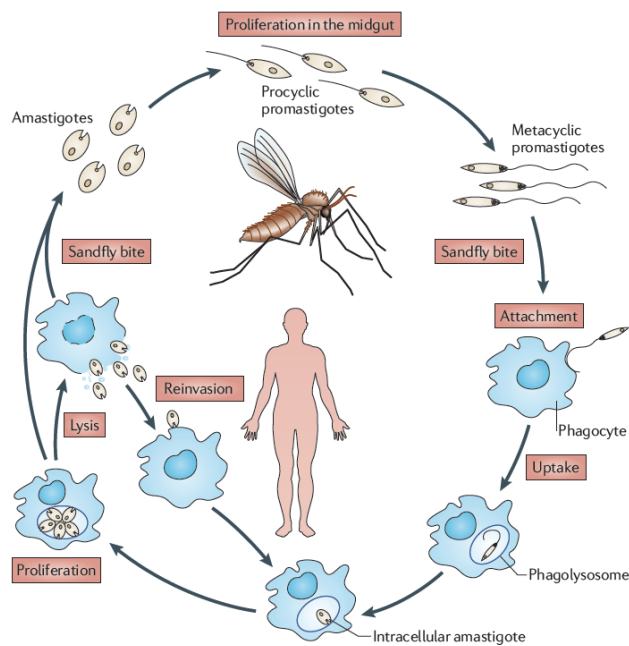


Figure 4: Life cycle of *Leishmania* parasite. After inoculation in the mammalian host, parasites recruit neutrophils by production of *Leishmania* chemotactic factor (LCF) (van Zandbergen et al., 2007). Recruitment and uptake of viable and apoptotic parasites by neutrophils occurs in the first 24 hours where the parasites remain in a non-developmental state. Apoptotic parasites mediate the silencing of neutrophils allowing the survival of viable parasites inside this cell. Within 48 hours, monocytes are recruited, which differentiate into macrophages able to phagocytize the phosphatidylserine (PS) positive apoptotic neutrophils containing *Leishmania*, allowing the parasite to silently enter and develop to the amastigote state, able to spread and to re-infect different macrophages (Kaye and Scott, 2011).

2.6 Human host macrophages

Macrophages are known to be the final host cell for *Leishmania* parasites (Kaye and Scott, 2011; Chávez-Galán et al., 2015). Monocytes, which circulate in the bloodstream, continually migrate into tissues where they differentiate into distinct phenotypes of mature macrophages (Martinez et al., 2006). After a stimulus, monocytes can be differentiated in M1 or M2 macrophages. The M1, also termed classical activated macrophages, are differentiated upon stimulation of monocytes with LPS, IFN gamma, TNF alpha or GM-CSF, which primarily occurs in tissue upon monocyte infiltration into sites of inflammation (Neu et al., 2013; Mia et al., 2014). Classical activated macrophages are characterized by secretion of pro-inflammatory cytokines such as TNF alpha, IL1, IL23, and IL12. In addition, M1 macrophages express CD14 and Mannose Receptor (CD206) as surface markers and are responsible for phagocytosis and clearance of infection. The M1 macrophages are morphologically characterized by a fried egg shape (**Figure 5**). In contrast, M-CSF, present in the blood, or stimulation with IL10 or IL4, promotes monocytes to differentiate into an alternative activated phenotype, also termed M2 macrophages. The M2 macrophages secrete the anti-inflammatory cytokine IL10 and express Scavenger Receptor (CD163) as a specific surface marker. The cells have an elongated shape (**Figure 5**). The M2 can be further divided in different subsets such as M2a, M2b, M2c and M2d; all of them exhibit an anti-inflammatory profile. Under normal conditions, anti-inflammatory macrophages are related with tissue repair, lacking a strong antimicrobial activity (Stout, 2010; Labonte et al., 2014; Martinez and Gordon, 2014).

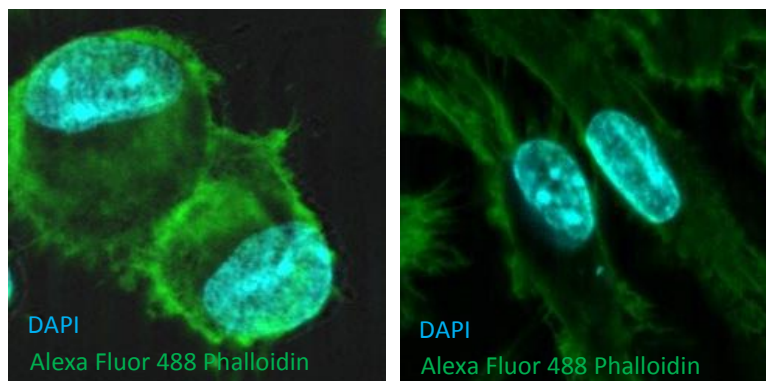


Figure 5: Fluorescent staining of a pro-inflammatory type 1 macrophage (left) and an anti-inflammatory type 2 macrophage (right). Cells were stained using DAPI (blue staining for the cell nucleus) and Alexa Fluor 488 Phalloidin (green staining for cell cytoplasm) and micrographs were taken using a Life Cell Imaging platform and ZEN 2012 Software.

2.7 Entry mechanism

Leishmania parasites can enter macrophages through the infected apoptotic neutrophils (Trojan horse model) or can bind directly to the macrophage surface. Entry into macrophages involves recognition of specific parasite ligands by receptors on the macrophage surface leading to internalization of the parasite. The binding of promastigote or amastigote parasites followed by phagocytosis by macrophages is managed by different receptors (**Figure 6**). Macrophages possess a broad arsenal of receptors that are involved in pathogen phagocytosis such as Mannose Receptor, Fc Receptor, Complement Receptor of the Immunoglobulin superfamily (CRIg), and Complement Receptors (CRs) 1, 2, 3 and 4. Mannose Receptor, a C-type lectin binding protein, serves as a broad recognition receptor detecting mannose on the surface of pathogens (Da Silva et al., 1989; Mosser and Karp, 1999; Dasgupta et al., 2000; Helmy et al., 2006; Akilov et al., 2007; van Lookeren Campagne et al., 2007; Polando et al., 2013). The Fc Receptors are known to bind the Fc fragment of the immunoglobulin G and to phagocyte particles attached to antibodies. The CRIg is member of the complement receptor family, suggested to have a pivotal role in the clearance of pathogens and autologous cells (Ueno and Wilson, 2012). However, *Leishmania* uptake is not exclusively regulated by a single receptor. In contrast, there is an interplay between several host cell receptors and this protozoan parasite (He et al., 2008; Ueno and Wilson, 2012). Two important receptors, CR1 (CD35) and CR3 (CD11b/CD18), have been described as the main CRs involved in the uptake of *Leishmania major* and *Leishmania donovani* parasites by human macrophages (Rosenthal et al., 1996). Moreover, complement receptors also bind complement factors, after which they are named. The complement system is a central component of the immune response and consists of a well-balanced network of circulating proteins and surface receptors which can be activated through the classical pathway, the alternative pathway or the lectin pathway. The opsonization and fixation of non-self-structures

by complement components lead to a massive amplification of the immune response and activation of the cell-killing membrane attack complex. The alternative pathway plays a central role in *Leishmania* infection starting with the hydrolysis of the third component of complement system (C3) and ending with parasite opsonization and recognition by complement receptor expressed on the surface of phagocytic cells (Lambris et al., 2008; Dunkelberger and Song, 2010). After cleavage of C3, parasites are opsonized either by C3b (CR1 ligand) or iC3b (CR3 ligand). *Leishmania* parasites opsonized with C3b are taken up by macrophages via CR1 while opsonization with iC3b leads to the uptake via CR3 (Isnard et al., 2012).

After the recognition of foreign antigens/pathogens, macrophages initialize a process called phagocytosis. The cell receptors recognize the pathogen and this event is followed by membrane polarization at the binding site (Attila Trájer, 1999). Next, membrane extensions embrace the pathogen internalizing it in an early phagosome compartment, marked by the Early Endosome Antigen 1 (EEA1) and Rab5 proteins. Phagosome maturation will follow through binding of several membrane-molecules such Lysosomal-associated membrane protein 1 (LAMP-1) and Rab7, followed by lysosomal fusion and the formation of a mature phagolysosomal compartment (Henry et al., 2004; Thi and Reiner, 2012). The pathogen is killed in this acid compartment preceding antigen presentation. As a result, MHCII molecules are responsible for the transport of antigen fragments to the cells surface where the antigen presentation to the T cells of the adaptive immune system takes place (Mosser and Edwards, 2008). Macrophage activation is a complex event where many important molecules are involved, such as ULK1 that contributes to the initialization of the autophagy machinery. Autophagy activity leads to the formation of autolysosomal compartments responsible for maintaining cell homeostasis, but also for pathogen degradation/survival (Vural and Kehrl, 2014). Furthermore, the process of phagosomal maturation leads to the expression of a cationic antimicrobial peptide, LL-37, that is also responsible for upregulation of gene involved in the immune response (Scott et al., 2002). Moreover, the phagocytosis process is regulated by different key molecules such as Synaptotagmins, responsible for vesicle fusion and cytokine secretion, playing a role in compartment acidification and parasite killing (Arango Duque et al., 2013).

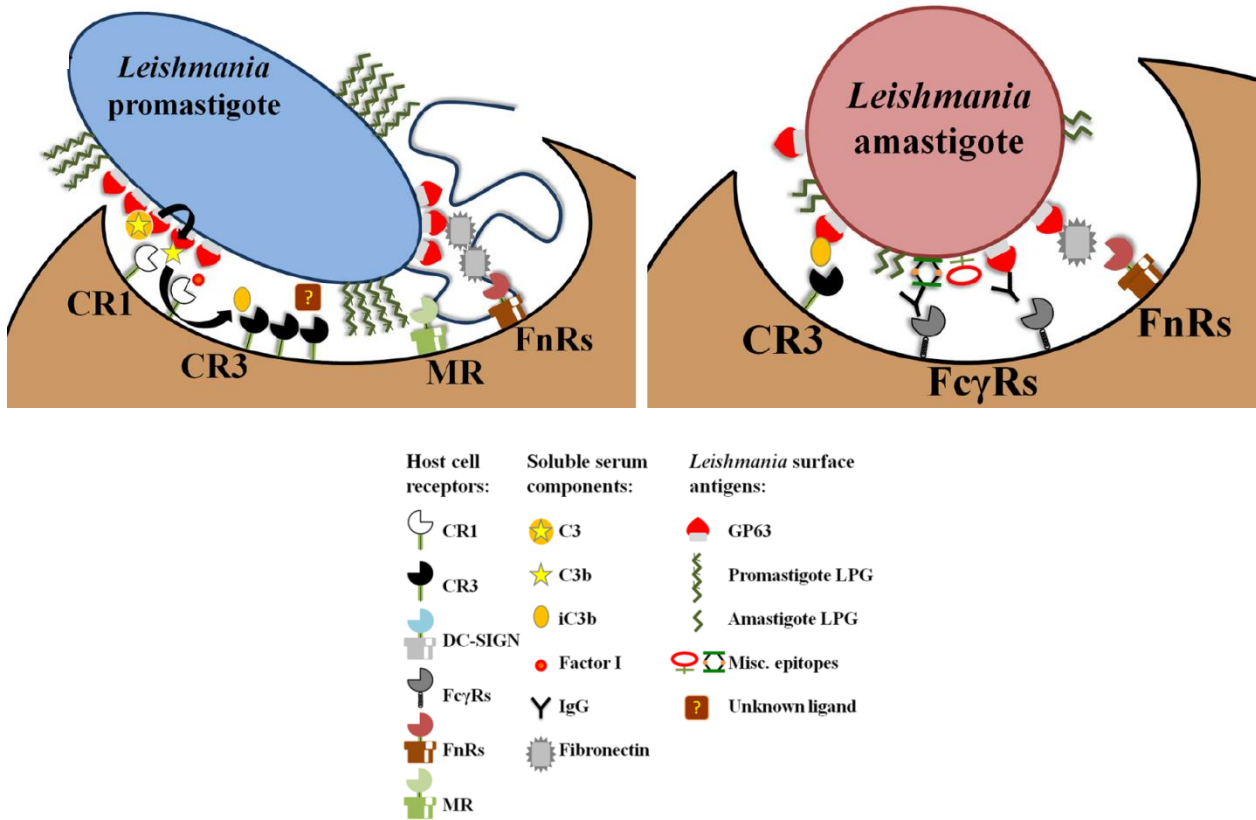


Figure 6: Representation of *Leishmania* parasite uptake by macrophages based on the set of expressed receptors. Based on molecules expressed on the surface of promastigote (left) and amastigote (right) parasites, different macrophage receptors take part in the recognition and phagocytosis of *Leishmania* (Ueno and Wilson, 2012).

2.8 The role of CR1 and CR3 in the outcome of *Leishmania* infection in macrophages

CR3 is a transmembrane glycoprotein formed by a heterodimer of α (CD11b) and β (CD18) chains and is closely related with parasite survival and development in macrophages. It has been described as a factor contributing in delaying phagosomal maturation, as well as for its inability to trigger a respiratory burst in macrophages after phagocytosis of *Leishmania* parasites (Ueno and Wilson, 2012; Polando et al., 2013). The recognition of *Leishmania* species by CR3 occurs after the parasite is opsonized by iC3b, the product of C3 cleavage, which binds specifically to CR3 expressed on macrophages (Berton and Lowell, 1999; Rodríguez et al., 2006). On the other

Introduction

hand, CR1 is a single chain type 1 transmembrane protein and has been suggested to be involved with phagocytosis and clearance of complement opsonized immune complexes (Krych-Goldberg and Atkinson, 2001; Smith et al., 2002). The phagocytosis of *Leishmania* parasites by macrophages via CR1 occurs after the C3 cleavage and parasite opsonization with C3b, which is specifically recognized by CR1. The effect of CR1 on intracellular signaling after *Leishmania* phagocytosis remains unclear. Many of the molecules involved in phagocytosis and phagosomal maturation are possibly affected by CR-mediated phagocytosis since CRs have been shown to be involved in intracellular vesicle binding and trafficking after the uptake of pathogens by phagocytic cells (Arango Duque and Descoteaux, 2015).

3. AIMS OF THE STUDY

Leishmaniasis is one of the 17 neglected tropical diseases (NTD) that has been identified by the WHO in 2015. This report aims to present the progression achieved by more than 74 countries worldwide engaged in combatting neglected diseases. The main clinical forms found in humans are the self-healing cutaneous Leishmaniasis (*Leishmania major* and *Leishmania aethiopica*) and the more lethal form, visceral Leishmaniasis (*Leishmania donovani*). Much about leishmanial pathogenicity has been learned from different infectious murine models. However interactions between different parasite species and different human macrophage phenotypes, as well as the specific role of complement receptor 1 in parasite control are mainly unknown.

We hypothesize that:

- I. **Being the potential lethal form, *Leishmania donovani* is more infective and able to survive longer in human macrophages as compared to cutaneous inducing strains.**
- II. **Complement receptor 1 mediated uptake of *Leishmania* leads to parasite elimination in pro-inflammatory human macrophages.**

In order to assess the hypotheses above we aimed to:

- i. Characterize the phenotype of hMDM I and II focusing on CR1 and CR3 expression.
- ii. Characterize the *Leishmania* species (*Lm*, *Lae*, *Ld*) and life stage (promastigote and amastigote) specific growth kinetics.
- iii. Assess the number of pro- and anti-inflammatory macrophages infected after co-incubation with different *Leishmania* species stages, based on histological stainings and flow cytometry using eGFP/DsRed-expressing *Leishmania* parasites.
- iv. Down regulate or inhibit CR1 and CR3 activity and analyze the effects on uptake and survival of *Leishmania* parasites, using microscopy, flow cytometry analysis and qRT-PCR. Here we will focus on infection rates and parasite load as well as parasite stage specific genes and macrophage mechanisms potentially involved in parasite killing.

4. MATERIAL AND METHODS

4.1 Materials

4.1.1 Chemicals and compounds

| | |
|---|---|
| β-Mercaptoethanol | Sigma-Aldrich, Steinheim (GER) |
| Ammonium chloride (0.15 M) | Medienküche PEI, Langen (GER) |
| Aqua distilled | Medienküche PEI, Langen (GER) |
| Bovine Serum Albumin | Sigma-Aldrich, Steinheim (GER) |
| CASYton | Roche Innovatis AG, Reutlingen (GER) |
| Difco™ Brain Heart Infusion Agar | Becton Dickenson, Sparks (USA) |
| Diff Quick Fixative, Solution I and II | Medion Diagnostics, Düdingen (CH) |
| Dimethylsulfoxid | Sigma-Aldrich Chemie, Steinheim (GER) |
| DNA loading buffer (10x) | New England Biolabs, Ipswich (USA) |
| dNTP: dATP, dCTP, dGTP, dTTP (100mM) | PeqLab, Erlangen (GER) |
| Dithiothreitol (DTT) | Sigma-Aldrich Chemie, Steinheim (GER) |
| Ethanol, absolute FACS Clean | VWR, Bruchsal (GER) Medienküche PEI, Langen (GER) |
| FACS Flow (Sheath Solution) | Medienküche PEI, Langen (GER) |
| FACS Rinse | Medienküche PEI, Langen (GER) |
| FACS Staining buffer | Medienküche PEI, Langen (GER) |
| Fetal Calf Serum | Sigma-Aldrich Chemie |
| Glutamine (L-Glutamine) | Biochrom AG, Berlin (GER) |
| Glycerol (99 %) | Citifluor, London (UK) |
| HEPES-Buffer (1 M) | Biochrom AG, Berlin (GER) |
| Histopaque 1077 | PAA, Pasching (AUT) |
| Human recombinant Granulocyte Macrophage Colony Stimulation Factor (GM-CSF) | Bayer Healthcare Pharmaceutical, Leverkusen (GER) |

Material and methods

| | |
|---|---|
| Human recombinant Macrophage Colony Stimulating Factor (M-CSF) | R&D Systems, Minneapolis (USA) |
| Hydrochloric acid (37 %) | VWR International, Fontenay Sous Bois (FR) |
| Hygromycin B, solution | Invitrogen, San Diego (USA) |
| Immersion Oil | Carl Zeiss, Jena (GER) |
| Isopropyl alcohol | Sigma-Aldrich Chemie, Steinheim (GER) |
| Paraformaldehyde | Sigma-Aldrich Chemie, Deisenhof (GER) |
| Penicillin/ Streptomycin | Biochrom AG, Berlin (GER) |
| Phosphate buffered saline (1x PBS) wo/ Ca ²⁺ , Mg ²⁺ ; pH 7.1 | Medienküche PEI, Langen (GER) |
| ProLong [®] Gold Antifade Reagent Rabbit Blood, defibrinated | Invitrogen, Darmstadt (GER) Elocin-Lab GmbH, Gladbeck (GER) |
| Ringer-Solution | B. Braun Melsungen AG, Melsungen (GER) |
| RNase AWAY | VWR, Darmstadt (GER) |
| Roswell Park Memorial Institute (RPMI) 1640 Medium | Sigma-Aldrich Chemie, Steinheim |
| Saponin from <i>Quillaja</i> bark | Sigma-Aldrich Chemie, Steinheim (GER) |
| Sodium Acetat | Sigma-Aldrich Chemie, Deisenhof (GER) |
| Sodium Azide | Sigma-Aldrich Chemie, Deisenhof (GER) |
| Sodium Chloride | Sodium Chloride |
| Sodium Hydroxide 1M | Merck, Darmstadt (GER) |

4.1.2 Culture medium and buffers

| | |
|---------------------------------------|----------------------------------|
| Novy-Nicolle-McNeal blood agar medium | 16.6 % Rabbit blood defibrinated |
| | 16.6 % 1x PBS |
| | 66.2 % Brain Heart Infusion Agar |
| | 66.2 U/ml Penicillin |

Material and methods

| | |
|---------------------------------------|--|
| <i>Leishmania</i> promastigote medium | 66.2 µg/ml Streptomycin RPMI 1640 Medium 5 % FCS 2 mM L-Glutamine 50 µM β-Mercaptoethanol 100 U/ml Penicillin 100 µg/ml Streptomycin 10 mM HEPES Buffer |
| <i>Lm</i> -Suspension-Medium | Medium 199 10 % FCS 100 U/ml Penicillin 100 µg/ml Streptomycin 40 mM Hepes Bu_er 5 ml 10 mM Adenine, in 50 mM Hepes 1 ml 0.25 % Hemin, in 50 % Triethanolamine 0.5 ml 0.1 % Biotin, in 95 % Ethanol |
| <i>Leishmania</i> amastigote medium | RPMI 1640 Medium 10 % FCS 3 mM L-Glutamine 50 µM β-Mercaptoethanol 100 U/ml Penicillin 100 µg/ml Streptomycin pH 5.5, adjusted with 38 % HCl Sterile filtrated |
| Complete-(macrophages) Medium | RPMI 1640 Medium |

Material and methods

| | |
|-------------------------------------|-------------------------------------|
| | 10 % FCS |
| | 2 mM L-Glutamine |
| | 50 μ M β -Mercaptoethanol |
| | 100 U/ml Penicillin |
| | 100 μ g/ml Streptomycin |
| | 10 mM HEPES Buffer |
| Macrophage generation - Wash buffer | 1x PBS |
| | 5 % Complete-(macrophages) Medium |
| MACS-Buffer pH 7.2 | 1x PBS |
| | 2 mM EDTA |
| PFA fixation solution | 1x PBS |
| | 4 % PFA |
| FACS-Buffer I | 1x PBS |
| | 1 % FCS |
| | 1 % BSA |
| | 1 % Human serum |
| FACS-Buffer II | 1x PBS |
| | 1 % FCS |
| | 1 % BSA |
| | 1 % Human serum |
| | 0.5 % Saponin |
| | Sterile filtrated |

4.1.3 Human leukocytes

Human peripheral blood mononuclear cells (PBMCs) were obtained from buffy coats of healthy donors from the DRK-Blutspendedienst in Frankfurt. Subsequently, cells were isolated and macrophages were generated as described in the Methods section.

4.1.4 *Leishmania* strains

Leishmania major WT *Leishmania major* isolate MHOM/IL/81/FEBNI originally obtained from a skin biopsy of an Israeli patient. Parasites were kindly provided by Dr. Frank Ebert (Bernhard Nocht Institute for Tropical Medicine, Hamburg, GER)

Leishmania major eGFP *Leishmania major* isolate MHOM/IL/81/FEBNI genetically transfected with the green fluorescent eGFP gene

Leishmania major DsRed *Leishmania major* isolate MHOM/IL/81/FEBNI genetically transfected with the red fluorescent DsRed gene

Leishmania aethiopica WT *Leishmania aethiopica* isolate MHOM/ET/72/L100 Z14

Leishmania aethiopica eGFP *Leishmania aethiopica* isolate MHOM/ET/72/L100 Z14 genetically transfected with the green fluorescent eGFP gene

Leishmania aethiopica DsRed *Leishmania aethiopica* isolate MHOM/ET/72/L100 Z14 genetically transfected with the red fluorescent DsRed gene

Material and methods

Leishmania donovani WT *Leishmania donovani* isolate MHOM/ET/67/HU3 Z18

Leishmania donovani eGFP *Leishmania donovani* isolate MHOM/ET/67/HU3 Z18 genetically transfected with the green fluorescent eGFP gene

Leishmania aethiopica and *Leishmania donovani* strains used in this study were obtained from The *Leishmania* collection of Montpellier, France (http://www.parasitologie.univ-montp1.fr/english_vers/en_cnrl.htm).

4.1.5 Ready to use kits

| | |
|--|---|
| CD14 MicroBeads, human | Miltenyi Biotec,, Bergisch Gladbach (GER) |
| DNeasy Blood and Tissue Kit | Promega, Mannheim (GER) |
| MESA Blue qPCR MasterMix Plus for SYBR | Eurogentec, Köln (GER) |
| RNeasy Plus Mini kit | Qiagen, Hilden (GER) |

4.1.6 Antibodies

| | |
|--|--|
| Mouse, α -human-IgG1k Isotype (PE) | BD Pharmingen |
| Mouse, α -human-CD11b/Mac-1 (PE) | BD Pharmingen |
| Mouse, α -human CD35 (PE) | BD Pharmingen |
| α -CR1, rabbit | Kind gift of Prof. Dr. Mohamed Daha and Ngaisah Klar-Mohamad (University of Leiden, Netherlands) |
| Rabbit serum | Plesker (PEI, GER) |
| Mouse, α -human CD11b/Mac-1 | BD Pharmingen |
| Mouse, α -human- Isotype | R&D Systems |
| Mouse, α -human-CD14 (Pacific Blue) | BD Pharmingen, Heidelberg (GER) |
| Mouse, α -human-CD206 (PE) | BD Pharmingen, Heidelberg (GER) |
| Mouse, α -human-CD163 (PE) | BD Pharmingen, Heidelberg (GER) |

Material and methods

| | |
|-------------------------------|---------------------------------|
| Mouse, α -human-IgG2ak | BD Pharmingen, Heidelberg (GER) |
| Isotype (Pacific Blue) | BD Pharmingen, Heidelberg (GER) |

4.1.7 Marker and dyes

| | |
|----------------------------|---|
| Annexin-V-Alexa Fluor 647 | Invitrogen Molecular Probes, Eugene (USA) |
| Alexa Fluor 488 Phalloidin | Invitrogen Life technologies |
| Alexa Fluor 568 | Invitrogen, Darmstadt (DE) |
| DAPI | Molecular Probes Invitrogen (GER) |
| 1 kb DNA Ladder | New England Biolabs, Ipswich (USA) |
| 100 bp DNA Ladder | Promega, Madison (USA) |
| Ethidium bromide | Merck, Darmstadt (GER) |
| LysoTracker® Green DND-26 | Molecular Probes Invitrogen (GER) |
| LysoTracker® Red DND-99 | Molecular Probes Invitrogen (GER) |

4.1.8 Oligonucleotides

| | |
|-------------|---------------------------------|
| 45 rRNA fwd | 5'- CCTACCATGCCGTGTCCTTCTA -3' |
| 45 rRNA rev | 5'- AACGACCCCTGCAGCAATAC -3' |
| ABC fwd | 5'- CGGGTTTGTCTTTTCAGTCGT -3' |
| ABC rev | 5'- CACCAGAGAGCATTGATGGA -3' |
| SHERP fwd | 5'- GACGCTCTGCCCTTCACATAC -3' |
| SHERP rev | 5'- TCTCTCAGCTCTCGGATCTTGTC -3' |
| GP63 fwd | 5'- ACTGCCCGTTTGTATCGAC -3' |
| GP63 rev | 5'- CCGGCGTACGACTTGACTAT -3' |
| ULK1 fwd | 5'- AGCACGATTTGGAGGTCGC -3' |
| ULK1 rev | 5'- GCCACGATGTTTTTCATGTTTCA -3' |
| CTSD_1 fwd | 5'- TGCTCAAGAACTACATGGACGC -3' |

Material and methods

| | |
|---------------------------|----------------------------------|
| CTSD_1 rev | 5'- CGAAGACGACTGTGAAGCACT -3' |
| CTSD_2 fwd | 5'- CACCACAAGTACAACAGCGAC -3' |
| CTSD_2 rev | 5'- CCCGAGCCATAGTGGATGT -3' |
| CTSD_3 fwd | 5'- ATTCAGGGCGAGTACATGATCC -3' |
| CTSD_3 rev | 5'- CGACACCTTGAGCGTGTAG -3' |
| SYT11_1 fwd | 5'- ACCAATATCCGACCTAGCTTTGA -3' |
| SYT11_1 rev | 5'- TCTGGGTATATGCTGATGCCTT -3' |
| SYT11_2 fwd | 5'- GGGAAGGTGGACGTAGGAAC -3' |
| SYT11_2 rev | 5'- GGGGTCAGGCTTGTAATAGGG -3' |
| SYT11_3 fwd | 5'- AGAGGAGGATGTCATGCTAGG -3' |
| SYT11_3 rev | 5'- GATGTAGGGGTCAGATCCCTG -3' |
| GAPDH fwd | 5'- GAGTCAACGGATTTGGTCGT -3' |
| GAPDH rev | 5'- TTGATTTTGGAGGGATCTCG -3' |
| LL-37 fwd | 5'- GGACCCAGACACGCCAAA -3' |
| LL-37 rev | 5'- GCACACTGTCTCCTTCACTGTGA -3' |
| Calpain C2 fwd | 5'- CTGTTCAATGTCAGGACCTG -3' |
| Calpain C2 rev | 5'- TCCTGAGCTAAGTACTCGG -3' |
| Adenylate kinase fwd | 5'- CTACCACCTCAAGTACAACC -3' |
| Adenylate kinase rev | 5'- GATACATGATGGACCCGTAG -3' |
| Metallo peptidase M32 fwd | 5'- GGAGTTCATGAAGATCTGGC -3' |
| Metallo peptidase M32 rev | 5'- CAGTCCTCCTTCGTCATTC -3' |
| SAP2 fwd | 5'- GTGGAGCTCTTGGAAATCAC -3' |
| SAP2 rev | 5'- CCAGCTGCTGTATTCTCTC -3' |
| Cysteine peptidase fwd | 5'- GAGAAAAGCTACCCCTACG -3' |
| Cysteine peptidase rev | 5'- CAGGGACATGTAACCACTG -3' |
| Alkyl Synthase fwd | 5'- GTATGGGTGTCAAGTCCTTC -3' |
| Alkyl Synthase rev | 5'- CTTCTTATCCTGCCACGTAG -3' |
| GAPDH fwd | 5'-GAG TCA ACG GAT TTG GTC GT-3' |
| GAPDH rev | 5'-TTG ATT TTG GAG GGA TCT CG-3' |

Material and methods

| | |
|----------|-----------------------------------|
| CR3 fwd3 | 5'-CGG CAA TAC AAG GAC ATG-3' |
| CR3 rev3 | 5'-CAC TTG CAC ACA GAC ACT TTG-3' |
| CR1 fwd3 | 5'-TTC AAC CTC ATT GGG GAG AG-3' |
| CR1 rev3 | 5'-ATC GTA GGA CTG GCA AAT GG-3' |

4.1.9 siRNA

- CR1: Qiagen, Gene Solution, #1027146 CR1 GeneID 1378, 10µM, Hilden (DE)

| | | |
|----------|-----------------------------------|------------|
| Hs_CR1_2 | 5'-CAG TCC TAC GAT CCC AAT TAA-3' | S100012068 |
| Hs_CR1_3 | 5'-CTG GAG CCA ATT GGA TCA TTA-3' | S100012075 |
| Hs_CR1_4 | 5'-CTG CAT GGT GAG CAT ACC CTA-3' | S100012082 |
| Hs_CR1_5 | 5'-TGC GAT GAA GGG TTC CGA TTA-3' | S103118759 |

- CR3: Qiagen, Gene Solution, #1027146 CR1 (ITGAM) GeneID 3684, 10 µM, Hilden (DE)

| | | |
|------------|-----------------------------------|------------|
| Hs_ITGAM_1 | 5'-CTC GTT TGA CTG GTA CAT CAA-3' | S100013202 |
| Hs_ITGAM_3 | 5'-TCG GGT CAT GCA GCA TCA ATA-3' | S100013216 |
| Hs_ITGAM_4 | 5'-TCA GAC ATC GGT TCA TAT TAA-3' | S100013223 |
| Hs_ITGAM_5 | 5'-TGC CGC CAT CAT CTT ACG GAA-3' | S103118430 |

- AllStars *Negative Control* siRNA #1027280, Qiagen, 10µM, Hilden (DE)

4.1.10 Enzymes

| | |
|--------------------------------------|--|
| Taq DNA Polymerase | New England Biolabs, Frankfurt am Main (Ger) |
| <i>Hae</i> III (restriction enzyme) | New England Biolabs, Frankfurt am Main (Ger) |
| Phusion High Fidelity DNA Polymerase | Thermo Scientific , Dreieich (GER) |

Material and methods

| | |
|---------------------------------------|--|
| Phusion High-Fidelity PCR kit | New England Biolabs, Frankfurt am Main (Ger) |
| Recombinant DNase I | Roche, Mannheim (Ger) |
| RNaseOUT™ recombinant RNase Inhibitor | Invitrogen, Darmstadt (Ger) |

4.1.11 Laboratory supplies

| | |
|--|--|
| Cell culture flasks with filter (25 cm ²) | BD labware Europe, Le Pont de Claix (FR) |
| Cell culture plates (6 well flat bottom and 96 well flat and V-shaped bottom) | Sarstedt, Nümbrecht (GER) |
| Cellfunnel | Tharmac GmbH, Waldsolms (GER) |
| Cellspin filter cards | Tharmac GmbH, Waldsolms (GER) |
| Centrifuge tubes (15 and 50 ml) | BD labware Europe, Le Pont de Claix (FR) |
| Chamber Slide™ 8 well | Thermo Scientific, Bonn (GER) |
| Cytoslides (One circle, uncoated) | Tharmac GmbH, Waldsolms (GER) |
| FACS tubes (2 ml) | Micronic, Lelystad (NL) |
| FACS tubes | BD labware Europe, Le Pont de Claix (FR) |
| Light Cycler 96-well plates with foil, white | Roche Applied Science, Darmstadt (GER) |
| Microcentrifuge tubes (1,5 and 2 ml) | Eppendorf, Hamburg (GER) |
| Pipette tips (1-10 µl, 10-200 µl, 100-1000 µl) | Eppendorf, Hamburg (GER) |
| Pipette filter tips (1-10 µl, 10-200 µl, 100-1000 µl) | Nerbe plus, Winsen/Luhe (GER) |
| PCR tube Multiply® Pro (0,2 ml) | Sarstedt, Nümbrecht (GER) |
| Serological pipettes, sterile (2,5 ml, 5 ml, 10 ml, 25 ml) | Greiner Bio-One, Kremsmünster (AT) |
| Tissue culture dishes (94 mm x 16 mm) | Greiner Bio-One, Kremsmünster (AT) |

4.1.12 Instruments

| | |
|---|--|
| Centrifuges 5430 and 5430R | Eppendorf, Hamburg (GER) |
| Centrifuge „Heraeus Megafuge 40R“ | Thermo Scientific , Dreieich (GER) |
| Cytocentrifuge Cellspin II Universal 320R | Tharmac GmbH, Waldsolms (GER) |
| Sprout Mini-Centrifuge | Biozym, Hamburg (GER) |
| Flow Cytometer LSR SORP | Becton Dickinson, Heidelberg (GER) |
| AxioCam IC | Carl Zeiss, Jena (GER) |
| Microscope Axiophot | Carl Zeiss, Jena (GER) |
| Microscope Axio Vert.A1 | Carl Zeiss, Jena (GER) |
| Microscope Primo Star | Carl Zeiss, Jena (GER) |
| Microscope LSM7 Live | Carl Zeiss, Jena (GER) |
| CO ₂ -Incubator Forma Series II Water Jacket | Thermo Scientific, Marietta (US) |
| CO ₂ -Incubator, Heraeus Auto Zero | Thermo Scientific, Dreieich (GER) |
| Light Cycler® 480 System | Roche applied Science, Mannheim (GER) |
| Analytical balance KB BA 100 | Sartorius, Göttingen (GER) |
| AutoMACS Pro separator | Miltenyi Biotec, Bergisch Gladbach (GER) |
| CASY Modell TT | Roche Innovatis AG, Reutlingen (GER) |
| Freezer (-20°C) | Bosch, Stuttgart (GER) |
| Freezer U725-G (-80°C) | New Brunswick, Eppendorf, Hamburg (GER) |
| Laminar flow workbench MSC-Advantage | Thermo Scientific, Dreieich (GER) |
| Multichannel Pipette (Research® plus) | Eppendorf, Hamburg (GER) |
| NanoDrop 2000c | PeqLab, Erlangen (GER) |
| Neubauer improved cell counting chamber (depth 0,1 mm and 0,02 mm) | VWR International, Darmstadt (GER) |
| Nitrogen container “Chronos” | Messer, Bad Soden (GER) |
| pH Meter PB-11 | Sartorius, Göttingen (GER) |
| Pipette controller (accu-jet® pro) | BRAND, Wertheim (GER) |
| Pipettes (Research® plus: 0,5-10 µl, 10-100 | Eppendorf, Hamburg (GER) |

Material and methods

µl, 20-200 µl, 100-1000 µl)

Recirculating cooler

Julabo, Seebach (GER)

Thermomixer comfort (1,5 ml)

Eppendorf, Hamburg (GER)

Thermomixer 5437 (1,5 ml)

Eppendorf, Hamburg (GER)

Vortex mixer VV3

VWR International, Darmstadt (GER)

Water bath

Köttermann VWR International, Darmstadt (GER)

4.1.13 Software

Axiovision 4.7

Carl Zeiss, Jena (DE)

BD Diva software v6.1.3

Becton Dickinson, Heidelberg (DE)

FlowJo vX

Miltenyi Biotec GmbH, Bergisch Gladbach (DE)

GraphPad Prism 6

GraphPad Software, Inc., La Jolla (USA)

LightCycler® software v3.5

Roche Applied Science, Mannheim (GER)

Microsoft® Office 2010

Microsoft, Redmont (USA)

4.2 METHODS

4.2.1 Cell culture

Cell culture work was performed in a laminar air flow under endotoxin free and sterile conditions. Both human cells and *Leishmania* parasites were cultivated in humidified incubators with 5% CO₂.

4.2.2 Cultivation of *Leishmania* promastigote parasites

Leishmania major (*Lm*), *Leishmania aethiopica* (*Lae*) and *Leishmania donovani* (*Ld*) promastigotes were cultured in biphasic Novy-Nicolle-McNeal (NNN) blood agar medium at 27°C and 5% CO₂. During the first 3 days of culture the parasites are in logarithmic growth phase (log. phase) characterized by an exponential cell division. After 7 days, parasite growth reach a plateau and remain in a stationary growth phase (stat. phase), after which *Lm* and *Lae* promastigote cultures were passaged at a concentration of 12×10^6 parasites / 12 ml *Leishmania* medium up to eight serial passages before the cultures were discarded. For *Leishmania donovani*, the cultures were passaged at a concentration of 24×10^6 parasites / 12 ml *Leishmania* medium each third day and at a concentration of 18×10^6 parasites / 12 ml *Leishmania* medium each fourth day up to eight serial passages.

For a long-time period storage, stat. phase parasites were pelleted at 2400 g for 8 min and resuspended in ice-cold *Leishmania* medium supplemented with 20% FCS and 10% DMSO. Cells concentration was adjusted to 200×10^6 parasites / ml. The cells were transferred into Cryo Tubes and were kept at -80°C overnight before storage in liquid nitrogen.

To start a new culture, parasites were thawed at 37°C in a water-bath and added to *Leishmania* medium. After pelleting, parasites were washed to remove residual DMSO and the final pellet was resuspended in 12 ml *Leishmania* medium and added on biphasic NNN blood agar plates. For eGFP and DsRed – expressing promastigotes, medium supplemented with 20 µg / ml hygromycin B was used.

4.2.3 Generation and cultivation of *Leishmania* amastigote parasites *in vitro*

From a log. phase NNN blood agar plate of *Lm* and *Lae* promastigotes culture, 400 µl (4 wells) were transferred and cultured in 5 ml *Lm*-Suspensions-Medium supplemented with 0.5 mL Fetal Calf Serum (FCS) for 3 days at 27°C. Next, promastigotes were harvested and pelleted at 1400 g for 8 min. The pellet was washed in 10 ml Alex Amastigote Medium (AAM) and centrifuged for 8 min at 1400 g. This step was repeated using 2400 g in order to collect all parasites. The final pellet was resuspended in AAM and adjusted to 20 x 10⁶ parasites / ml. The cells were incubated in 25 cm² culture flasks for 10 – 14 days at 33°C.

Using the same protocol, the generation of *Leishmania donovani* amastigotes was not successful. Different variations of the protocol were tested as listed (**Table 1**).

| Trials | Parasites (x10⁶) /mL | pH | Temperature (°C) |
|---------------|--|-------------|-------------------------|
| 1° | 5 | 5 | 33 |
| 2° | 20 | 5,5 | 35 |
| 3° | 20 | 6 | 37 |
| 4° | 20 | 6,25 | 37 |

Table 1 – Different conditions used in the attempt to generate *Ld* amastigotes.

4.2.4 Annexin-binding

Phosphatidylserine (PS) is an indicator of apoptosis, which is present on the outer cell membrane during the process of programmed cell death. To detect this feature, Annexin A5 (AnxA5)-FITC or AnxA5-Fluos was applied. For the PS expression analysis, 2 x 10⁶ *Leishmania* parasites were washed in Ringer buffer and incubated with 0.5 µl / 2 x 10⁶ parasites in Ringer buffer for 20 min in ice in the dark. The parasites were washed and resuspended in 400 µl Ringer solution and analyzed by Flow cytometry (FACS-Calibur II with CellQuest R Pro software or LSR II with BD Diva software).

4.2.5 Amastigote isolation

To obtain a pure fraction of *Lm* amastigotes, a Histopaque® 1119 density gradient was used to separate amastigotes from the remaining promastigotes and dead cells. The pre-culture was harvested and centrifuged at 2400 g for 8 min. The pellet was resuspended in 50% (1.0595 g/ml) Histopaque® 1119 and carefully layered on a discontinuous Histopaque® 1119 density gradient consisting of layers with densities of 1.0833 g / ml (70%), 1.0952 g / ml (80%), 1.1071 g / ml (90%) and 1.119 g / ml (100%), from top to bottom. This gradient was centrifuged at 2400 g for 35 min without brake. The interphases between 70 - 80% and 80 - 90% were collected, washed twice with AAM and adjusted to a concentration of 20×10^6 parasites / ml and cultured in 25 cm² culture flasks at 33°C. Parasites were used for experiments within four days after the isolation procedure.

Regarding generation of *Leishmania aethiopica* amastigotes, a similar protocol was used. Nevertheless, the parasites turned into amastigote stage already after 24 h in AAM. Moreover, the amastigote culture presented a low percentage of promastigote parasites, not requiring a Histopaque® 1119 density gradient separation.

4.2.6 Promastigote transformation from an amastigote culture

In order to assure a constant infectivity of the parasites, a pure culture containing over 95% axenic amastigotes was transferred into a NNN blood agar medium and cultured for 7 days to assure the transformation of amastigotes back to the promastigote stage.

4.2.7 Isolation of human peripheral blood mononuclear cells (PBMC)

The peripheral blood mononuclear cells (PBMC) were isolated from buffy coats of healthy donors obtained from the DRK blood donation center in Frankfurt. The approximate 50 ml of blood was diluted 1:5 in sterile prewarmed PBS. Next, 25 ml of diluted blood was carefully layered on top of

15 ml Lymphocyte Separation Medium 1077 and centrifuged at 545 g for 30 min (with acceleration and deceleration set at the lowest level). After centrifugation, plasma and the interphase containing the PBMCs were collected and washed in 50 ml wash buffer (PBS + 5% complete medium) at 1024 g for 8 min. Pellet was resuspended and washed with wash buffer at 545 g and then at 135 g for 8 min. The pellet was resuspended in 10 ml of 0.15 M Ammoniumchloride and the erythrocyte lysis was performed for 10 - 15 min at room temperature. Subsequently, the cells were washed with wash buffer to remove remaining thrombocytes. Then, cells were pooled and the concentration was determined either by manual counting (Neubauer chamber slide, depth 0.1) or CASY cell counter.

4.2.8 Generation of monocytes derived macrophages

4.2.8.1 Plastic adherence

Isolated PBMCs were seeded in a 25 cm² culture flasks at a concentration of 8×10^6 PBMCs / ml (final volume of 5 ml complete medium) supplemented with 1% human serum for 1.5 hour at 37°C. After, non-adherent cells were washed with wash buffer. The remaining adherent cells were cultured in complete medium supplemented with 10 ng / ml GM-CSF (for hMDM I) or with 30 ng / ml M-CSF (for hMDM II) during 6 - 7 days at 37°C with 5% CO₂.

4.2.8.2 Monocyte isolation using CD14 positive selection (AutoMACS separation)

To perform this protocol, 100×10^6 PBMCs were washed with 10 ml cold MACS buffer at 300 g for 8 min. The pellet was resuspended in 400 µl MACS buffer and 100 µl of CD14 beads were added. The mixture was incubated at 4°C for 15 min. Subsequently, cells were washed with 10 ml MACS buffer at 300 g for 8 min and the pellet was resuspended in 500 µl MACS buffer before proceed with the automatic separation. Labeled cells were placed into an AutoMACS device and the separation program “posseld” (positive selection using double columns) was selected to run. After separation, the isolated CD14 positive monocytes were counted and incubated in a 6-well

plates at a concentration of 1.6×10^6 cells / ml in complete medium supplemented with 10 ng / ml GM-CSF (for hMDM I) or with 30 ng / ml M-CSF (for hMDM II) during 6 - 7 days at 37°C with 5% CO₂.

4.2.9 Co-incubation of macrophage with *Leishmania* parasites

After 6 - 7 days of culture, both hMDM I and hMDM II were placed on ice for 30 min, harvested using a cell scraper and counted. Co-incubation experiments were performed by two different methods.

4.2.10 Co-incubation in 96-well plate

To perform this experiment, 1×10^5 macrophages were transferred to a 96-well cell culture plates. The cells were left at 37°C for 1 h to adhere. After, the non-adherent cells were removed by discarding the supernatant. Stat. phase *Lm*, *Lae* or *Ld* promastigotes or amastigotes were added to the cells with a multiplicity of infection (MOI) of 1:10 or 1:5, depending on the experiment. The plates were centrifuged at 300 g for 4 min before incubating for 3 h at 37°C. Next, macrophages were washed with wash-buffer in order to remove extracellular parasites. Cells and supernatants were collected at the time points of interest for further analyses. Infection rates were determined by counting 400 macrophages after the DiffQuick staining procedure.

4.2.11 Co-incubation in centrifuge tubes

For a centrifuge tube, 1×10^6 macrophages / ml were transferred into 1.5 ml Eppendorf tubes. Stat. phase *Lm*, *Lae* or *Ld* promastigotes and / or amastigotes were added to the macrophages with a MOI of 1:10 or 1:5, depending on the experiment. After 3 h of co-incubation, extracellular parasites were removed by washing the cells with complete medium and centrifuging at 135 g for 8 min. After washing, macrophages were cultured till the defined time points of interest at

37°C. Cells were collected after 18, 48, 72 or 120 h of culture for further analyses. Infection rates were determined by Flow cytometry.

4.2.12 CR1 and CR3 staining on hMDM I and hMDM II

For CR1 and CR3 staining, 2×10^5 to 2.5×10^5 macrophages were used for each condition. The cells were pipetted in a 96-well-V-plate and centrifuged at 300 g for 4 min at 4°C. After discarding the supernatant, the pellets were washed in 100 µl FACS buffer. Next, FACS buffer was discarded and pellets were resuspended in antibody staining solution for 30 min at 4°C and kept in dark. For CR1, 5 µl of CD35 anti-human PE labeled antibody was used per 1×10^6 cells, while for CR3 1 µl of CD11b/Mac-1 anti-human PE labeled antibody was used per 1×10^6 cells. Isotype control PE labeled was used at the same volume to the corresponding CR1 or CR3 antibody. The antibody solution was prepared in 100 µl FACS buffer. After incubation, plate was centrifuged and the cells were washed and resuspended in 100 µl FACS buffer. Staining was analyzed by Flow cytometry.

4.2.13 Blocking Complement Receptor 1 and 3

For CR1 and CR3 blocking on hMDM I and hMDM II, specific anti-CR1 and anti-CR3 antibodies and respective isotype controls were diluted in complete medium and added to the cells for 30 min at 37 °C. For blocking CR1, cells were incubated with 10 µg / 1×10^5 cells of a rabbit anti human CR1. In order to block CR3, 1 µg / 1×10^5 cells of purified mouse anti-human CD11b/Mac-1 was used. After incubation the cells were centrifuged at 135 g for 8 min and washed with complete medium. Macrophages were used for staining experiments or infection with *Leishmania* parasites.

4.2.14 Microscopy

The following techniques were used for microscopical analysis.

4.2.14.1 Cytospins

To perform either *Leishmania* or macrophages cytopins, 1×10^6 parasites / 100 μ l were used while $0,1 \times 10^6$ cells 100 μ l were used for cytopins of macrophages. The cells were centrifuged in a Cyto centrifuge at 75 g for 5 min for macrophages and 500 g for 10 min for *Leishmania* parasites. Afterwards the slides were dried on air and stained using DiffQuick staining kit.

4.2.14.2 DiffQuick staining

96-well plates or cytospin slides were fixated for 2 min with Fixation-Methanol solution. Subsequently, cells were stained with staining-solution 1 (Eosin) for 2 minutes followed by incubation in staining-solution 2 (Thiazine) for 2 minutes. Next, the cells were washed with water and dried on air.

4.2.14.3 DAPI staining of *Leishmania*

For the detection of *Leishmania* wild-type, parasites were counted and resuspended in *Lm*-medium at a concentration of 1×10^6 parasites / 100 μ l. Next, DAPI was directly added to the parasites in a dilution 1:20 and incubated for 1 h at 27 °C. After incubation, the parasites were washed with complete medium. Parasites were centrifuged at 2400 g for 5 min and resuspended in appropriate volume of complete medium. Stained parasites were used for infection experiments.

4.2.14.4 Lysosome staining

To identify acidic organelles, 2×10^5 macrophages were seeded in chamber slides and incubated overnight at 37 °C and 5% CO₂. On the next day, cells were blocked with α -CR1 and infected for 3 h using *Lm* wild-type, which was previously stained with DAPI. Next, the cells were washed with complete medium, stained with either LysoTracker® Red DND-99 (1:1000) for 15 min at 37 °C and directly used for microscopy. For LysoTracker® Green DND-26 staining, *Lm* DsRed were used for infection and LysoTracker was diluted 1:20000 and incubated for 15 min at 37 °C

4.2.15 Molecular biology methods

4.2.15.1 siRNA knockdown approach in human primary cells

For the siRNA approach, human monocytes were isolated by CD14 positive selection using AutoMACS. The isolated cells were seeded in a 6-well plate (4×10^6 cells / well). After 3 days, new medium supplemented with growth factors was added. After the differentiation in a period of 5 days, medium was removed. Cells were washed with PBS to remove non-adherent cells. For transfection, cells were washed with 1 ml RPMI-medium without supplements (FCS and antibiotics). For each well, 2 μ l of each 10 μ M siRNA solution (4 different siRNAs) was mixed with 20 μ l of buffer. In a separated tube, 4.6 μ l of Stemfect reagent with 20 μ l buffer was mixed. In timeframe of 5 min, both solutions were mixed together and added to the cells for 7 h at 37°C, 5% CO₂. Next, new medium was replaced and cells were incubated for the next 2 days. After, cells were harvested for further experiments comprising RNA isolation, FACS staining, infection experiments and microscopical analysis.

4.2.15.2 DNA isolation

Genomic DNA was isolated from *Leishmania* parasites using QIAgen Blood and Tissue Kit according to the manufacturer's instructions. Beforehand, 100×10^6 stat. phase *Lm*, *Lae* and *Ld* promastigotes were washed in cold PBS and resuspended in 200 μ l PBS. Next, 20 μ l proteinase K and 200 μ l buffer AL were added and the cells were lysed for 10 min at 56°C. Subsequently, 200 μ l ethanol was added, samples were vortexed, transferred to a DNeasy Mini spin column and centrifuged at 6000 g for 1 min at room temperature. The flow-through was discarded and the column washed with 500 μ l buffer AW1 by centrifugation at 6000 g for 1 min at room temperature. An additional washing step was performed with 500 μ l buffer AW2 by centrifugation at 18000 g for 3 min. The remaining content of the column was collected in a fresh collection tube by centrifugation at 18000 g for 1 min. After, the spinning column containing DNA was placed in a fresh 1.5 ml tube and 200 μ l buffer AE was added and incubated for 1 min before centrifuged at 6000 g for 1 min. The isolated DNA was stored at -20°C.

4.2.15.3 Amplification of the ribosomal internal transcribed spacer 1 (ITS1)

After genomic DNA isolation, the ITS1 of the different *Leishmania* species was amplified by PCR using specific oligonucleotides. The products were analyzed by electrophoresis on a 1% agarose gel and visualized under ultraviolet light. The reagents and amounts used for one reaction:

| Reagent | Volume |
|-------------------------|--------------|
| Dest Water | 35.5 μ l |
| Primer fwd (10 μ M) | 2.5 μ l |
| Primer rev (10 μ M) | 2.5 μ l |
| dNTPs (2mM) | 1 μ l |
| DMSO | 1.5 μ l |

Material and methods

| | |
|--------------------|------------------------------|
| 10x NEB Taq-Buffer | 5 μ l |
| NEB-TaqPolymerase | 0.5 μ l |
| <u>gDNA</u> | <u>1.5 μl</u> |
| | ad 50 μ l |

4.2.15.4 Restriction digest

Each PCR products (40 μ l) of the different *Leishmania* species were incubated with 1 μ l of *Hae*III enzyme for restriction digest at 37°C for 1 h according to the manufacturer's instructions. The restriction fragments were analyzed by electrophoresis on a 2% agarose gel and visualized under ultraviolet light.

4.2.15.5 RNA Isolation

Macrophages were harvested and the RNA was isolated using the RNeasy Plus Mini Kit according to the manufacturer's instructions. At least 0.5×10^6 cells were used for isolation. Macrophages were pelleted and washed with cold PBS at 1024 g for 8 min. The pellet was lysed in 350 μ l RLT-Plus-Buffer after which the lysate was transferred to a gDNA Eliminator spin column. Centrifuging at 15300 g for 30 sec, genomic DNA was removed by being retained in the column and RNA was collected. The flow-through was mixed with 70% ethanol (1:1) and the mixture was transferred to an RNeasy spin column. Columns were centrifuged at 15300 g for 30 sec. After, the flow-through was discarded and the column was washed twice with 500 μ l RPE-buffer (15300 g, 30 sec and 2 min). Subsequently the column was placed in a fresh 1.5 ml centrifuge tube. To elute the RNA from the column, 30 μ l RNase-free water was added following centrifugation of 15300 g for 1 min. The samples were placed on ice for further use or frozen at -80°C for a later use. For measuring RNA concentrations (duplicates), a NanoDrop2000c was used. RNA was verified to be DNA-free by a test-PCR.

4.2.15.6 DNase treatment

The isolated RNA was incubated with 1 μ l of DNase I recombinant (10 U / μ l) and 1 U / μ l) and 1 μ l of RNase Out™ Ribonuclease Inhibitor (40 U / μ l) for 20 min at 37°C and subsequently, 10 min at 75°C for enzyme inactivation. The DNase digestion was performed two times in order to ensure the elimination of remaining genomic DNA.

4.2.15.7 Test-PCR

In order to guarantee that no genomic DNA is present in the isolated RNA, a Test-PCR was performed after RNA isolation. A specific GAPDH primer was used for macrophages as well as rRNA45 or ABC (ABC transporter homologue) primer for *Leishmania* samples. For all samples, a Master-Mix was prepared and divided into PCR tubes. Afterwards, the RNA and the required volume of H₂O were added. For positive control 2 μ l (100 ng) of cDNA was added while for the negative control H₂O was used. After PCR, the products were mixed with 5.5 μ l 10x AAP and loaded on a 1% agarose gel with EtBr and visualized with UV light after separation.

Reagents and volumes used for Test-PCR

| Reagent | Volume |
|--------------------|--------------|
| 10x NEB Taq-Buffer | 5 μ l |
| dNTPs | 5 μ l |
| Primer forward | 1 μ l |
| Primer reverse | 1 μ l |
| NEB Taq-Polymerase | 0,25 μ l |

Material and methods

| | |
|------------------|----------|
| H ₂ O | X |
| RNA | 100 ng |
| <hr/> | |
| | ad 50 µl |

4.2.15.8 cDNA Synthesis

For cDNA synthesis, ImProm-II Reverse Transcription System was used according to the manufacturer's instructions. For that, 1 µl Random Primer (0.5 µg) was added to 50 ng RNA and mixed. Water was added to a final volume of 5 µl. The samples were incubated for 5 min at 70°C and 5 min at 4°C. In the next step 15 µl master mix was added to each reaction tube. After the reaction, the cDNA was stored at -20°C.

Reagents and volumes used for cDNA Synthesis:

| Reagent | Volume [µl] |
|-----------------------|-------------|
| H ₂ O | 6,5 |
| 5x Reaction Buffer | 4 |
| Magnesiumchloride | 2 |
| dNTPs Mix | 1 |
| RNasin Inhibitor | 0.5 |
| Reverse Transcriptase | 1 |

Material and methods

Performed program for cDNA synthesis:

| | Temp [°C] | Time [min] |
|----------------|-----------|------------|
| Annealing | 25 | 5 |
| cDNA Synthesis | 42 | 60 |
| Inactivation | 70 | 15 |
| Cooling | 4 | ∞ |

4.2.15.9 Quantitative real-time PCR

In order to measure the amount of cDNA in each sample, the MESA Blue qPCR MasterMix Plus for SYBR Assay No Rox was performed according to the manufacturer's instructions. Based on the fluorescence intensity, which is proportional to the DNA amount, the amplification of the target genes was measured, using specific primers. The reactions were performed in duplicates in a withe 96-well LightCycler plate. For analysis of parasite gene expression, normalization was performed against housekeeping gene rRNA45 of *Leishmania* promastigote. To perform the analysis of macrophage gene expression, normalization was performed against the housekeeping gene GAPDH of macrophages.

Performed program for qRT-PCR at LightCycler:

| | Temp [°C] | Time | $\Delta^{\circ}\text{C}/\text{s}$ |
|---------------------------|-----------|--------|-----------------------------------|
| Activation | 95 | 10 min | 4.4 |
| Amplification (45 Cycles) | | | |
| Denaturation | 95 | 10 s | 4.4 |
| Annealing | 60 | 10 s | 2.2 |
| Elongation | 72 | 15 s | 4.4 |

Material and methods

| | | | |
|------------------|-------|--------|------|
| Final Elongation | 85 | 10 s | 4.4 |
| Melting Curve | 60-99 | | 0.11 |
| Cooling | 40 | 20 min | 2.2 |

4.2.15.10 siRNA screen in primary human macrophages

In a collaboration project, we tested several macrophage targets that maybe involved in the increase and decrease of *Leishmania* infection in this cell. The experiments were performed in the Scottish Bioscreening Facility in the University of Glasgow under the supervision of Prof. Dr. Markus Meissner.

Anti-inflammatory macrophages were generated by negative selection using Monocyte Isolation Kit II human von Miltenyi Biotec. A total of 18×10^6 cells were cultured in Lumox Dish 50 for 3 days at 37°C. After, siRNA library was transferred to the 384 well plates (7500 cells / well) using a liquid handling robot platform, Beckman BioMek FXP©. After, macrophages were harvested and added to the plates using a Multidrop Dispenser. The mixture of cells and siRNA was incubated for 4 days at 37°C. Next, stat. phase *Lm* wild-type promastigotes was added to the cells with a MOI of 10 during 2 h. Adherent cells were washed with PBS for the removal of extracellular parasites. Cells were fixed with 3.6% Formaldehyde solution during 25 min at RT. After washing, 0.1% TritonX (in PBS) was added for 25 min. Cells were washed twice with PBS and incubated with mouse Anti-*Leishmania* serum (1:100) for 40 min at RT. After washing, PBS including Hoechst (1:50000), Phalloidin (1:500) and secondary Anti-Rabbit-Alexa555 (1:1000) was added and incubated for 40 min at RT. Adherent cells were washed twice with PBS and submitted to imaging with GE IN Cell 2000©.

4.2.15.11 Statistical analysis

Data normality was tested using the D'Agostino-Pearson omnibus test. Data regarding $n > 7$ was normally distributed. Data regarding $n < 7$ which was following a Gaussian distribution was assumed to be normally distributed. Statistical analyses were performed using a paired Student's t-test using the software package GraphPad Prism 6 (Graph-Pad Software, USA). Data are presented as mean \pm standard deviation (SD). Values of $p < 0.05$ (*), $p < 0.01$ (**), $p < 0.001$ (***) and $p < 0.0001$ (****) were considered as significant.

5. RESULTS

5.1 Phenotypical characterization of different human macrophage phenotypes

In this thesis, we used primary human monocytes and generated macrophages *in vitro*. First we characterized the phenotype of both pro-inflammatory (hMDM I) and anti-inflammatory (hMDM II) macrophages. By using flow cytometry analysis, specific cell surface markers were assessed. After macrophage differentiation (6-7 days) with either GM-CSF for hMDM I or M-CSF for hMDM II, we investigated the positivity (%) and Mean Fluorescent Intensity (MFI) of molecules already known as phenotype specific markers. We found that CD14 was lower expressed on hMDM I ($87.5\% \pm 0.4$; MFI = 1786 ± 1682.9) in comparison to hMDM II ($98.3\% \pm 1.1$; MFI = 6761.5 ± 1703.4). An already known characteristic of hMDM II is the presence of scavenger receptor CD163 (Martinez and Gordon, 2014). Indeed the expression of CD163 on hMDM I ($7.2\% \pm 6.6$; MFI = 515.5 ± 382.9) was much lower when compared to hMDM II ($85.4\% \pm 10.9$; MFI = 3773.5 ± 3109.4). The hMDM I cells showed a high expression of the mannose receptor CD206 ($96\% \pm 4.7$; MFI = 2021 ± 485.5), which was presented in lower amounts on hMDM II ($79.8\% \pm 20.5$; MFI = 1059.3 ± 572.7) (**Figure 7**).

Results

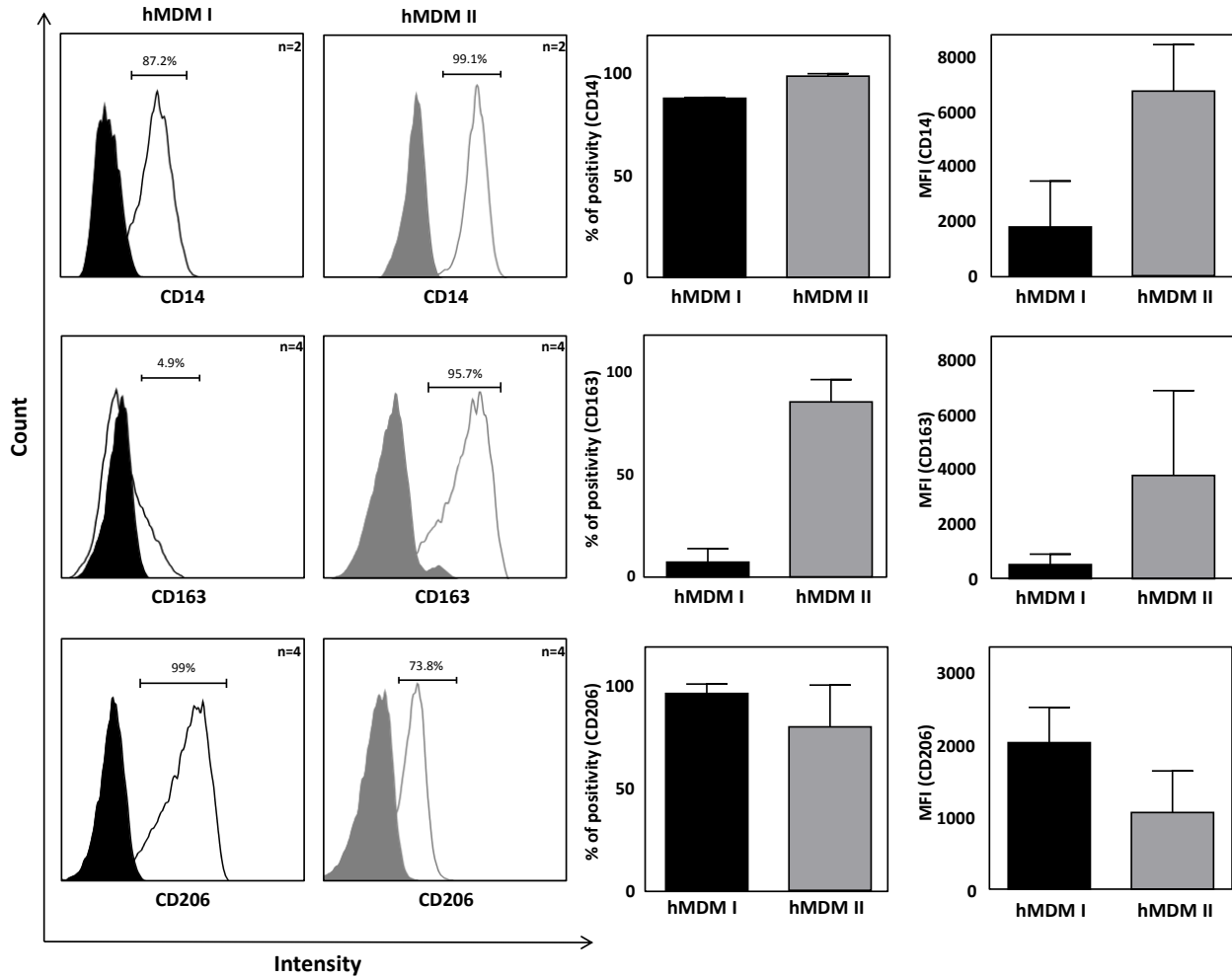


Figure 7: Phenotypical characterization of human macrophages. Human primary CD14⁺ monocytes were differentiated into pro-inflammatory (hMDM I) and anti-inflammatory macrophages (hMDM II) using GM-CSF (10 ng/ml) and M-CSF (30 ng/ml) respectively. After 6-7 days of culture, the surface expression of CD14, CD163 and CD206 was assessed using specific CD14 Pacific Blue labeled, CD163 and CD206 PE labeled antibodies. Flow cytometry was used for the measurement of positivity (%) and Mean Fluorescent Intensity (MFI). Histograms and data, as mean \pm SD, are representative of at least 2 independent experiments.

5.2 Complement Receptor 1 and 3 expression on pro- and anti-inflammatory human macrophages

In search of additional macrophage phenotype markers, we focused on the complement receptors CD35 (CR1) and CD11b/CD18 (CR3). We found that expression of CR1 on hMDM I ($71.2\% \pm 25$) is significantly higher in comparison to hMDM II ($18.4\% \pm 16$) (**Figure 8A**). When comparing this high number ($n=65$) of donors, we found a large variability in CR1 expression on hMDM I, in contrast to a much lower variability and lower expression on hMDM II. The MFI of CR1 was similar between hMDM I (4433.8 ± 2511.3) and hMDM II (5429.2 ± 2690.8) (**Figure 8B**). Focusing on CR3, we found that the expression of CR3 on hMDM I ($99.3\% \pm 1.7$) and hMDM II ($94.7\% \pm 7.5$) was equal (**Figure 8C**). Moreover, the MFI of CR3 was slightly higher on hMDM I (13101.5 ± 6884.7) in comparison to hMDM II (10175.9 ± 4894.9) (**Figure 8D**). Taken together, we found that pro-inflammatory human macrophages have higher expression levels of CR1 when compared to anti-inflammatory macrophages.

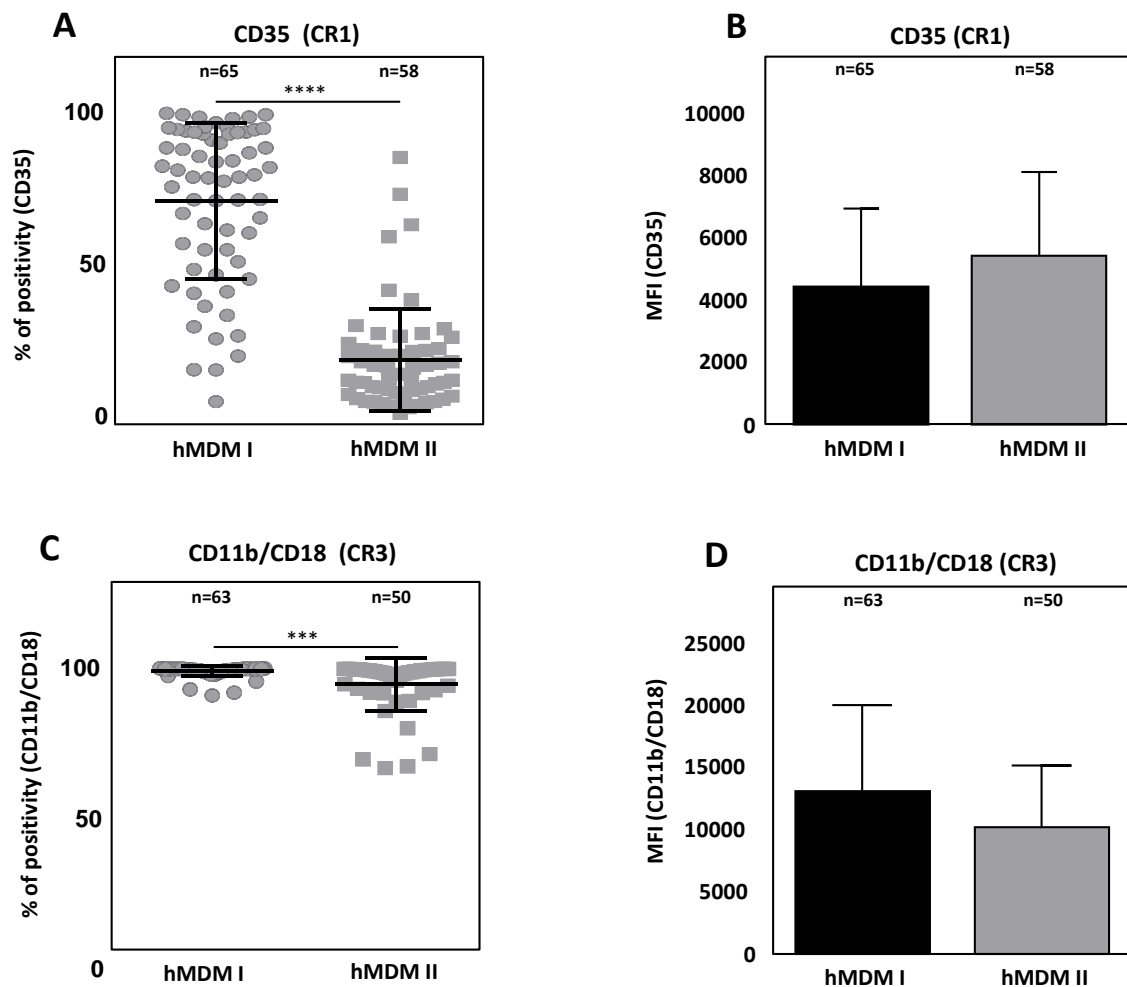


Figure 8: Assessment of the expression levels of CR1 and CR3 on hMDM I and hMDM II. After 6-7 days in culture, the expression levels of CD35 (CR1) and CD11b/CD18 (CR3) was analyzed on both hMDM I and hMDM II using PE labeled specific antibodies by flow cytometry analysis. **(A)** Quantification of CR1 positivity (%) on hMDM I (grey dots) and hMDM II (grey squares). **(B)** Measurement and quantification of the MFI of CR1 on hMDM I (black bar) and hMDM II (grey bar). **(C)** CR3 positivity (%) on hMDM I (grey dots) and hMDM II (grey squares). **(D)** MFI quantification of CR3 on hMDM I (black bar) and hMDM II (grey bar). Data are presented as mean \pm SD of at least 3 independent experiments (***: $p < 0.001$; ****: $p < 0.0001$).

5.3 Characterization of different *Leishmania* species by restriction fragment length polymorphism analysis of ITS1

Complement receptors are known to be involved in the uptake of different *Leishmania* species. We aimed to compare macrophage interactions with *Leishmania major* (*Lm*), *Leishmania aethiopia* (*Lae*) and *Leishmania donovani* (*Ld*) parasites. First, we ensured the identity of the different parasite species by performing a restriction fragment length polymorphism (RFLP) analysis of the internal transcribed spacer 1 (ITS1), used as a marker for the parasite species. After genomic DNA isolation of parasites, which resided in a logarithmic growth phase (log. phase), the amplicons of ITS1 of *Lm*, *Lae* and *Ld* wild-type and eGFP and DsRed-expressing *Leishmania* were digested with the restriction enzyme *HaeIII*. We observed that *Lm* showed three DNA fragments (± 150 / 210 / 300bp); *Lae* ITS1 showed two clearly visible DNA fragments (± 80 / 200bp) and two weakly visible DNA fragments (± 20 / 150bp); *Ld* ITS1 showed three clearly visible DNA fragments (± 60 / 90 / 200bp) and one weakly visible DNA fragment (± 150 bp). Within one species, the transgenic variants (eGFP/DsRed-expressing parasites) had a similar RFLP profile as compared to the wild type (**Figure 9**).

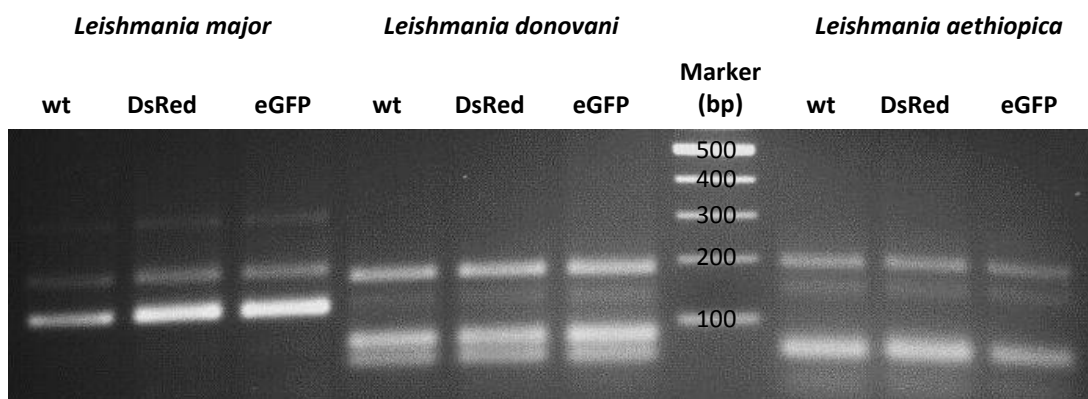


Figure 9: Restriction fragment length polymorphism of different *Leishmania* species. Genomic DNA isolated from log. phase *Lm*, *Lae* and *Ld* promastigotes was amplified with ITS1 specific primers. The digestion of the amplified ITS1 with *HaeIII* showed a distinct species specific band pattern for *Lm*, *Lae* and *Ld*. The samples were loaded in a 2% agarose gel in parallel with a 100 bp marker and analyzed under UV light. A representative restriction pattern is depicted.

5.4 Growth kinetics and morphological assessment of promastigote stage of different *Leishmania* species

After confirming their identity, promastigote stages of *Lm*, *Lae* and *Ld* wild-type were analyzed for their growth kinetics. We found that the growth of all three strains was first characterized by a log. phase followed by a plateau stage so called as stationary growth (stat.) phase. During the first three days of cultivation, *Lm* promastigotes expanded 19.2-fold (d1: $7 \times 10^6 \pm 3.9$ parasites/ml; d3: $135.4 \times 10^6 \pm 16.9$ parasites/ml). *Lae* promastigotes, also causing cutaneous Leishmaniasis, expanded 11.4-fold (d1: $5.2 \times 10^6 \pm 1.8$ parasites/ml; d3: $59.0 \times 10^6 \pm 7.9$ parasites/ml) and, at d3, presented significant less parasites as compared to *Lm*. *Ld*, causative for visceral Leishmaniasis, grew at a much lower speed, only expanding 4.9-fold, and the parasite number was significantly lower as compared to the growth kinetics of both *Lm* and *Lae* at d3 of culture (d1: $3.5 \times 10^6 \pm 1.3$ parasites/ml; d3: $17.4 \times 10^6 \pm 4.8$ parasites/ml). From day 6 on, parasites entered a stat. phase. By analyzing the species specific growth kinetics, it could be demonstrated that *Lm* showed the highest expansion (d7: $247.5 \times 10^6 \pm 2.4$ parasites/ml) followed by *Lae* (d7: $113.6 \times 10^6 \pm 26.4$ parasites/ml) and *Ld* ($54.8 \times 10^6 \pm 22.1$ parasites/ml) (**Figure 10A**). Moreover, parasite morphology was assessed by microscopy and DiffQuick staining. Log. phase promastigotes from either *Lm*, *Lae* or *Ld* species, were elongated shaped with an apical flagellum and a clearly visible nucleus and kinetoplast (white arrows) (**Figure 10B, upper row**). Microscopical analysis of stat. phase promastigotes showed a mixture of elongated promastigotes and round shaped promastigotes (black arrows) (**Figure 10B, lower row**). Round shaped parasites were observed to have less nuclear and mitochondrial structures, typical for the infective stationary phase.

As already published by our group using *Lm* parasites (Wenzel et al., 2012), the virulent inoculum (stat. phase) consists of a mixture of viable and apoptotic parasites. Therefore, we compared the three *Leishmania* species for their ability to bind AnnexinA5 as an early marker for apoptosis (van Zandbergen et al., 2006). Even though *Lm*, *Lae* and *Ld* species possess a unique and different growth profile, we found that stat. phase parasites of *Lm* ($57.4\% \pm 9.5$), *Lae* ($46.4\% \pm 8.1$) and *Ld* ($47.7\% \pm 10.6$) all bind AnnexinA5 to a similar extent (**Figure 10C**). In all, the stat. phase

Results

(infectious inoculum), independent of the *Leishmania* species, comprises a viable and apoptotic parasite population in a ratio of about 1:1.

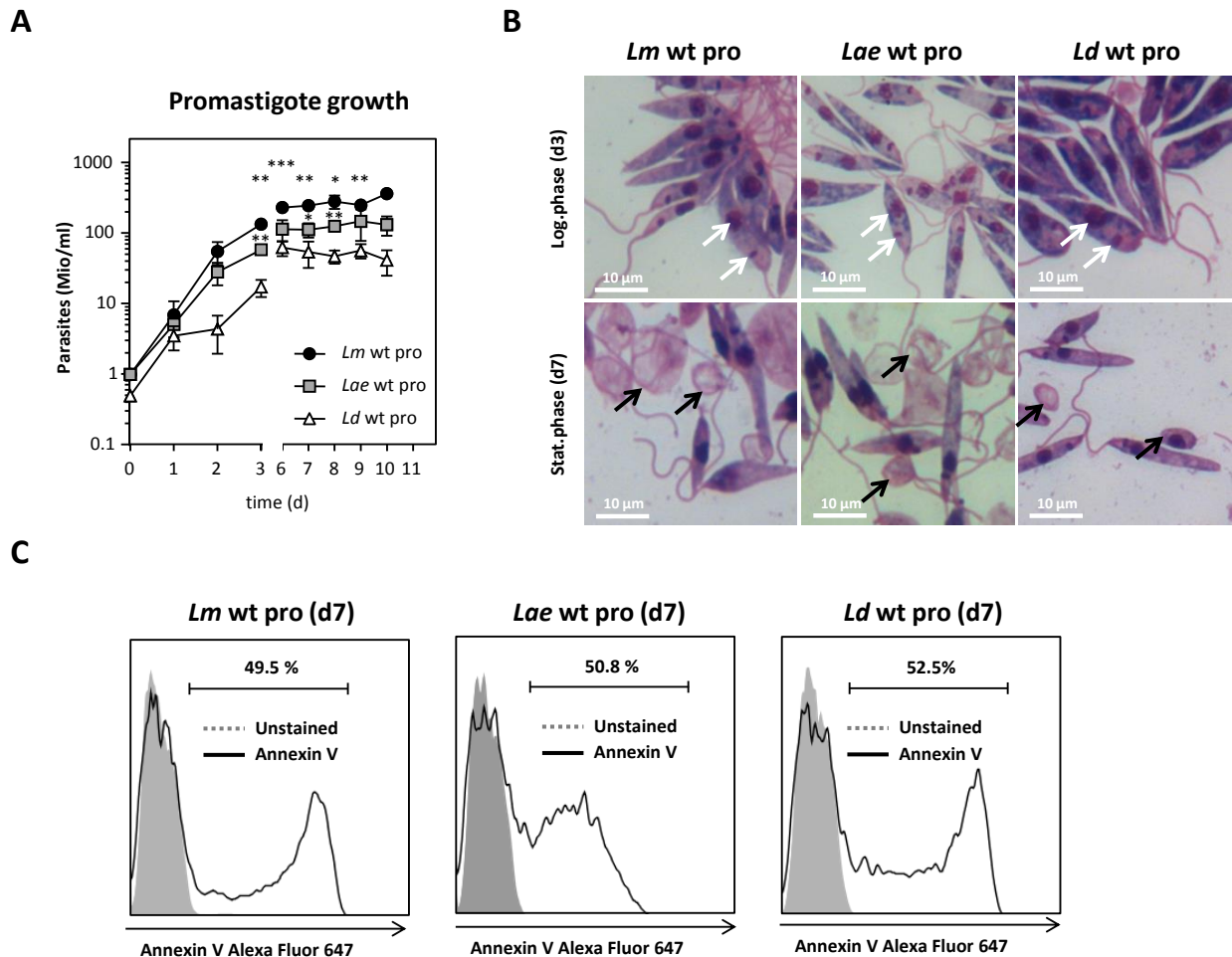


Figure 10: Growth kinetics and morphology profile of distinct *Leishmania* promastigote species. (A) Promastigotes of *Lm* (filled black circles), *Lae* (filled grey squares), *Ld* (open triangles) were cultivated in a biphasic culture system. Parasite numbers were counted daily microscopically over a time span of 10 days, depicted in growth curves. (B) Histological assessment of log. and stat. phase *Lm*, *Lae* and *Ld* promastigotes using DiffQuick. Elongated parasites (white arrows) depicted in the upper row and a mixture of elongated and round shaped (black arrows) parasites in lower row. (C) AnnexinA5 binding of stat. phase *Lm*, *Lae* and *Ld* was assessed by flow cytometry. Micrographs and histograms are representative and data, presented as mean \pm SD, are representative for at least 3 independent experiments (*: $p < 0.05$; **: $p < 0.01$; ***: $p < 0.001$).

5.5 Growth kinetics and morphological analysis of amastigote parasites

We generated axenic *Lm* and *Lae* amastigotes as described for *Lm* (Wenzel et al., 2012) and compared growth characteristics as for promastigotes. We could demonstrate *Lm* amastigotes to expand 5-fold (d0: $10.0 \times 10^6 \pm 0.0$ parasites/ml; d7: $50.0 \times 10^6 \pm 25.6$ parasites/ml) over a time span of 7 days, which did not significantly differ from the growth profile of *Lae* amastigotes, expanding 3.3-fold (d0: $10.0 \times 10^6 \pm 0.0$ parasites/ml; d7: $31.3 \times 10^6 \pm 7.4$ parasites/ml) (**Figure 11A**). Furthermore, morphology of both *Lm* and *Lae* amastigotes was analyzed using DiffQuick staining and microscopy. Axenic amastigotes were generated by transferring log. phase promastigotes, previously cultivated in biphasic medium, to an acidified medium. Unlike promastigotes, amastigotes have a droplet shaped morphology and are non-motile, as the flagellum does not protrude beyond the body's surface. The nucleus and kinetoplast were present as well and the presence of dividing amastigotes was observed. Although *Lae* amastigotes showed an elliptic form, they were not as uniform as *Lm* (**Figure 11B**). By using the system established in our group, we were able to generate viable axenic amastigote cultures of *Lm* and *Lae* with the presence of 96% droplet shape multiplying parasites. Applying this protocol on *Ld* log. phase promastigotes, we were not able to generate *Ld* axenic amastigote cultures, since no viable multiplying amastigote parasites were observed after 3 days of culture in pH 5.5 amastigote medium. Next, the pH was adjusted from 5.5 to 5 and still 16% of remaining promastigotes was observed. After changing the temperature from 33°C to 35°C and 37°C, we still found 20% of promastigote parasites to be present.

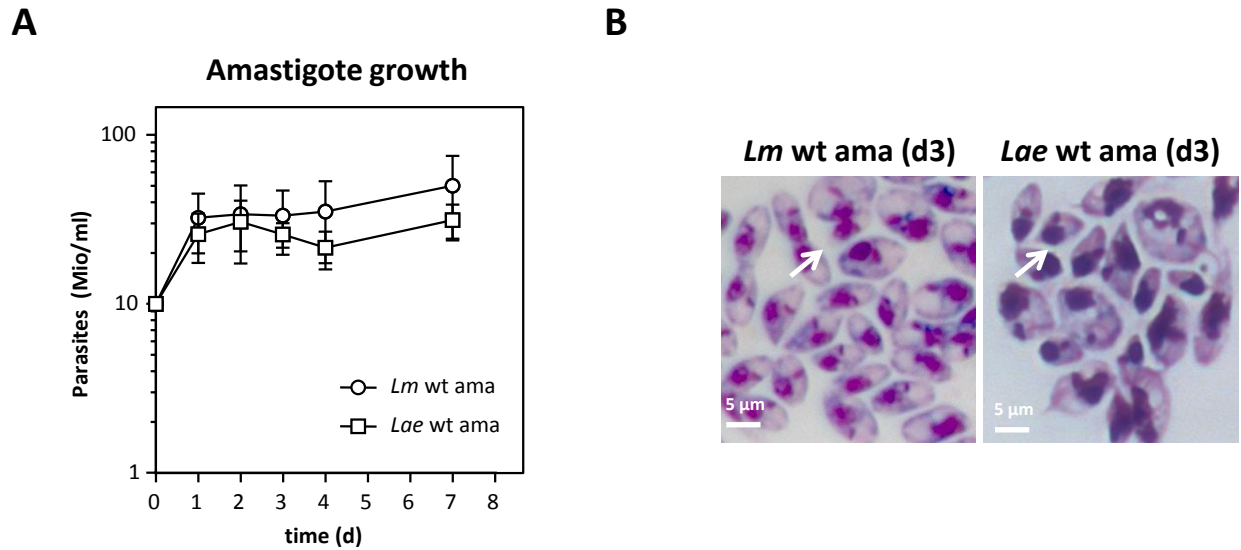


Figure 11: Growth kinetics and morphology analysis of the amastigote stage of different *Leishmania* species. (A) Axenic amastigotes were cultured in acid AAM. Growth curves of *Lm* (open circles) and *Lae* (open squares) amastigotes determined by microscopical counting over 7 days. (B) DiffQuick staining of amastigote axenic cultures (d3) of both *Lm* and *Lae*. Dividing amastigotes are highlighted by white arrows. Micrographs are representative and data, presented as mean \pm SD, are representative for at least 3 independent experiments.

5.6 *Leishmania* stage-specific gene expression analysis

To further characterize the promastigote and amastigote growth stages, we assessed specific gene expression levels. Initially, the gene expression of the promastigote marker SHERP (small hydrophilic endoplasmatic reticulum associated protein) as well as the amastigote markers ABC-transporter homologue and glycoprotein 63 (GP63) were analyzed.

In addition, we selected additional genes based on a mass spectrometry screen, in which promastigote and amastigote specific proteins were identified. Based on this study, performed in a previous project, Adenylate Kinase, Calpain Peptidase, Metallo Peptidase and a Surface Antigen Protein were identified as being promastigote stage specific and Alkyl dihydroxyacetone phosphate as well as Cysteine Peptidase as amastigote stage specific (data not shown). Corresponding promastigote genes IDs (5651684, 5651484, 5654678 and 5649987 respectively) and amastigote genes IDs (5653530 and 5651252 respectively) were selected for RT-PCR analysis.

Results

Primer specificity was verified after the PCR products showed, for each target, one single band with the expected size on an agarose gel. Respective negative controls (H₂O) were negative, or showed primer dimers (**Figure 12A**). We observed a higher gene expression of Adenylate Kinase in promastigote parasites in comparison to the amastigote stage (**Figure 12B**). In agreement, Calpain Peptidase (**Figure 12C**), Metallo Peptidase (**Figure 12D**) and Surface Antigen Protein (**Figure 12E**) were all significantly higher expressed in promastigote when compared to the amastigote parasites.

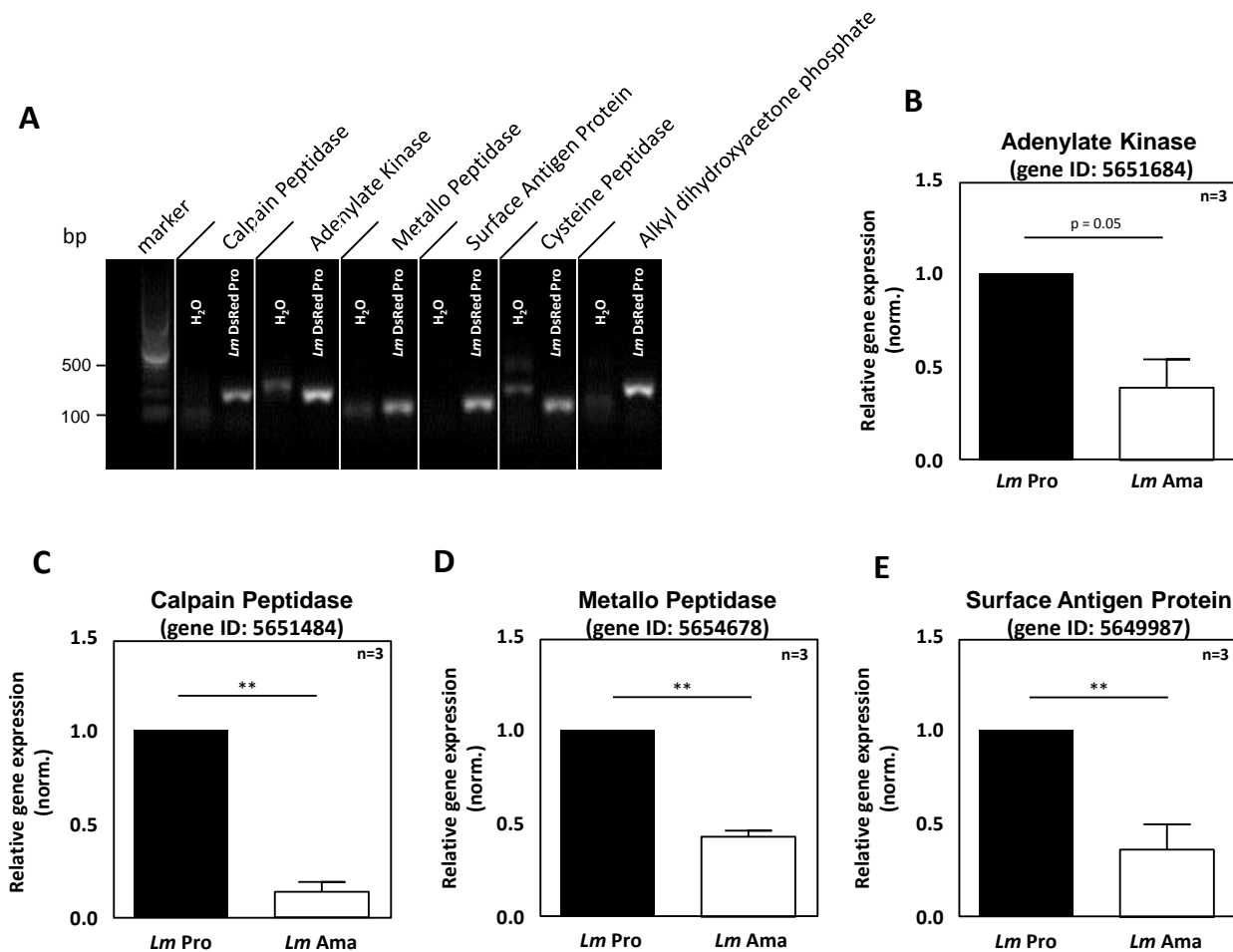


Figure 12: *Leishmania* promastigote stage specific gene expression. RNA was isolated from DsRed-expressing *Lm* promastigotes and amastigotes. After cDNA synthesis a qRT-PCR, using optimized primers (**A**), was performed in order to compare the gene expression levels of specific promastigote proteins in both parasite stages. (**B-E**) Relative gene expression of Adenylate Kinase (**B**), Calpain Peptidase (**C**), Metallo Peptidase (**D**) and Surface Antigen Protein (**E**) in promastigote (black bar) and amastigote (white bar) parasites. The relative gene expression was calculated and normalized based on the housekeeping gene rRNA45 of *Leishmania* promastigote parasites. Data, presented as means \pm SD, are representative of at least 3 independent experiments (**: $p < 0.01$).

Results

Cysteine Peptidase, as expected, was higher expressed in amastigotes when compared to the promastigote parasites (**Figure 13A**). In contrast to our expectation, we found that Alkyl dihydroxyacetone phosphate was less expressed in amastigote parasites in comparison to the promastigote stage (**Figure 13B**).

We could demonstrate that the gene expression levels of the different promastigotes genes are promastigote stage-specific, whereas only the Cysteine Peptidase gene was shown to be amastigote stage-specific.

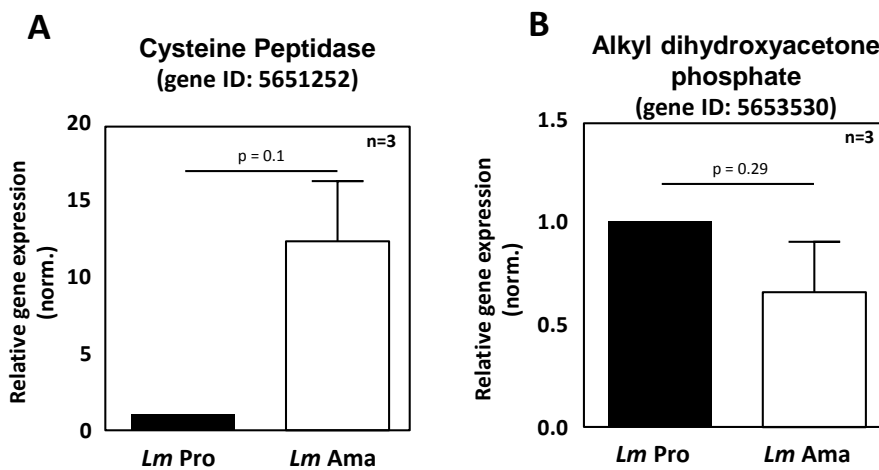
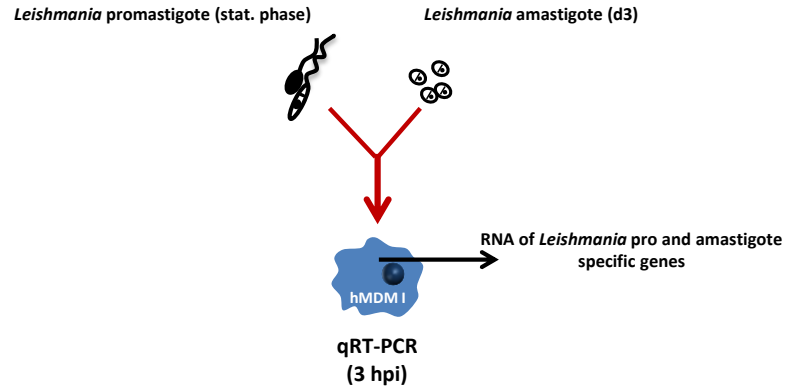


Figure 13: *Leishmania* amastigote stage specific gene expression. RNA was isolated from DsRed-expressing *Lm* pro and amastigote. After cDNA synthesis a qRT-PCR was performed in order to assess the gene expression levels of specific promastigote proteins in both parasite stages. (A-B) Relative gene expression of Cysteine Peptidase (A) and Alkyl dihydroxyacetone phosphate (B) of promastigote (black bar) and amastigote (white bar) parasites. The relative gene expression was calculated and normalized based on the housekeeping gene rRNA45 of *Leishmania* promastigote parasites. Data, presented as means \pm SD, are representative of at least 3 independent experiments.

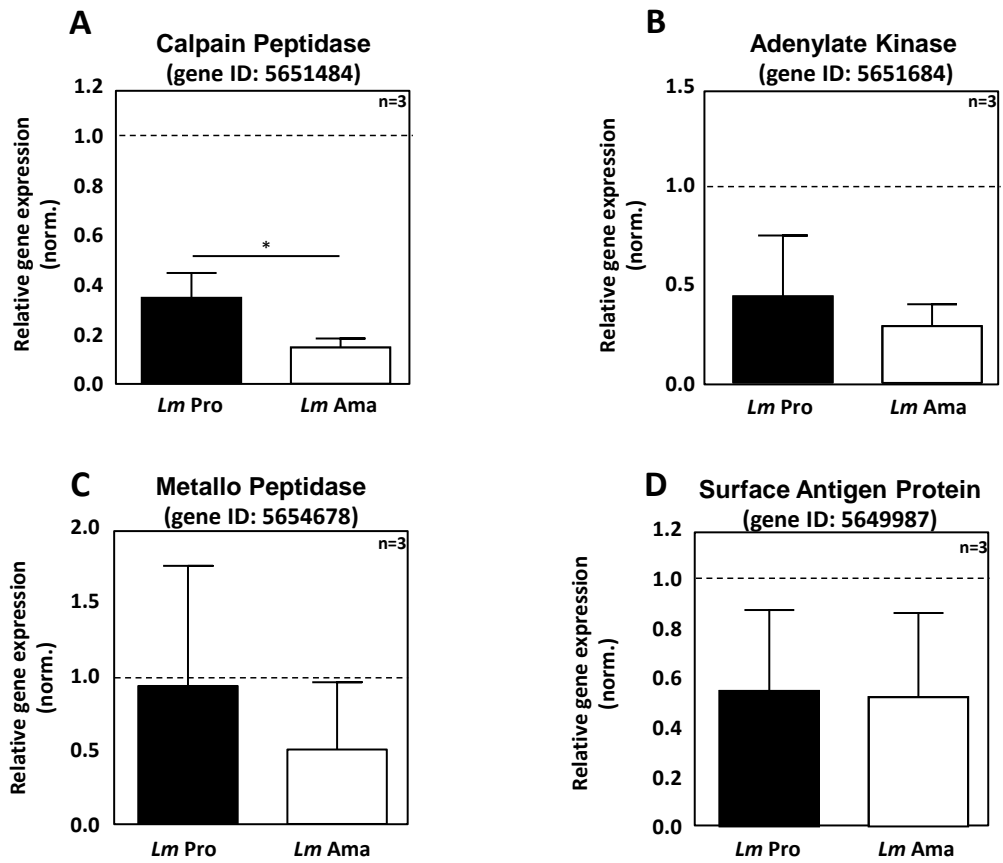
5.7 Promastigote and amastigote stage specific gene expression in infected hMDM I.

In a next step, hMDM I were infected with either promastigotes or amastigotes after which these stage-specific genes were assessed. The gene expression of Adenylate Kinase, Calpain Peptidase, Metallo Peptidase and Surface Antigen Protein (promastigote specific) as well as Alkyl dihydroxyacetone and Cysteine Peptidase (amastigote specific) were assessed 3 hpi. After *Lm* promastigote infection, we found the promastigote specific gene Calpain Peptidase to be significantly higher expressed in the promastigote stage. Adenylate Kinase and Metallo Peptidase genes were upregulated in promastigote compared to amastigote parasites. In contrast, Surface Antigen Protein gene was similarly regulated in both pro and amastigote parasites (**Figure 14A-D**). The amastigote specific genes, Alkyl dihydroxyacetone and Cysteine Peptidase, were both high expressed in cells infected with the amastigote stage as compared to the promastigote infected cells (**Figure 14E-F**). In all, we demonstrated that after macrophage infection, gene expression remained parasite stage-specific.

Results



Promastigote specific



Amastigote specific

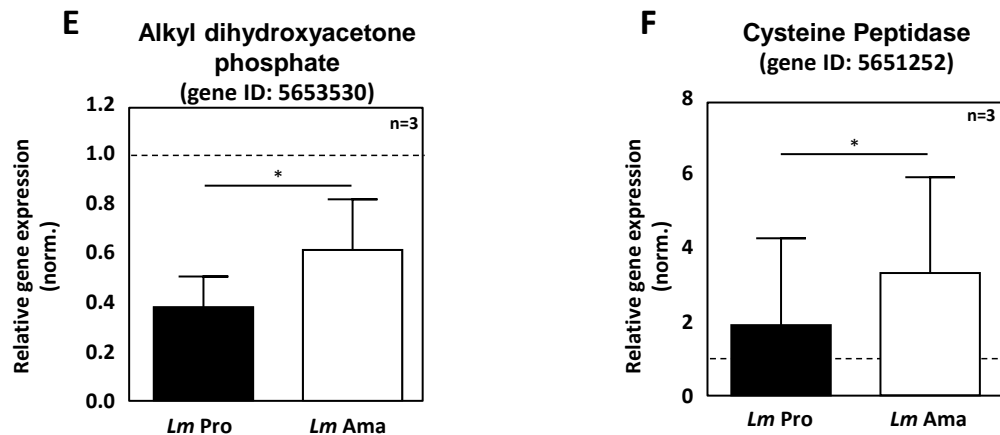


Figure 14: Relative gene expression of *Leishmania* stage specific genes after infection of hMDM I cells. After 3 hpi of hMDM I with transgenic *Lm* promastigote (black bar) or amastigote (white bar), RNA was isolated and after cDNA synthesis, qRT-PCR was performed to assess the relative gene expression of promastigote proteins. (A-F) Relative gene expression of Calpain Peptidase (A), Adenylate Kinase (B), Metallo Peptidase (C), Surface Antigen Protein (D), Alkyl dihydroxyacetone phosphate (E) and Cysteine Peptidase (F) in hMDM I infected with *Lm* promastigotes or amastigotes. Data are presented as mean \pm SD of at least 3 independent experiments (*: $p < 0.05$).

5.8 *Leishmania* parasite species and promastigote specific infection of hMDM I and hMDM II

It remains unclear which phenotype of macrophages is responsible for parasite killing or parasite survival and disease development. In addition, it is unclear whether parasite species and stages infect differentially. Therefore hMDM I and hMDM II were infected with either promastigotes or amastigotes of different species. At 24 hours post infection (24 hpi), infection rates were analyzed microscopically by using DiffQuick staining. We first investigated the infection and persistence of infection over time of *Lm* in hMDM I and hMDM II cells. After 24 hpi, *Lm* infected hMDM II (38.1 ± 4.4) significantly higher in comparison to hMDM I ($27.2\% \pm 6.3$) and we observed that the infection persisted stable over time in both cell types. After 48 hpi, hMDM II ($39.5\% \pm 11.4$) was significantly higher infected as compared to hMDM I ($29.2\% \pm 5.9$) cells. Similar persistence of infection was found after 72 hpi in hMDM II ($38.7\% \pm 6.9$) and hMDM I ($27.9\% \pm 5.1$) as well as after 120 hpi in both hMDM II ($38.1\% \pm 8.7$) and hMDM I ($24.9\% \pm 5.9$) (Figure 15A).

Next, we investigated whether the *Lae* species behave differently when infecting hMDM I and hMDM II. After 24 hpi we observed that *Lae* infects macrophages at a similar level. Interestingly, no differences were found between *Lae* infection of hMDM I ($41.9\% \pm 6.8$) and of hMDM II ($44.1\% \pm 13.2$) Moreover, parasite infection rates dropped significantly over time (Figure 15B). Subsequently, we assessed the interaction of *Ld* with hMDM I and hMDM II. After 24 hpi, macrophages showed a reduced rate of infection as compared to both *Lm* and *Lae* promastigotes. As with *Lm*, hMDM II ($18.1\% \pm 8.1$) were more susceptible to *Ld* infection as compared to hMDM I ($10.9\% \pm 0.91$). At 48 hpi the infection rate was reduced in both cell types.

Results

Furthermore, at both 48 and 120 hpi we observed a decrease of *Ld* infection in both hMDM I and hMDM II (**Figure 15C**). Of note, after infection (24 hpi) of hMDM I and hMDM II, with either *Lm*, *Lae* or *Ld*, DiffQuick stainings were performed, of which representative micrographs are depicted (**Figure 15A-C**).

In all, we found, independent of the analyzed time points, hMDM II to be more susceptible to *Lm* infection in comparison to hMDM I. Over time, *Lm* infection showed to be sustained, whereas *Lae* and *Ld* infection decreases. In addition, infection with *Ld* parasites was less effective in both hMDM I and hMDM II in comparison to *Lm* and *Lae*.

Results

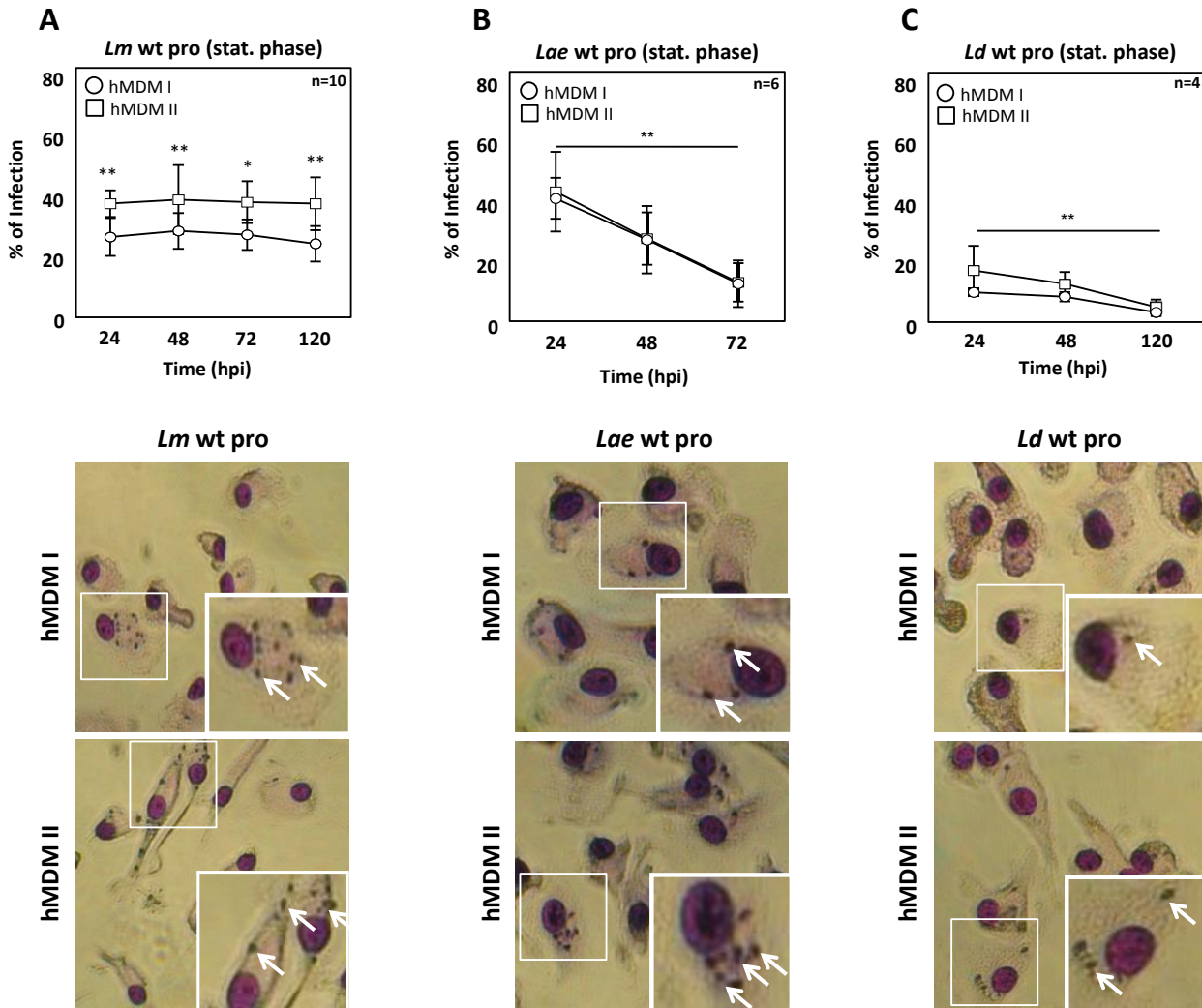


Figure 15: Infection and development of different *Leishmania* promastigote species in pro- and anti-inflammatory human macrophages. Both hMDM I (white circles) and hMDM II (white squares) were infected with promastigotes wild-type of distinct *Leishmania* species, at MOI 10. After 3 hours extracellular parasites were removed by washing and the infection rates were measured at different time points (24, 48, 72 hpi and 5 dpi) by DiffQuick staining and microscopical assessment. Parasites are indicated by white arrows. (A-C) Quantification of *Lm* (A), *Lae* (B) and *Ld* (C) infection rate and survival in both hMDM I and hMDM II at the indicated time points. Micrographs (24hpi) and data, presented as mean \pm SD, are representative of at least 3 independent experiments (*: $p < 0.05$; **: $p < 0.01$).

5.9 *Leishmania* parasite species and amastigote specific infection of hMDM I and hMDM II

After analysis of wild-type promastigote infection of different *Leishmania* species in human cells, we investigated the interaction of *Lm* and *Lae* amastigotes with both hMDM I and hMDM II and the outcome of infection at different time points. At 24 hours post infection (24 hpi), infection rates were analyzed microscopically by using DiffQuick staining. After 24 hpi, *Lm* established a significant higher infection in hMDM II ($83.6\% \pm 4.8$) in comparison to hMDM I ($67.4\% \pm 9.1$). After 48 hpi, the infection was similar in both hMDM II ($70.4\% \pm 16.7$) and hMDM I ($69.1\% \pm 8.5$) and remained stable after 72 hpi in hMDM II ($76.7\% \pm 7.7$) and hMDM I ($76.2\% \pm 8.5$) as well as after 120 hpi in hMDM II ($68.8\% \pm 6$) and hMDM I ($71.6\% \pm 70.8$) cells (**Figure 16A**).

Next, we investigated *Lae* amastigote infection in both macrophage phenotypes. In agreement with *Lm*, after 24 hpi, *Lae* amastigotes infected hMDM II ($79.5\% \pm 5.6$) significantly higher compared to the infection in hMDM I ($65.8\% \pm 10$) cells. Nevertheless, *Lae* infection significantly decreased over time in both cell types. (**Figure 16B**). Of note, after infection (24 hpi) of hMDM I and hMDM II, with either *Lm* or *Lae*, DiffQuick stainings were performed, of which representative micrographs are depicted (**Figure 16A-B**).

Taken together, both *Lm* and *Lae* amastigotes are able to initially infect hMDM II more efficiently compared to hMDM I. Over time, both hMDM cell types have an equal and stable *Lm* infection rate, whereas the *Lae* infection decreases.

Results

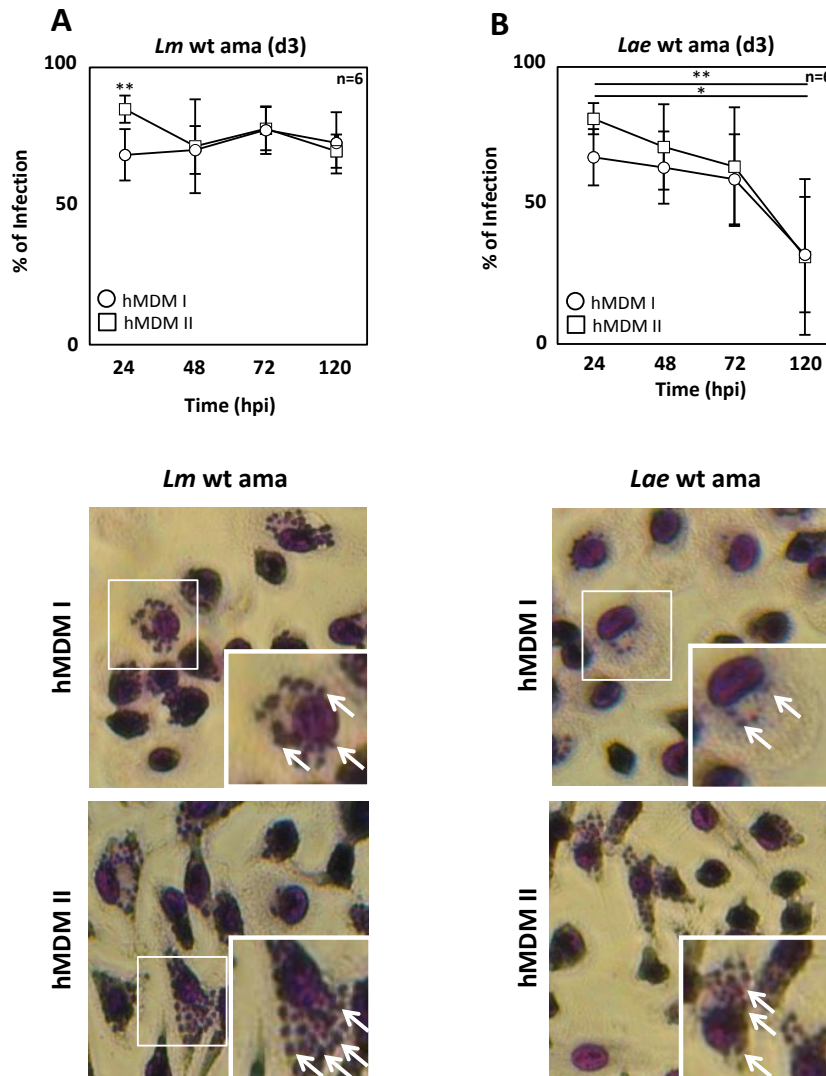


Figure 16: Infection of *Lm* and *Lae* amastigotes and analysis of infection over time in pro- and anti-inflammatory macrophages. Human macrophages, hMDM I (white circles) and hMDM II (white squares), were infected with *Lm* and *Lae* wild-type amastigote (MOI 10) and infection rates were measured from 24 hpi – 5 dpi by DiffQuick staining and microscopical assessment. Parasites are indicated by white arrows. (A-B) Quantification of *Lm* (A) and *Lae* (B) amastigote infection and parasite development in hMDM I and hMDM II at the indicated time points. Micrographs (24hpi) and data, presented as mean \pm SD, are representative of at least 3 independent experiments (*: $p < 0.05$; **: $p < 0.01$).

5.10 Expression of cell markers on hMDM I and hMDM II after *Lm* and *Ld* promastigote infection

Assessing the hMDM phenotypic markers (**Figure 17**), we found that the CD163 expression levels on hMDM II ($73.8\% \pm 3.1$) was decreased after infection with *Ld* ($37\% \pm 21.3$) and even more after infection with *Lm* ($14.8\% \pm 17.2$). In agreement, CD163 MFI on hMDM II after infection was reduced accordingly (**Figure 17A**). CD206, CR1 and CR3 expressions on both hMDM I and hMDM II did not change significantly by either *Lm* or *Ld* infection (**Figure 17B-D**).

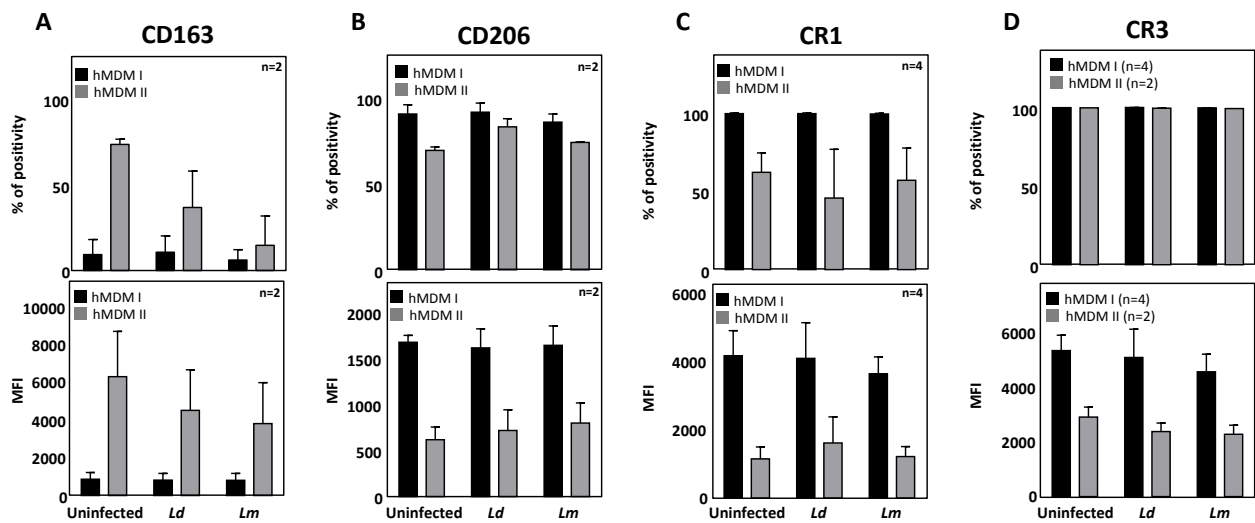


Figure 17: Expression of surface markers on hMDM I and hMDM II after *Leishmania* infection. The hMDM I (black bars) and hMDM II (grey bars) were infected with *Ld* and *Lm* promastigotes (MOI 10). After 3 hours, cells were washed and macrophages were further incubated. After 24 hpi, the surface expression of CD163, CD206, CR1 and CR3 was assessed using specific PE labeled antibodies and flow cytometry. (**A-D**) Quantification of marker positivity (% , upper row) and Mean Fluorescent Intensity (MFI, lower row) respectively of CD163 (**A**), CD206 (**B**), CR1 (**C**) and CR3 (**D**). Data are presented as mean \pm SD of 2 independent experiments for CD163 and CD206 and at least 3 independent experiments of CR1 and CR3.

5.11 Infection of hMDM I and hMDM II using fluorescent protein expressing *Lm* and *Lae* promastigotes

We could already demonstrate, by a microscopical analyses and subsequent quantification, that both the cutaneous *Leishmania* strains efficiently infect primary human macrophages. By DiffQuick staining however, both viable and apoptotic parasites are stained. To investigate parasite viability, we made use of transgenic parasites, as only the viable parasites express either the eGFP or DsRed transgenic protein, which can be quantified by FACS analysis (Stenger and van Zandbergen, 2011) . A representative histogram shows that the percentage of macrophages infected with viable *Lm* eGFP remains stable from 24 to 48 hpi. In contrast the number macrophages containing fluorescent and viable *Lae* eGFP is lower after 24 hpi and decreases at 48 hpi (**Figure 18A**). By quantifying infection rates, it could be indeed seen that *Lm* eGFP infection remained stable when comparing infection at 24 hpi (hMDM I: 34.1% \pm 3.2; hMDM II: 57.7% \pm 7.6) to 48 hpi (hMDM I: 38.2% \pm 6.2; hMDM II: 66.2% \pm 6.5). Interestingly, *Lae* eGFP, also causing cutaneous Leishmaniasis, was not able to sustain infection, resulting in a significant lower infection rate 48 hpi (hMDM I: 4.4% \pm 1.2; hMDM II: 9.3% \pm 1.3), as compared to 24 hpi (hMDM I: 12% \pm 1.6; hMDM II: 22.4% \pm 3.4) in pro-inflammatory macrophages. Moreover, *Lm* eGFP infection of macrophages was significantly higher compared to *Lae* eGFP infection (**Figure 18B-C**). Comparing DsRed expressing *Lm* with *Lae* in both hMDM I and II and sustainment of infection over time, we could show the results to be in line with the above data from eGFP expressing *Lm* and *Lae* (**Figure 18D-F**).

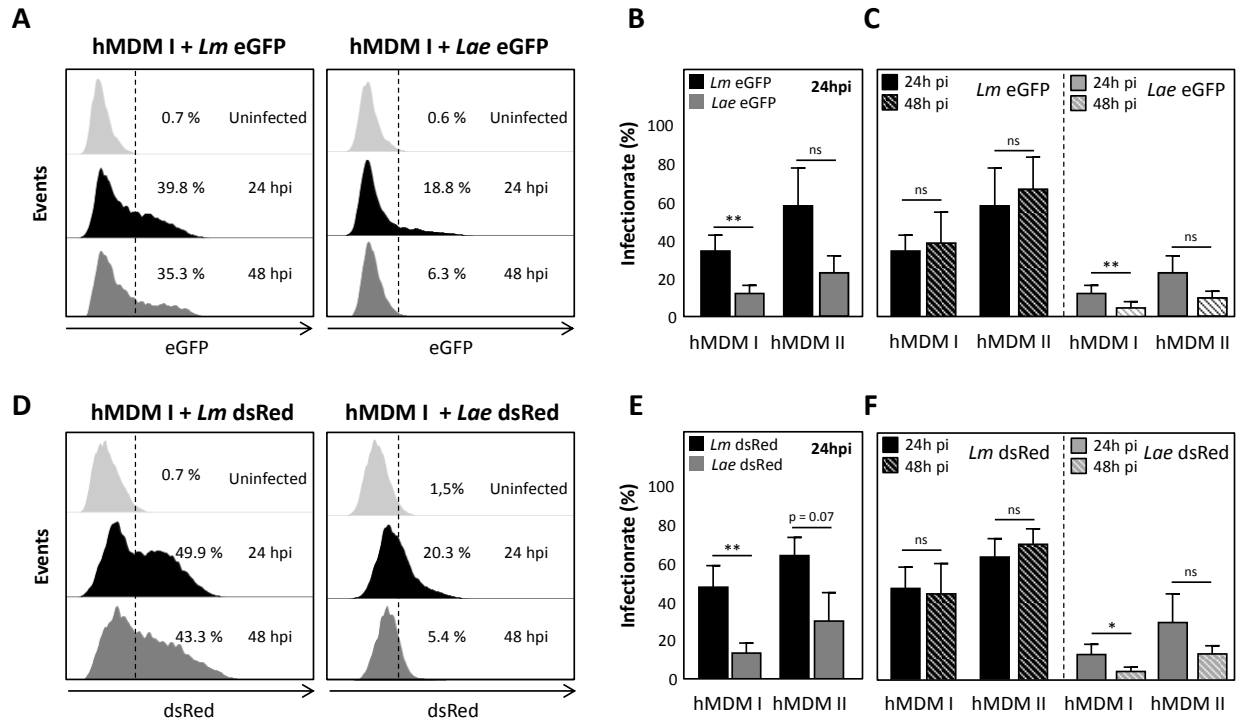


Figure 18: Infection and development of different transgenic *Leishmania* promastigote species in pro- and anti-inflammatory human macrophages. Human macrophages, hMDM I and hMDM II, were infected with transgenic *Lm* or *Lae* for 3 hours, after which extracellular parasites were removed by washing. Infection rates were assessed 24 hpi by flow cytometry. **(A, D)** Representative histograms, showing the infection rates of eGFP expressing *Lm* and *Lae* **(A)** and DsRed expressing *Lm* and *Lae* **(D)**. Histograms depicted uninfected hMDM I cells (light grey), 24 hpi (black) and 48 hpi (dark grey) **(B, E)**. Quantification of infection rates of transgenic *Lm* (black bars) **(B, E, *Lm* eGFP; E, *Lm* DsRed)** and transgenic *Lae* (grey bars) **(B, E, *Lae* eGFP; E, *Lae* DsRed)** in hMDM I and hMDM II, at 24 hpi. **(C, F)** Assessing infection rates of eGFP **(C)** and DsRed **(F)** expressing *Lm* (black bars) and *Lae* (grey bars) over time at 24 hpi (filled bars) and 48 hpi (dashed bars) in hMDM I and hMDM II. Data are presented as mean \pm SD of at least 3 independent experiments (* $p < 0.05$; ** $p < 0.01$; ns not significant).

5.12 Infection of hMDM I and hMDM II using fluorescent protein expressing *Lm* and *Lae* amastigotes

Although *Lm* and *Lae* promastigotes effectively infected macrophages, *Lae* promastigotes were not able to sustain infection. In a next step, we assessed both infectivity and persistence of infection of the amastigote life stage from both cutaneous *Leishmania* strains. Both hMDM I and hMDM II were infected with transgenic *Lm* and *Lae* amastigotes. After 24 hours, no differences in

Results

infection rates of *Lm* (hMDM I: 75.5% ± 9.4; hMDM II: 83.4% ± 4.8) and *Lae* (hMDM I: 67.9% ± 21.4; hMDM II: 81.9% ± 18.4) were observed (**Figure 19A**). Over time, *Lm* amastigotes were found to sustain infection (hMDM I: 76.6% ± 5.5; hMDM II: 83.2% ± 4.3). In contrast, infection with *Lae* amastigotes was reduced in hMDM I (53.5% ± 13.9) and remained stable in hMDM II (73.2% ± 22.4) (**Figure 19B**). Quantifying parasite load, by assessing the mean fluorescent intensity (MFI), both phenotypes of macrophages were found to harbor significantly greater numbers of *Lm* amastigotes (hMDM I: 14299.5 ± 6806.5; hMDM II: 18497.5 ± 8002.5), as compared to *Lae* amastigotes (hMDM I: 512 ± 152.5; hMDM II: 684.8 ± 197.6) (**Figure 19C**). Subsequently, amastigote load after 48 h was investigated. *Lm* amastigotes were able to sustain parasite load numbers in hMDM I (15870.8 ± 8851.4) and hMDM II (18103.8 ± 7378.7). A significantly lower amount of *Lae* amastigotes was observed 48 hours after infection in hMDM I (412.5 ± 102.9) and hMDM II (554.3 ± 297.2), compared to infection with *Lm* amastigotes. *Lm* amastigote infection was sustained over time while *Lae* amastigote parasites infection showed a tendency to decrease (**Figure 19D**). When comparing amastigote to promastigote parasites, we showed an increased infectivity and parasite load, as depicted for *Lm* (**Figure 19E**). Using fluorescent microscope, the increased parasite load and infection rate upon infection with *Lm* amastigotes, compared to promastigotes, could also be visualized (**Figure 19F-G**). Taken together, amastigote parasites infect both macrophage phenotypes more efficiently as compared to the promastigote stage. In agreement, we found that both stages of *Lm* are able to sustain infection over time while both promastigote and amastigote stages of *Lae* showed a decreased infection. Moreover, the parasite load of *Lm* amastigote was stable over time in comparison to *Lae* amastigote.

Results

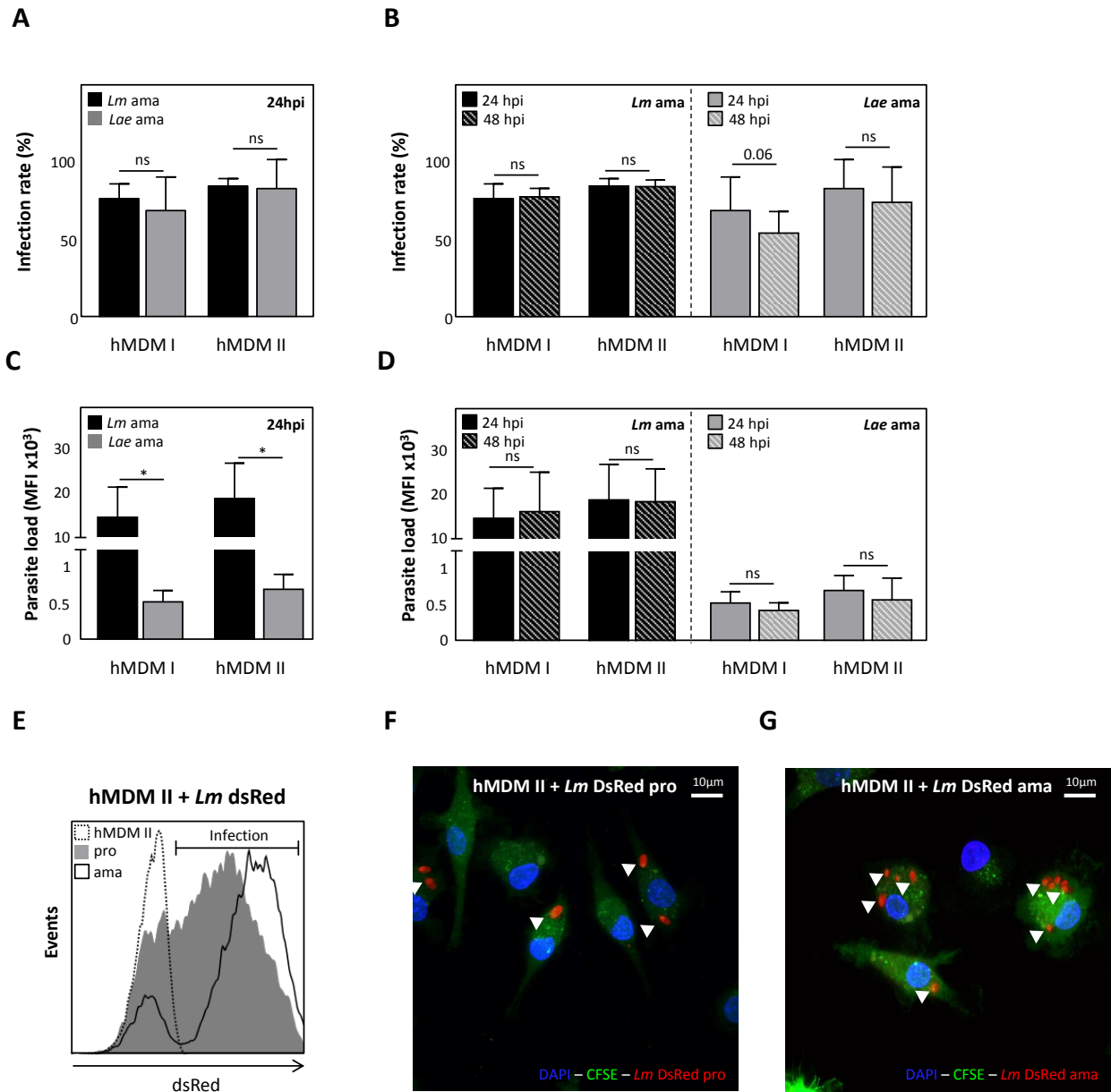


Figure 19: In contrast to *Lae*, *Lm* amastigotes establish a sustained infection in human primary macrophages. Human macrophages, hMDM I and hMDM II, were generated and infected with transgenic *Lm* and *Lae* amastigotes (MOI 10). After 3 hours, cells were washed and macrophages were further incubated for 24 h or 48 h after which infection rates were assessed by flow cytometry. Quantification of infection rates (**A**) and parasite load, as mean fluorescent intensity (MFI) (**C**) of transgenic *Lm* amastigote (black bars) and transgenic *Lae* amastigote (grey bars) in hMDM I and hMDM II, at 24 hpi. (**B**, **D**) Assessing infection rates (**B**) and parasite load (**D**) of transgenic *Lm* amastigote (black bars) and *Lae* amastigote (grey bars) over time at 24 hpi (filled bars) and 48 hpi (dashed bars) in hMDM I and hMDM II. (**E**) Representative histograms depicted an uninfected (dotted histogram) control and hMDM II cells 24 hpi after infection with either *Lm* promastigote (filled histogram) and amastigote (white histogram). (**F**, **G**) Live Cell Imaging analysis of transgenic *Lm* promastigote infection. The hMDM II were stained using Carboxyfluorescein succinimidyl ester (CFSE) and Hoechst. Next, cells were

infected using *Lm* DsRed promastigotes (**F**) or amastigotes (**G**) (MOI 10) for 3 hours and washed subsequently. After 24 hours, images were taken. Data, presented as mean \pm SD, and histograms are representative for at least 3 independent experiments (* $p < 0.05$; ns not significant).

5.13 High Throughput Screening in primary human macrophages and modulation of proteins, potentially involved in parasite uptake and/or control

To identify, both known and unknown proteins involved in uptake and control of *Leishmania* in macrophages, a siRNA screen was performed in the Scottish Bioscreening Facility in the University of Glasgow in cooperation with the group of Dr. Markus Meissner in the Division of Infection and Immunity in the Wellcome Center for Molecular Parasitology of the University of Glasgow (Glasgow, UK). Based on literature, a library of targets, focusing on surface markers and proteins involved in intracellular trafficking, was generated (**Table 2**). Accordingly siRNAs were designed to specifically enable mRNA knockdown and potentially subsequent protein downregulation in human primary macrophages in a 384 well based system. We used an automated liquid handling robot platform, Beckman BioMek FXp© and microscopical approach (GE IN Cell 2000) in a High Content Image Based Screening, to quantify the uptake of *Lm* parasites. The siRNA library was applied to the macrophages using the automated liquid handling robot platform able to optimize the entire process (**Figure 20A**). The death control was applied to cells in order to assure the successful siRNA transfection. After the siRNA knockdown was performed in macrophages and allowed to downregulate specific mRNA and protein for 4 days, macrophages were co-incubated with *Lm* using a multidrop system. Subsequent, washing of non-phagocytosed parasites was performed after 2 hpi using the liquid handling robot platform, Beckman BioMek FXp©. After 2 hpi, cells were stained for *Lm* infection. A minimal amount of 2000 macrophages were necessary to perform the analysis between the several targets. However, after each experiment, we observed less than 1000 cells in different wells. The intensity of the washing steps was reduced in order to minimize cell loss. After, such optimizations (**Figure 20B**), we compared a well transfected with the non-target siRNA to previous experiments (**Figure 20C**) and observed a higher number of cells, which however was

Results

difficult to reproduce. Next, non-representative wells of a 384 well normal assay plate (**Figure 20D**) were compared to the non-representative wells of a high binding plate (**Figure 20E**). In this trial, the number of adherent cells was higher in the Normal assay plates and the infection rate was lower in the High binding plates. Next, we compared different MOIs in order to analyze the effect of parasite infection on the macrophage adherence to plastic. In only a few wells (non-representative) enough amounts of cells, infected with MOI 10 (**Figure 20F**) and MOI 20 (**Figure 20G**), were observed. The low numbers of cells was observed in random wells and was not related to any specific target effect. In all, after several trials and optimizations, no substantial data was obtained from the experiments and the correct analysis was not possible to be performed.

| | | | | | | | | | |
|--------------|---------|----------|---------|----------|---------|---------|---------|---------|---------|
| CD197 | ITGA5 | ITGAL | ITGAV | ITGAX | PDGF-Ra | PDGF-Rb | ADIPOR1 | ADIPOR2 | CD13 |
| Fibro-nectin | VEGFRa | CD331 | CD332 | CD333 | CD334 | CD317 | GPR13 | ITGB1 | ITGB2 |
| ITGB3 | ITGB5 | BAI1 | CLCA | CHC | ENG | LRP1 | NGFR | PTGER2 | NRAMP1 |
| VTN | STAB2 | TIMD4 | CLEC1A | CLEC2B | CLEC2Da | CLEC3B | CLEC4F | CLEC4G | CLEC10A |
| CR1 | MERTK | CAMP | CTSB | CTSD | CTSS | LAMP1 | LAMP2 | RAB5A | RAB7A |
| EEA1 | BECN1 | MAP1LC3B | CD200R1 | GPR114 | MSR1 | GPR120 | AFI-1 | CB2 | CSF1 |
| GJA1 | IGF1 | IKBKB | LBP | LGALS3BP | LTF | MAL | MAOB | CD136 | B220 |
| FCGBP | PGLYRP1 | CH25H | IL1RL1 | P2RY14 | CLEC4M | CLEC5A | CLEC4E | CLEC4K | CLEC4A |
| CLEC1B | SIGIRR | CLEC7A | COL23A1 | CLEC6A | SIRPA | TRIF | CLEC12A | CLEC4C | CLEC9A |
| CLEC6 | TRAM | CLEC12B | CD192 | CD192 | CD195 | BMPR1A | BMPR1B | BMPR2 | CAV1 |
| CAV2 | CAV3 | CD14 | SCARB1 | SCARB2 | CDH5 | CDH17 | CD191 | CD36 | CD115 |
| CD116 | CD131 | EDNRB | EGFR | CD32 | FCGR3A | FCGR3B | IL1R1 | TNF | IL1RAP |
| IL10RA | INSR | CD11B | ITGB2 | CD206 | CD204 | TGFBR1 | TGFBR2 | TGFRB3 | TLR1 |
| TLR2 | TLR3 | TLR4 | TLR5 | IL1R2 | CXCR4 | MARCO | IL1RL2 | CD163 | CD280 |
| TLR6 | NOD1 | CD85 | CD209 | TLR7 | TLR8 | GPRC5B | TLR9 | TLR10 | |

Table 2 – Representation of the siRNA library containing macrophage surface markers and molecules involved in cell trafficking.

Results

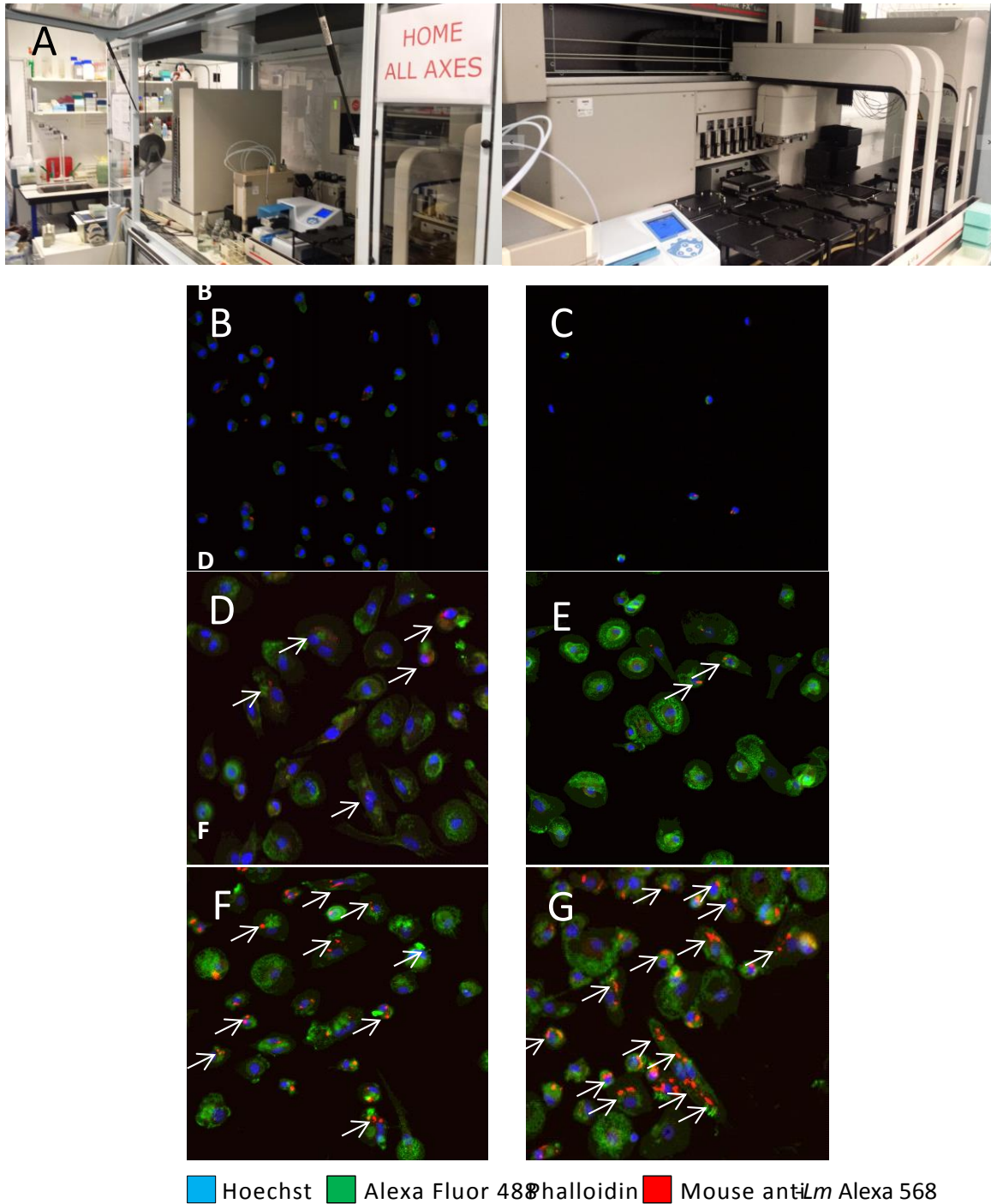


Figure 20: High Throughput Screening in primary human macrophages. siRNA library was added to the macrophages in a 384 well plate using the liquid handling robot platform, Beckman BioMek FXp©. After transfection with siRNAs, macrophages were infected with *Lm* wild-type (white arrows). After 2 hpi, macrophages were washed to remove extracellular parasites. Next, cells were stained using Hoechst (blue staining for the cell nucleus) and Alexa Fluor 488 Phalloidin (green staining for cell cytoplasm). *Leishmania* parasites were stained using Mouse anti-*Lm* Alexa 568 (red). (A) Automated system responsible for adding siRNA library and to perform the washing steps. (B) Normal amount of cells needed to perform a reliable analysis. (C) Amount of cells usually obtained after the experiments (D)

Normal assay plate containing macrophages infected with *Lm* parasites. (E) High binding plate after siRNA transduction and *Lm* infection. (F) Normal assay plate containing macrophages infected with *Lm* (MOI 10). (G) Normal assay plate containing macrophages infected with *Lm* (MOI 20).

5.14 Modulation of CR1 and CR3 using siRNA approach

Independent of the siRNA screen we used a single target siRNA approach in order to specifically target the CR1 and CR3 receptor to generate hMDM I and hMDM II knockdown cells. Upon treatment with CR1 siRNAs, we achieved a knockdown efficiency of 87% in hMDM I (**Figure 21A**). Consequently, we observed a decrease in the surface expression of the CR1 protein, assessed by flow cytometry (**Figure 21B**). In hMDM II cells, an efficiency of 88.4% was reached (**Figure 21C**) and a significant decrease in the surface expression of CR1 protein was observed (**Figure 21D**).

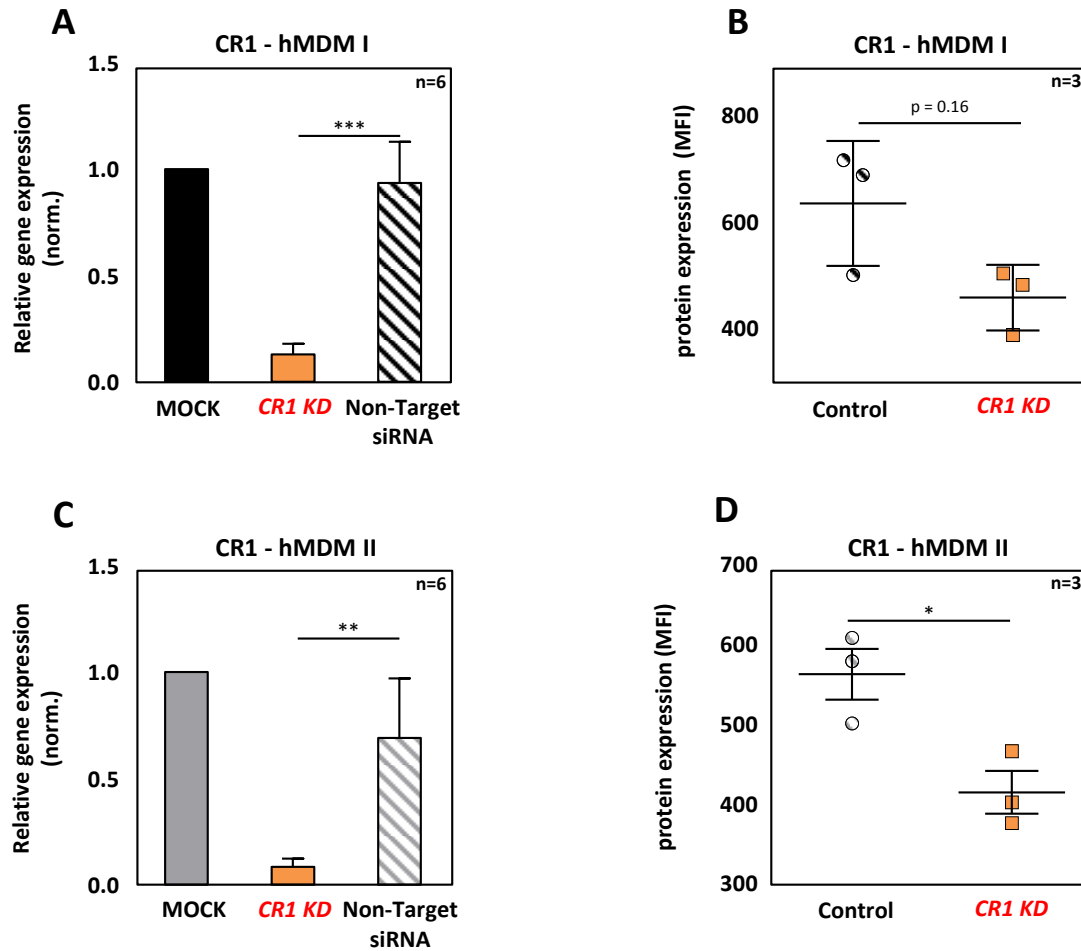


Figure 21: Knockdown efficiency and expression levels of CR1 in hMDM I and hMDM II after siRNA treatment. The hMDM I and hMDM II were transfected with specific siRNAs designed against CR1. After 48 h of transfection, cells were harvested for RNA isolation and flow cytometry analysis. (A, C) After cDNA synthesis, relative gene expression was analyzed by qRT-PCR. (B, D) Protein expression (MFI) of CR1 was analyzed by flow cytometry on hMDM I and hMDM II. Data are presented as mean \pm SD of at least 3 independent experiments (*: $p < 0.05$; **: $p < 0.01$; ***: $p < 0.001$).

A similar knockdown efficiency was observed after treatment with CR3 siRNAs in hMDM I (**Figure 22A**) followed by a significant reduction of surface expression of CR3 protein (**Figure 22B**). In line, a good knockdown efficiency was observed in hMDM II cells (**Figure 22C**) as well as the reduction of CR3 protein expression (**Figure 22D**).

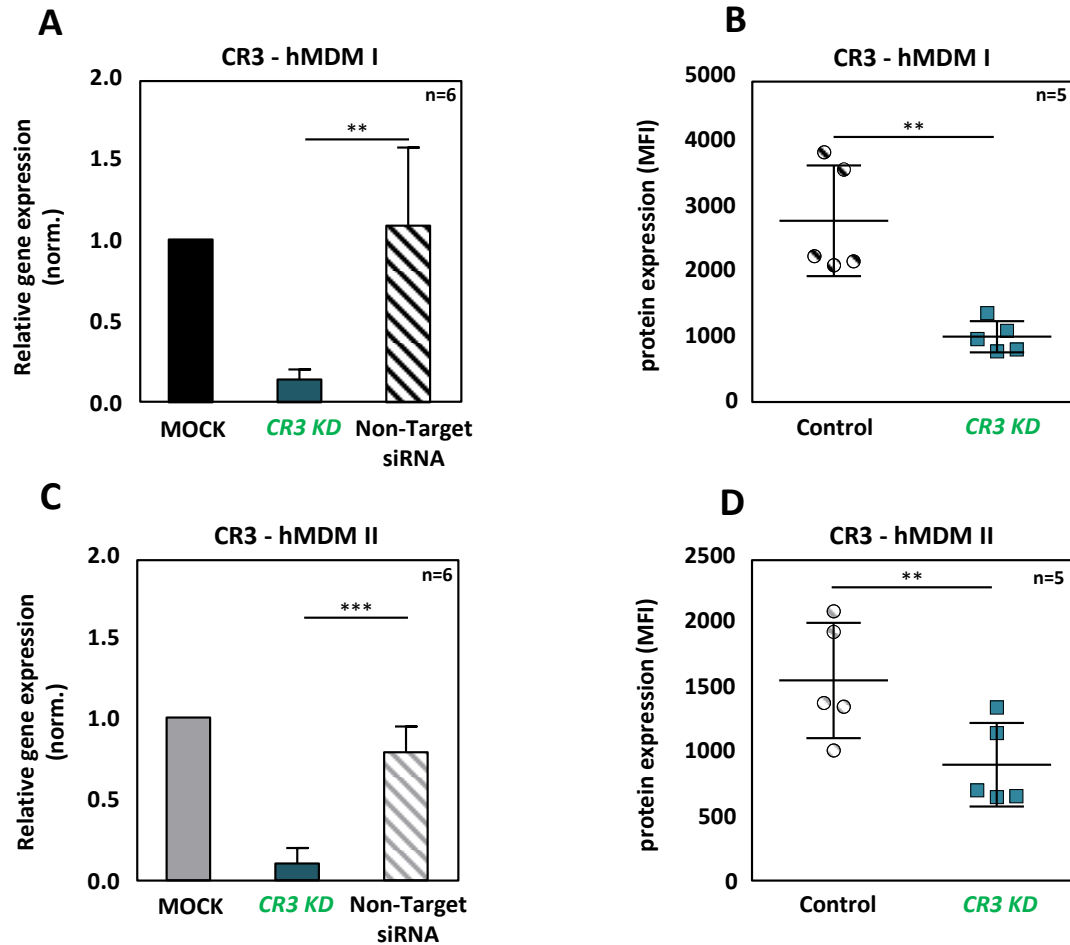


Figure 22: Knockdown efficiency and expression levels of CR3 in hMDM I and hMDM II after siRNA treatment. The hMDM I and hMDM II were transfected with specific siRNAs designed against CR3. After 48 h of transfection, cells were harvested for RNA isolation and flow cytometry analysis. (A, C) After cDNA synthesis, relative gene expression was analyzed by qRT-PCR. (B, D) Protein expression (MFI) of CR3 was analyzed by flow cytometry on hMDM I and hMDM II. Data are presented as mean \pm SD of at least 3 independent experiments (**: $p < 0.01$; ***: $p < 0.001$).

Next, knockdown macrophages were used in infection experiments to assess uptake of *Lm* wild-type. *Leishmania* infection was assessed by fluorescent microscopy. We found that CR1 knockdown in hMDM I resulted in a reduced uptake ($22.1\% \pm 0.6$) of *Lm* parasites, whereas this effect was not observed in hMDM II cells ($-1.6\% \pm 1.3$). By microscopical analysis, we were able to visualize the inhibitory effect on the parasite uptake by hMDM I which could not be seen in hMDM II treated cells (Figure 23A-B).

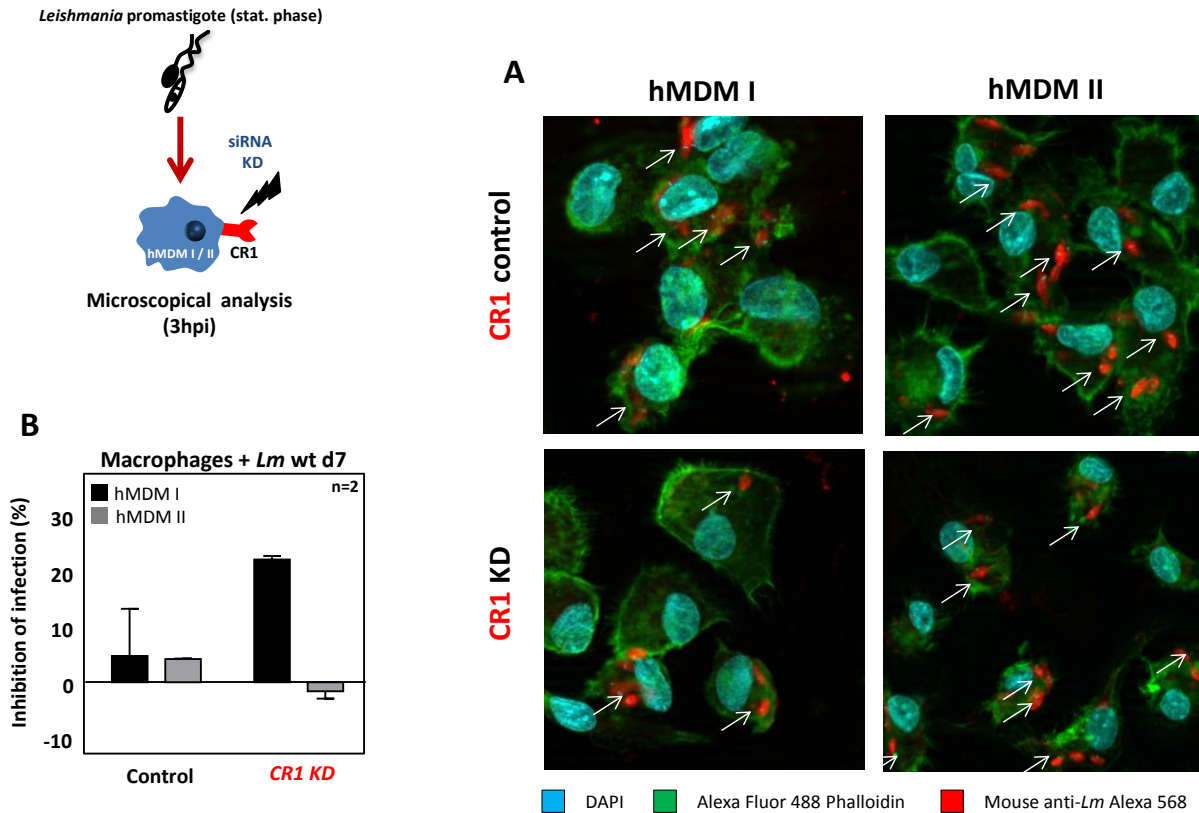


Figure 23: Effect of the CR1 KD on the uptake of *Leishmania* parasites after infection of hMDM I and hMDM II. Cells were treated using CR1 siRNAs or Non-Target control siRNA. After 48 h, cells were infected with *Lm* wild-type (MOI 10). After 3 hours, cells were washed and stained using DAPI (blue staining for the cell nucleus) and Alexa Fluor 488 Phalloidin. *Leishmania* parasites were stained using Mouse anti-*Lm* Alexa 568. **(A)** Representative immunofluorescence pictures of infected CR1 knockdown cells and cells treated with control siRNA. **(B)** Quantification of the infection rate in hMDM I (black bars) and hMDM II (grey bars) after CR1 knockdown by microscopical assessment. Data are presented as % inhibition, and depicted as mean \pm SD. Data and micrographs are representative and of 2 independent experiments.

Similar experiments were performed using both hMDM I and hMDM II, treated with siRNAs targeting CR3 mRNA. The microscopical quantification showed a reduction in the uptake of *Lm* by hMDM I (22.3% \pm 10.1), while a minor effect was found in the parasite uptake by hMDM II (7.2% \pm 8) **(Figure 24A-B)**.

In all, using a siRNA knockdown approach in hMDM I and hMDM II, we were able to reduce the expression of CR1 and CR3 on both gene and protein levels in primary human macrophages, reducing parasite uptake by hMDM I cells.

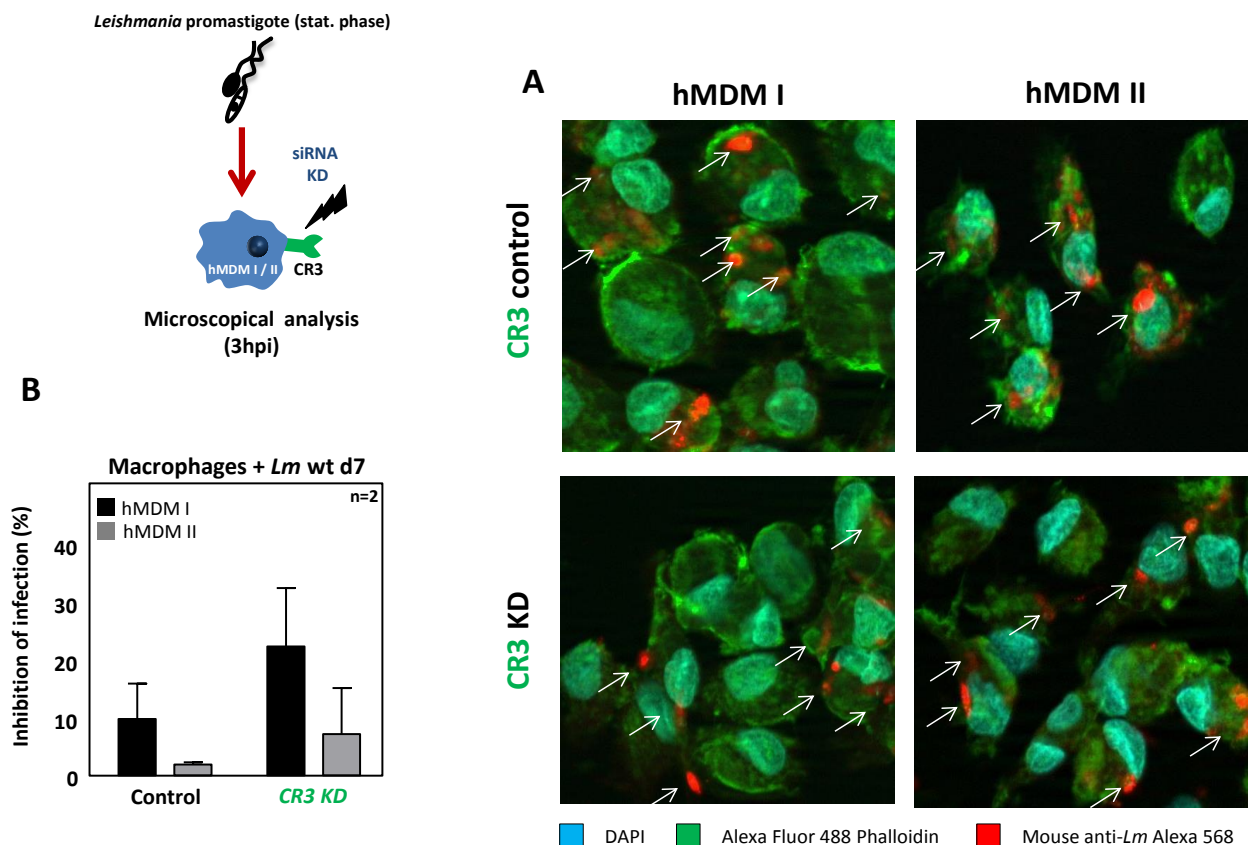


Figure 24: Effect of the CR3 KD on the uptake of *Leishmania* parasites after infection of hMDM I and hMDM II. Macrophages were treated with CR3 siRNAs or the Non-Target siRNA control for 48 h. Macrophages were infected with *Lm* wild-type (MOI 10). After 3 hours, cells were washed and stained using DAPI (blue staining for the cell nucleus) and Alexa Fluor 488 Phalloidin (green staining for cell cytoplasm). *Leishmania* parasites were stained using Mouse anti-*Lm* Alexa 568 (red). (A) Representative pictures of infected CR3 knockdown cells and cells treated with control siRNA. (B) Quantification of infection rate in hMDM I (black bars) and hMDM II (grey bars) by microscopical assessment. Data are presented as % inhibition, and depicted as mean \pm SD. Data and micrographs are representative and of 2 independent experiments.

5.15 Blocking of CR1 and CR3 using specific blocking antibodies

Using siRNA knockdown approach in hMDM, we demonstrated that CR1 and CR3 are involved in *Leishmania* uptake by hMDM I and hMDM II. In a next step, we used specific antibodies to block either CR1 or CR3 to confirm their role in both *Lm* and *Ld* uptake. After treatment with specific α -CR1 antibody, we observed an inhibition in the uptake of *Lm* parasites by hMDM I ($11.6\% \pm 9$) as compared to hMDM II ($-13.3\% \pm 13.7$). In addition, we found an inhibition in the uptake of *Ld* by

Results

hMDM II ($11.4\% \pm 2.2$) as compared to hMDM I ($-2\% \pm 15.4$) (Figure 25A). Using specific α -CR3, we found a significant inhibition on the uptake of *Lm* parasites by hMDM II ($8.6\% \pm 9.6$) (Figure 25B).

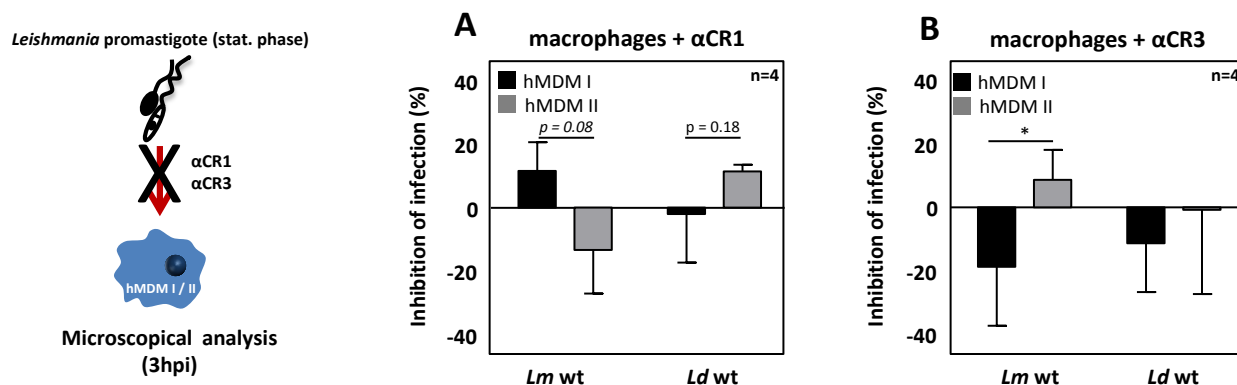


Figure 25: CR1 and CR3-mediated phagocytosis of *Leishmania* is species-specific and macrophage phenotype dependent. Both hMDM I (black bars) and hMDM II (grey bars) were co-incubated with *Lm* or *Ld* (MOI 10) after treatment with α -CR1 and α -CR3 antibodies or the respective isotype controls. After 3 hours, cells were washed and stained using Diff-Quick. The infection rates were quantified by microscopical analysis. (A-B) Quantification of the inhibition of *Lm* and *Ld* uptake by hMDM I and hMDM II after blocking of CR1 (A) or CR3 (B). The reduction in the parasite uptake is presented as % of inhibition. Data are presented as mean \pm SD of at least 3 independent experiments (*: p < 0.05).

5.16 The uptake of *Lm* and *Lae* is hMDM phenotype, parasite-stage and receptor dependent

In addition to comparing *Lm* with *Ld* promastigotes, we investigated the effect on the uptake of promastigote and amastigote stages from both cutaneous strains after blocking CR1 and CR3 on hMDM I and hMDM II (Figure 26). After treatment with α -CR1 antibody we showed a higher inhibition on the uptake of *Lm* promastigote ($16.4\% \pm 4.5$) and *Lae* amastigote ($15\% \pm 9.2$) by hMDM I (Figure 26A). The blocking of CR3 on hMDM I showed an inhibition in the uptake of *Lm* amastigote ($18.1\% \pm 4.6$) and *Lae* ($10.2\% \pm 1.4$) amastigote (Figure 26C). Analyzing hMDM II, the

Results

blocking of CR3 showed to inhibit the uptake of *Lm* promastigote ($15.6\% \pm 5.3$) and to significantly reduce the uptake of *Lae* promastigote ($12.9\% \pm 2.7$). (Figure 26D).

Blocking of CR1 on hMDM I inhibited the uptake of *Lm* promastigote and *Lae* amastigote. Uptake of *Lm* and *Lae* amastigotes was inhibited after blocking CR3 on hMDM I while the uptake of the promastigote form is CR3 dependent only in hMDM II. Since the effect of blocking CR1 and CR3 was only tested using wild-type parasites, we performed further experiments using fluorescent protein expressing parasites.

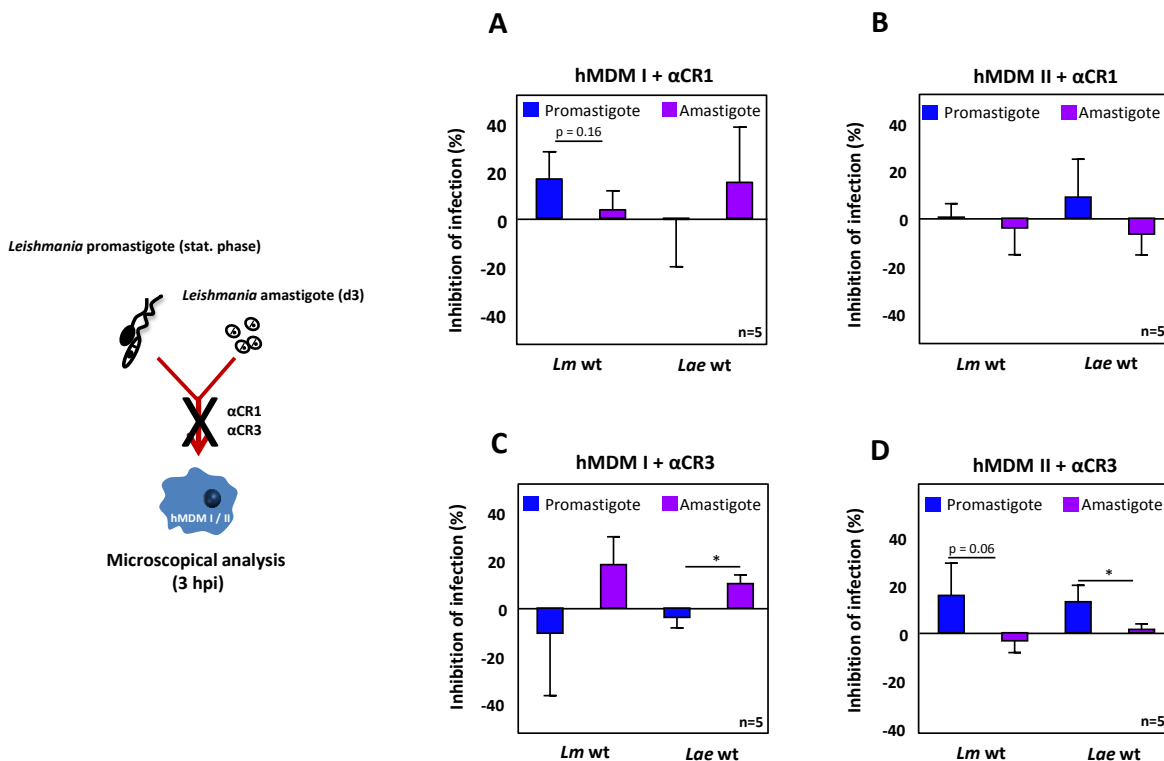


Figure 26: Phagocytosis of *Leishmania* is species/stage-specific and macrophage phenotype dependent after blocking of CR1 and CR3. The hMDM I and hMDM II were pre-incubated with α -CR1 and α -CR3 antibodies or the respective isotype controls preceding the *Leishmania* infection with *Lm* and *Lae* wt promastigotes (blue bars) and amastigotes (pink bars) (MOI 10). After 3 hours, cells were washed and stained using Diff-Quick. Infection rate was quantified by microscopical analysis. The reduced parasite uptake is presented as % of inhibition. (A-D) Inhibition of *Lm* and *Lae* pro and amastigote uptake after blocking CR1 (A, B) and CR3 (C, D) by hMDM I and hMDM II respectively. Data are presented as mean \pm SD of at least 3 independent experiments (*: $p < 0.05$).

5.17 Uptake of fluorescent protein expressing *Lm* and *Ld* promastigote is inhibited after blocking CR1 on hMDM I

To quantify the effect of CR1 and CR3 blocking on the uptake of fluorescent parasites by FACS we used eGFP-expressing *Lm* and *Ld* (Figure 27). A higher inhibition in the uptake of *Lm* was observed after blocking CR1 on hMDM I ($17\% \pm 4.3$) (Figure 27A). Blocking of CR3 did not inhibit *Lm* and *Ld* uptake by both type of macrophages.

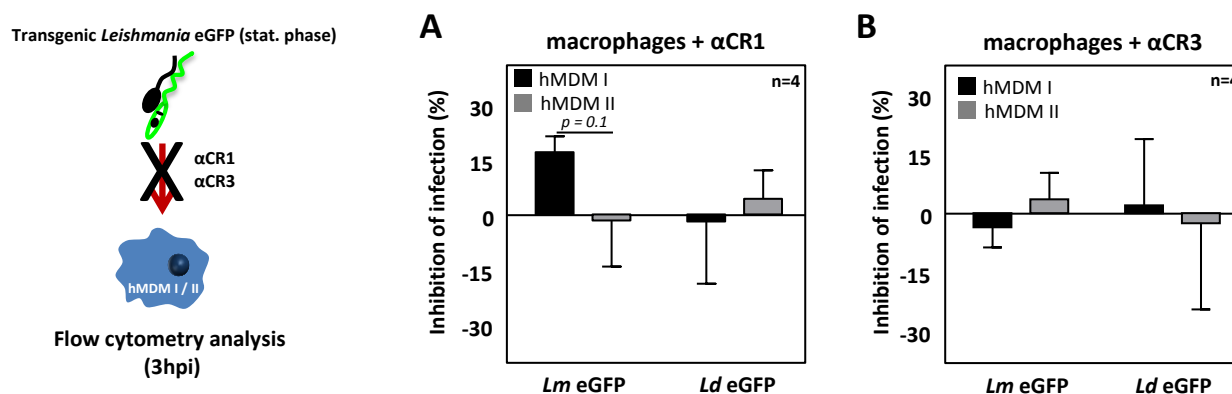


Figure 27: CR1 and CR3-mediated phagocytosis of eGFP-expressing *Lm* and *Ld* is species-specific and macrophage phenotype dependent. The hMDM I (black bars) and hMDM II (grey bars) were pre-incubated with α -CR1 and α -CR3 antibodies and the respective isotype controls. Cells were infected with transgenic *Lm* eGFP and *Ld* eGFP promastigotes (MOI 10). After 3 hours, parasite uptake was assessed by flow cytometry and the % of inhibition in uptake was calculated. (A-B) Quantification of the inhibition of *Lm* eGFP and *Ld* eGFP uptake by hMDM I and hMDM II cells after blocking of CR1 (A) or blocking of CR3 (B). Data are presented as mean \pm SD of at least 3 independent experiments.

Using both siRNA knockdown of CR1 and CR1 specific blocking antibodies, we found that uptake of *Lm* promastigotes in hMDM I is reduced. Now we investigated the consequence of CR1 specific blocking on sustainment of infection and parasite development. Using the transgenic parasites, uptake was measured after 3 hpi and parasite survival after 7 dpi. Comparing hMDM I cells treated with α -CR1 ($47.2\% \pm 11.2$) with isotype control ($50.4\% \pm 12.9$) we observed a very minor but significant reduction in the infection rate (Figure 28A). In concordance, taking the MFI as an indicator for parasite load, we found that CR1 blocking resulted in a minor but significant decrease in parasite numbers inside hMDM I (Figure 28C). 7 days later we found that the infection rate significantly increased when comparing α -CR1 ($37.6\% \pm 14.3$) with the isotype

Results

(27.4% ± 10.4) treated hMDM I (**Figure 28B**). In concordance, parasite load also increased significantly after CR1 blocking (**Figure 28D**). Taken together, we showed that the blocking of CR1 on pro-inflammatory human macrophages has a clear beneficial effect on *Lm* survival even after the inhibition of parasite uptake.

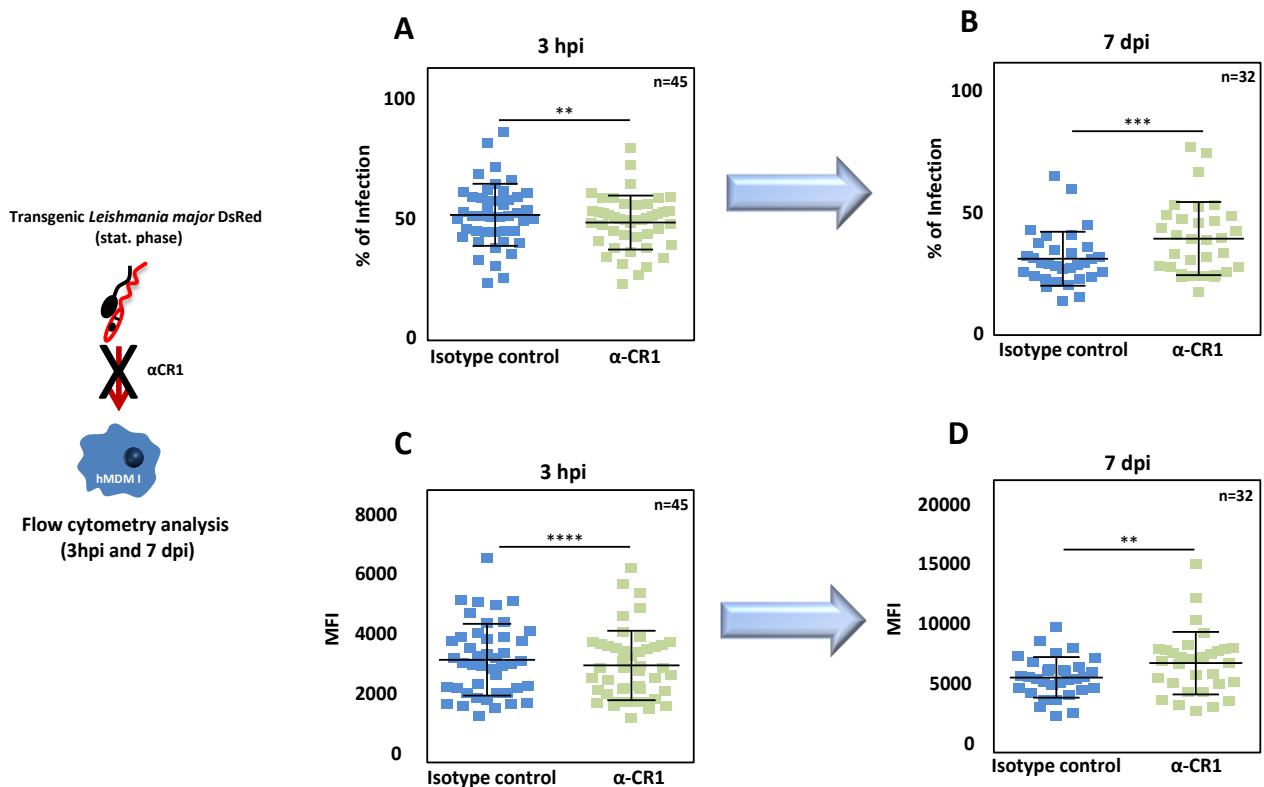


Figure 28: Uptake and intracellular survival of *Lm* DsRed after blocking of CR1 on hMDM I cells. The hMDM I were pre-incubated with an isotype control (blue squares) or α -CR1 specific antibody (green squares) before infection with *Lm* DsRed (MOI 5). Macrophages were washed and extracellular parasites were removed after 3 hpi. Subsequently cells were further incubated for 7 days in order to assess parasite intracellular survival or used for analysis (3hpi). Uptake and survival were measured by assessing the infection rate (%) and parasite load (MFI) by flow cytometry analysis. (**A-D**) Quantification of infection rates (**A, B**) and MFI (**C, D**) of hMDM I, after CR1 blocking, at 3hpi and 7dpi, respectively. Data are presented as mean \pm SD of at least 3 independent experiments (**: $p < 0.01$; ***: $p < 0.001$; ****: $p < 0.0001$).

5.18 Effect of CR1 blocking on the intracellular survival of *Ld* parasites in hMDM I

Blocking of CR1 on hMDM I appeared to have no effect on *Ld* promastigote uptake. Now we assessed the effect of CR1 blocking on *Ld* eGFP uptake (3 hpi) and survival (7 dpi) in hMDM I macrophages (**Figure 29**). We observed similar infection rates and parasite load when comparing cells treated with α -CR1 with cells treated with isotype control (**Figure 29A, C**). Interestingly, at 7 dpi infection rates significantly increased with α -CR1 (26.6% \pm 5.3) compared to isotype control (8.7% \pm 1.8) treated cells whereas the parasite load after CR1 blocking remained equal to isotype treated control cells (**Figure 29B, D**).

In all, blocking of CR1 on hMDM I cells does not affect the development of *Ld* parasites.

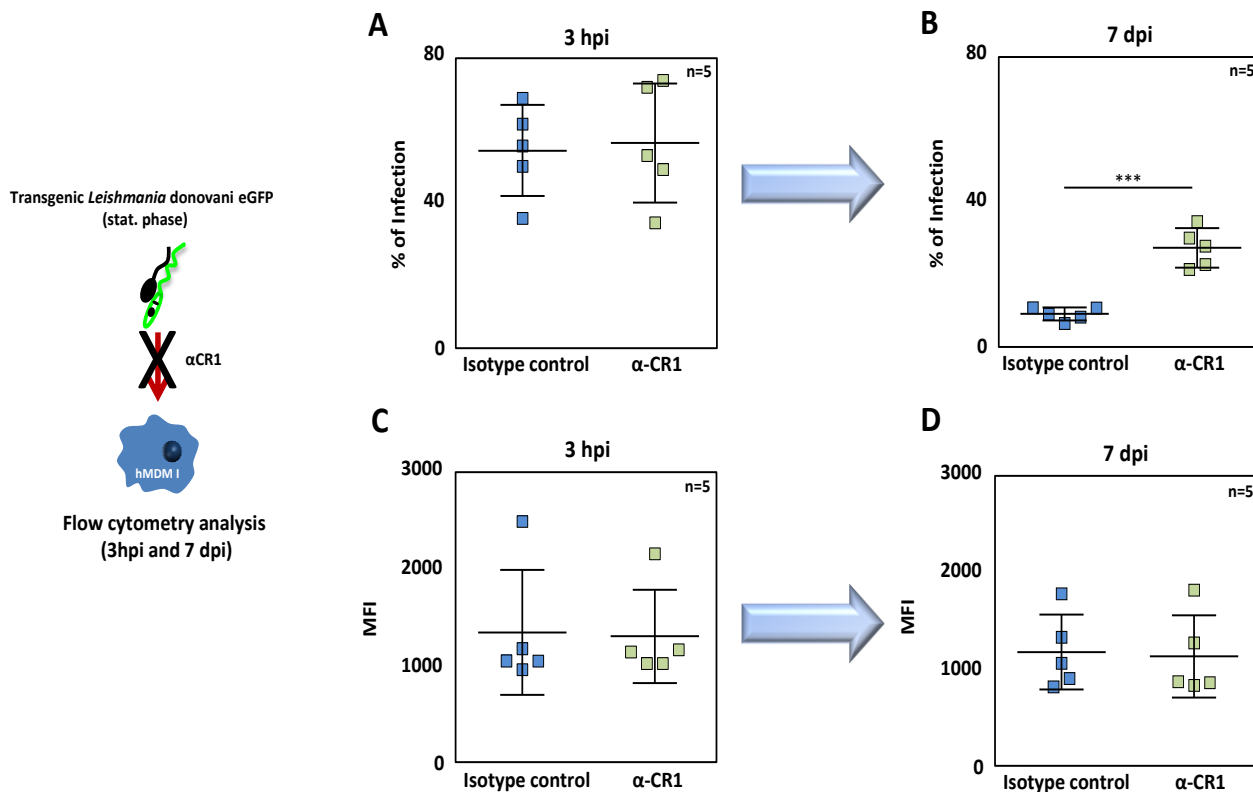


Figure 29: Effect of blocking CR1 on the uptake and intracellular survival of *Ld* eGFP in hMDM I cells. The hMDM I were pre-incubated with an isotype control (blue squares) or α -CR1 specific antibody (green squares) and infected *Ld* eGFP (MOI 5). After 3 hpi, cells were washed and extracellular parasites

were removed for measurement of parasite uptake. Cells were further incubated for 7 days in order to assess parasite intracellular survival. Uptake and survival were measured by assessing the number of infected cells (%) and parasite load (MFI) by flow cytometry analysis. (A-D) Quantification of infection rates (A, B) and MFI (C, D) of hMDM I, after CR1 blocking, at 3hpi and 7dpi, respectively. Data are presented as mean \pm SD of at least 3 independent experiments (***: $p < 0.001$).

5.19 Assessment of *Lm* survival in hMDM I based on stage specific gene expression

Next, we analyzed *Lm* intracellular development by measuring specific gene expression of amastigote parasites. For *Lm* parasites, we investigate the relative gene expression of the already mentioned glycoprotein 63 (GP63), ABC homologue transporter (ABC), as amastigote specific genes, and the small hydrophilic ER-associated protein (SHERP) as the promastigote specific gene. Gene expression was measured after 3 hpi and 7 dpi. The gene expression of ABC after 7 dpi showed to be statistically higher in hMDM I pretreated with α -CR1 (2 ± 0.9) compared to the cells treated with isotype control (0.7 ± 0.2) (**Figure 30A**). In agreement, GP63 gene expression was found to be statistically upregulated after 7 dpi in hMDM I after blocking of CR1 (1.2 ± 0.6) in comparison to cells treated with isotype control (0.5 ± 0.2) (**Figure 30B**). Unexpectedly, the gene expression of SHERP, a promastigote specific gene, was upregulated after 7 dpi in α CR1 treated hMDM I (2.2 ± 1.5) compared to isotype control treated cells (1.3 ± 0.6) (**Figure 30C**). Next, gene expression of Cysteine Peptidase and Alkyl dihydroxyacetone phosphate were analyzed. We found Cysteine Peptidase to be upregulated after blocking of CR1 (1.4 ± 0.5) (**Figure 30D**) in comparison to isotype control treated cells (0.8 ± 0.4). Contrary, no differences were observed in the relative gene expression of Alkyl dihydroxyacetone phosphate (**Figure 30E**). Taken together, the blocking of CR1 on hMDM I cells leads to an increase of amastigote specific gene expression, confirming the effect of CR1 on parasite development inside hMDM I cells.

Results

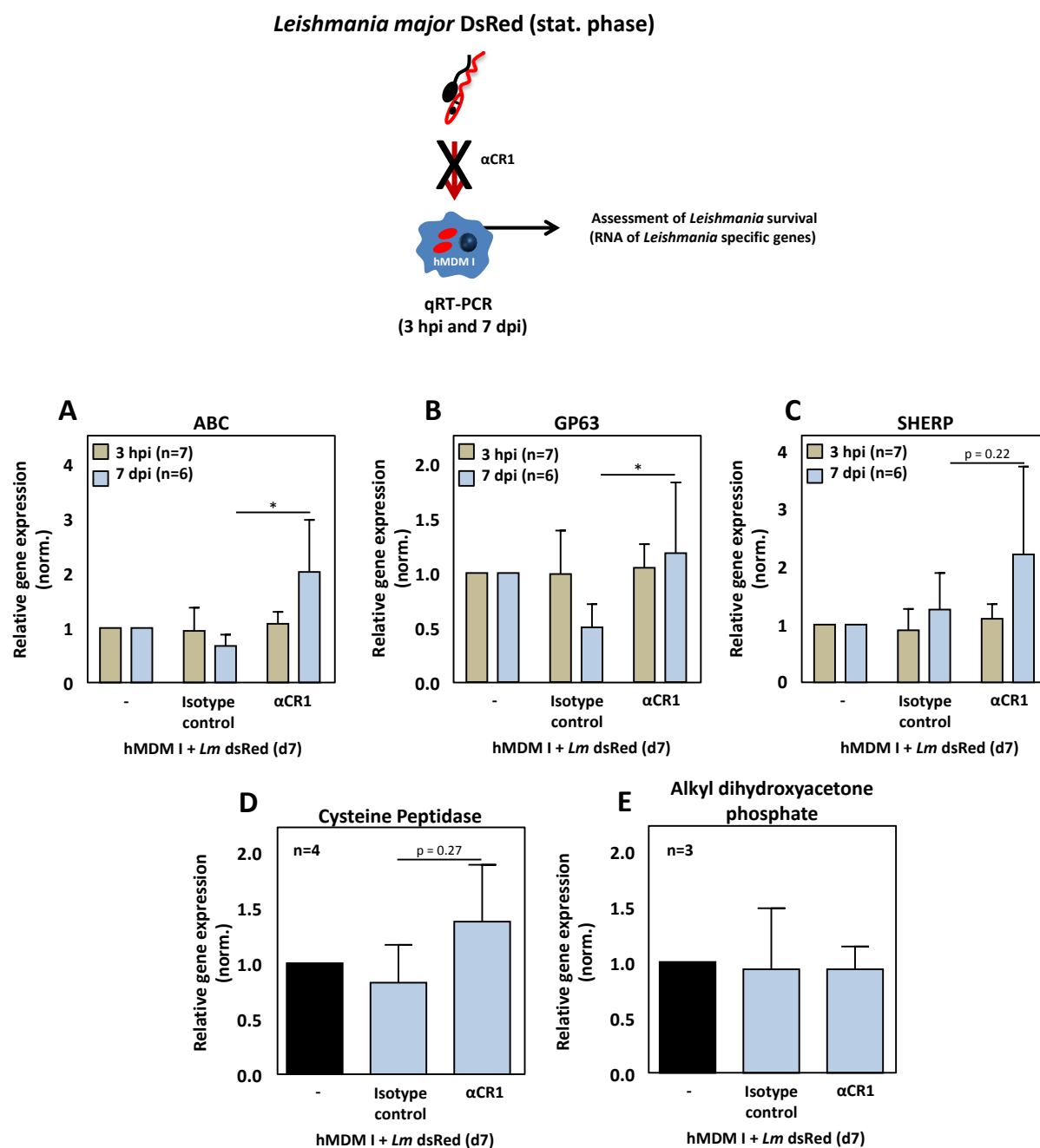


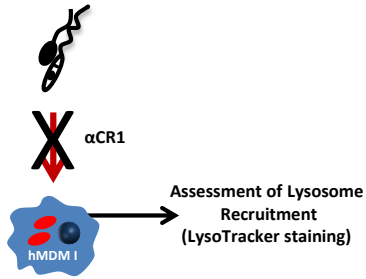
Figure 30: Assessing relative gene expression of *Leishmania* stage specific genes after CR1 blocking on hMDM I cells during infection. The hMDM I were pre-treated with either isotype control or α -CR1 preceding infection with *Lm* DsRed, MO110. (A-E) After 3h (brown bars), cells were used for RNA isolation or further cultivated for 7 days (blue bars), after which RNA was isolated. By qRT-PCR gene expression of ABC (A), GP63 (B), SHERP (C), Cysteine Peptidase (D) and Alkyl dihydroxyacetone phosphate (E) were assessed. The relative gene expression was calculated based on the *Leishmania* housekeeping gene rRNA45 and normalized against the relative gene expression obtained from the infected hMDM I. Data are presented as mean \pm SD of at least 3 independent experiments (*: $p < 0.05$).

5.20 Lysosomal recruitment in pro-inflammatory cells is increased after CR1 blocking

In addition to the parasite development analysis, the lysosomal recruitment was also measured. Initially, the presence/acidification of lysosomes was assessed in untreated and uninfected hMDM I and hMDM II, by flow cytometry using LysoTracker staining. We found a stronger LysoTracker positivity in hMDM II (11.3 ± 5.3) compared to hMDM I (8.1 ± 1.1) (**Figure 31A**). Next, the LysoTracker staining was repeated in infected hMDM I previously treated with α -CR1 or isotype control antibody. After 24 h infection, hMDM I was incubated with LysoTracker[®] Red DND-99 and the MFI was analyzed by FACS. We observed a stronger LysoTracker positivity in infected hMDM I pre-treated with α -CR1 (14.9 ± 2.5) when compared to isotype treated cells (10.5 ± 3) (**Figure 31B**). A representative picture of hMDM I is depicting the presence of lysosomes stained with LysoTracker[®] Red DND-99 post CR1 blocking and *Lm* infection (**Figure 31C**). Similar results were observed after lysosome staining using LysoTracker[®] Green DND-26 (**Figure 31D**). A representative picture of hMDM I is depicting the presence of lysosomes stained with LysoTracker[®] Green DND-26 post CR1 blocking and *Lm* infection (**Figure 31E**). In all, we found the lysosomal recruitment to be higher in hMDM II compared to hMDM I. A higher lysosomal recruitment was also observed in hMDM I after the blocking of CR1.

Results

Leishmania (stat. phase)



Flow cytometry analysis
(24 hpi)

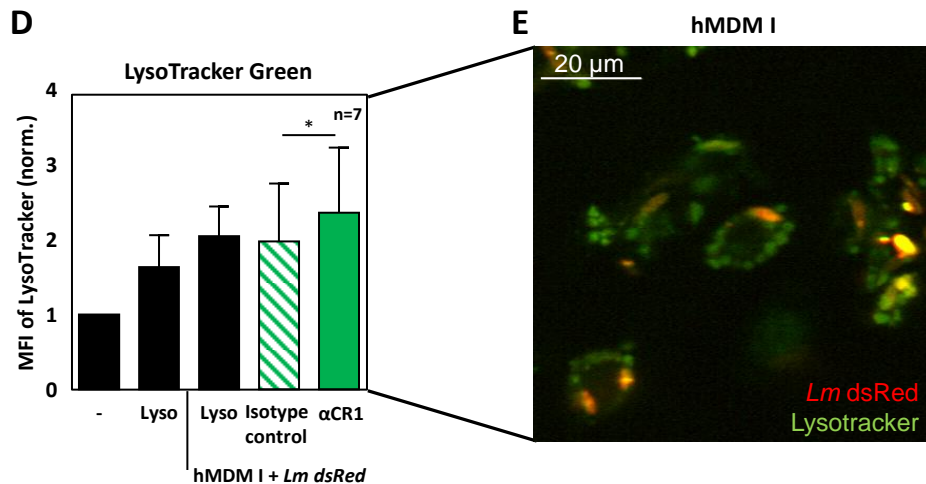
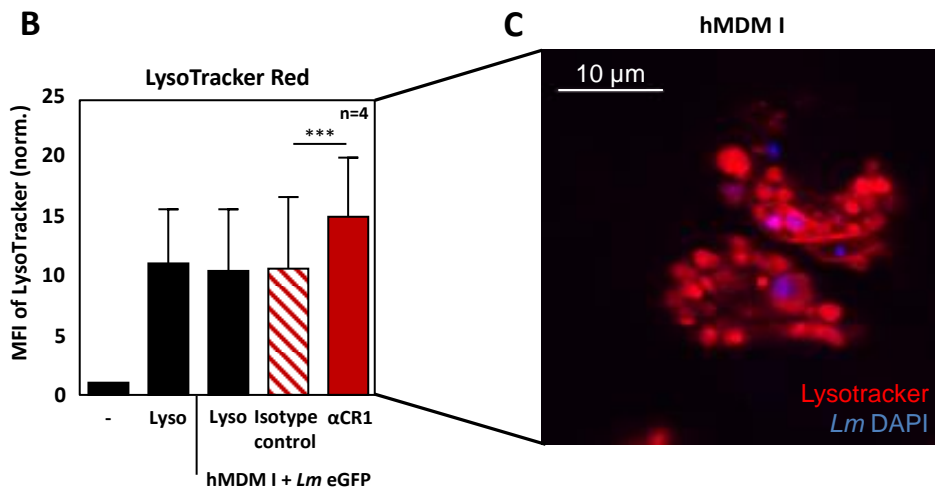
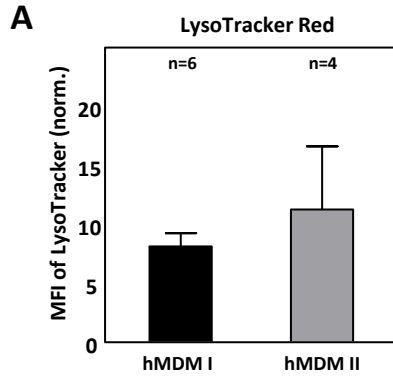


Figure 31: Assessing lysosomal acidification/recruitment in infected hMDM I after blocking of CR1 using LysoTracker® Red DND-99 and LysoTracker® Green. (A) Both hMDM I and hMDM II were stained with LysoTracker® stains for 15 min at 37°C. Subsequently, cells were washed and the MFI of the LysoTracker staining was measured by flow cytometry. The MFI of the LysoTracker staining in hMDM I (black bar)

and hMDM II (grey bar). **(B-D)** The hMDM I were pretreated with an isotype control (dashed colored bars) or α -CR1 (colored bar) and infected with transgenic *Lm* parasites. After 24 hpi LysoTracker staining was performed using either LysoTracker® Red DND-99 **(B)** or LysoTracker® Green DND-26 **(D)**. After washing, the MFI was assessed by flow cytometry and normalized against the MFI of untreated cells. In addition, fluorescent micrographs **(C, E)** were made, in which DAPI was used to counterstain the nuclei. Data are presented as mean \pm SD of at least 3 independent experiments (*: $p < 0.05$; ***: $p < 0.001$).

5.21 Blocking of CR1 on hMDM I and its effect on the gene expression of molecules involved in phagolysosome maturation

To elucidate on the intracellular mechanism, responsible for parasite survival inside macrophages, we assessed the gene expression, involved in cell activation and phagosomal maturation, after CR1 blocking and *Leishmania* infection of hMDM I.

Gene expression of Cathepsin D, Synaptotagmin XI, ULK1 and LL-37 were measured after blocking CR1 on hMDM I. Gene expression of α -CR1 treated hMDM I was compared to isotype control treated cells after 3 hpi and 7 dpi. No differences were found regarding the expression of Cathepsin D at 3 hpi as well as at 7 dpi **(Figure 32A)**. The gene expression of Synaptotagmin XI after 7 dpi was significantly increased in α -CR1 (3.7 ± 0.7) treated hMDM I in comparison to the isotype control (2.3 ± 0.6) treated hMDM I **(Figure 32B)**. The autophagy related gene, ULK1, was found to be significant higher expressed in α -CR1 (5.2 ± 2.7) treated cells when comparing to treatment using isotype control (3 ± 0.6) after 7 dpi **(Figure 32C)**. In agreement, similar results were observed for LL-37, being upregulated in α -CR1 (9.6 ± 8.8) pretreated hMDM I compared to the isotype control (4.2 ± 2.1) after 7 dpi **(Figure 32D)**.

Taken together, we demonstrated that CR1 plays a role in the gene expression of molecules involved in phagosomal maturation and cell activation.

Results

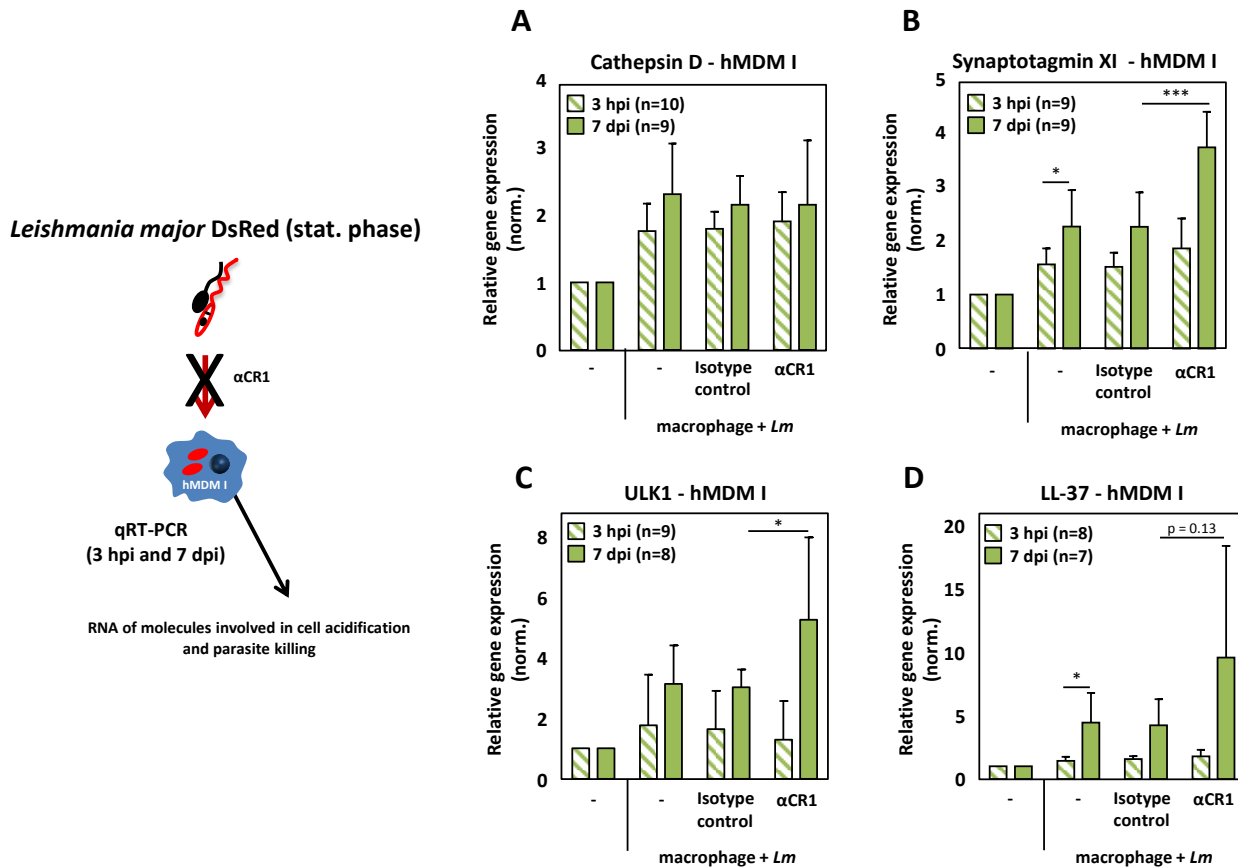


Figure 32: Relative gene expression of host cell genes involved in the phagolysosome formation after CR1 blocking and *Leishmania* infection. The hMDM I were pre-incubated with α-CR1 or isotype control previously infection with *Lm* DsRed, MOI10. (A-C) After 3h (dashed bars), cells were used for RNA isolation or further cultivated for 7 days (full bars), after which RNA was isolated. By qRT-PCR gene expression of Cathepsin D (A), Synaptotagmin XI (B), ULK1 (C) and LL-37 (D) was assessed. The relative gene expression was calculated based on the hMDM housekeeping gene GAPDH and normalized against the relative gene expression obtained from the uninfected hMDM I. Data are presented as mean ± SD of at least 3 independent experiments (*: p<0.05; ***: p<0.001).

6. DISCUSSION

Different *Leishmania* species are responsible for causing distinct clinical manifestations and even death in humans worldwide. The reason why individuals develop such mild or severe disease is not clear and is dependent on the parasite's virulence, in combination with the immunological status of human host, resulting in either disease susceptibility or disease control. In this study we hypothesize that *Ld*, causing visceral Leishmaniasis, presents a higher infectivity, being able to establish a stronger and more sustained infection in macrophages compared to cutaneous Leishmaniasis causative strains. Focusing on the parasite's host cell, the macrophage, we hypothesize that CR1-mediated phagocytosis is responsible for *Leishmania* killing.

Investigating the infectivity of different *Leishmania* promastigote species, we found *Ld* to infect human primary macrophages to a much lower degree, compared to *Lm* and *Lae*. Furthermore, *Lae* and *Ld* infection is decreased while *Lm* infection remained stable over time. In line, *Lm* amastigotes established a sustained infection, in contrast to *Lae* amastigotes, of which infection rates dropped over time. Of note, independent of the parasite species, hMDM II showed to be more susceptible to infection, with either promastigotes or amastigotes, as compared to hMDM I cells. The human macrophages, hMDM I and hMDM II were further characterized and defined to be CR1^{high} and CR1^{low}, respectively. By using specific siRNAs, targeting CR1 mRNA, we demonstrated CR1 to be involved in *Lm* uptake by hMDM I. Furthermore, CR1 mediated phagocytosis led to parasite elimination, as siRNA treatment or α -CR1 antibodies, increased parasite survival inside the macrophages. Gene expression analysis showed an upregulation of amastigote specific genes, nevertheless also host specific genes involved in lysosomal recruitment and acidification were found to be upregulated.

6.1 *Leishmania* and macrophage interaction

We found that visceral Leishmaniasis causative strain *Ld*, establishes a weaker and decreasing infection in human macrophages compared to *Lm* and *Lae* strains. Wilson et al. already showed that *Ld* progress from a virulent to an attenuated state during *in vitro* cultivation. In here, the

Discussion

virulence factor GP63 is affected, leading to an alternative attachment of parasites to human monocyte derived macrophages (Wilson et al., 1989). These data support our finding, that blocking CRs did not influence the uptake of *Ld* parasites. Live attenuated *Ld* parasites were also shown to induce a stronger pro-inflammatory response in murine macrophages, compared to wild-type *Ld* (Bhattacharya et al., 2015). This response was characterized by a classically activated macrophage phenotype, which is playing a crucial role in disease protection in BALB/c mice. Regarding the amastigote life stage, also differences in the parasite's virulence was observed. The group of G. Späth demonstrated an increased survival of hamster-derived compared with axenic parasites (Pescher et al., 2011). One could speculate that our *Leishmania donovani*, which are cultivated *in vitro*, lost their virulence and can be considered to be attenuated, explaining their reduced infectivity profile. Various virulence factors could be analyzed, e.g. GP63, but also expression of the A2 gene. The A2 gene is required for survival in visceral organs by *Ld*, which is only partially present in parasites like *Lm*, causative for cutaneous Leishmaniasis. Future experiments should focus on determining the presence or loss of virulence factors, to explain the reduced infectivity of *Ld*, compared to *Lm* and *Lae*.

Between the species *Lm* and *Lae*, both responsible for cutaneous Leishmaniasis, also strong differences in infectivity were observed. One would hypothesize that species, causing the same disease form, to interact similarly with the host. However, *Lm* strongly differs from *Lae* on a genetic level. Schönian et al. even revealed a strong genetic heterogeneity among several parasites strains of the same species (Schönian et al., 2000). Furthermore, cutaneous Leishmaniasis comprises a variety of clinical manifestations. Most patients have localized cutaneous Leishmaniasis, displaying either single or multiple skin lesions, in contrast to the more severe diffuse cutaneous Leishmaniasis (Carrada et al., 2007) . Therefore it may also not be unexpected that also differences in infectivity between *Lm* and *Lae* occur.

Focusing on the human host cell, the macrophage, we found an alteration of the macrophages' polarization status upon infection. *Ld* is able to down regulate the expression of CD163 on anti-inflammatory macrophages. A similar finding was observed after infection with *Lm*. Both cutaneous and visceral Leishmaniasis causative species were responsible to induce a change from anti- to a pro-inflammatory macrophage phenotype. It was already reported that

macrophages can change their functional phenotypes according to environmental influences (Stout et al., 2005). In line, it was showed that macrophage adopt an anti-inflammatory profile after phagocytosis of myelin, indicating that macrophage polarization may occur in both directions (Bogie et al., 2013). We observed this phenomenon only with regard to CD163, as this protein is exclusively expressed on anti-inflammatory cells. Previous work, in our group, showed also the cytokine secretion (TNF, IL10, IL12) to change towards a M1-polarisation, confirming the data presented in this work (Bank et al., unpublished).

6.2 Stage specific gene expression in *Lm* parasites

Previous work, obtained in our group, already demonstrated that the proteins Adenylate Kinase, Calpain Peptidase, Metallo Peptidase and Surface Antigen protein to be specifically upregulated in the promastigote life stage. On the other hand, Alkyl Dihydroxyacetone Phosphatase and Cysteine Peptidase were specifically upregulated during the amastigote life stage. In line with the protein data, we could show also the gene expression to be regulated in a stage specific manner. The stage specific markers are in line with other scientific reports. Kemp et al. also described the *Leishmania* surface antigen, to be promastigote specific, even playing an important antigen, able to trigger a Th1-mediated protection when used in vaccines (Kemp et al., 1998). In agreement, a drastically increase in *Leishmania* promastigote surface antigen from exponentially growing to stationary phase parasites was detected by Devault et al. (Devault and Bañuls, 2008). This overexpression of promastigote surface antigen proteins could even be linked to the virulence status of the parasites, as passaging cultures *in vitro* was shown to reduce this phenomenon (Beetham et al., 2003). One could conclude that surface antigen protein is indeed a good promastigote marker, and a potential indicator for parasite virulence in our *Lm* culture. Our findings for Adenylate Kinase are in agreement with Villa et al., which showed that this protein is present in the promastigote stage, especially in the parasite glycosomes (Villa et al., 2003). Moreover, Adenylate plays a role in the ATP-regenerating system required for flagellar movements, which would only make sense in promastigotes, not in amastigotes (Ginger et al.,

2005). On the other hand, Zufferey et al. suggested Alkyl Dihydroxyacetone Phosphatase to have an additional function in amastigote survival and infectivity as well as during lipophosphoglycan (LPG) and smaller glycosylinositolphospholipids (GIPLs) synthesis (Zufferey et al., 2003). Cysteine Peptidase is the best characterized peptidases in the genus *Leishmania* (Caroselli et al., 2012). In macrophages infected with *L. mexicana* amastigote, this protein is associated with inhibition of IL-12 production (Cameron et al., 2004). For other *Leishmania* species, Cysteine Peptidase is also considered a virulence factor that allows the parasite survival inside phagosome compartments of macrophages (Denise et al., 2006; Lima, A P C A et al., 2013). Our findings concerning to stage specific gene expression of *Leishmania* parasites are in agreement with what was found in previous studies and allows us to use these targets as *Leishmania* stage specificity markers.

6.3 The role of CR1 in *Leishmania major* survival inside human inflammatory macrophages

The blocking of CR1 on pro-inflammatory human macrophages resulted in a reduced *Lm* uptake followed by an increased parasite survival/development. These data are in line with results of Da Silva et al., showing a detrimental role for complement receptors in the uptake of *Leishmania* parasites. Nevertheless, CR1-mediated uptake of metacyclic promastigotes did not generate a respiratory burst, after which the authors speculated that CR1 usages may facilitate the parasite's subsequent intracellular survival (Da Silva et al., 1989). In contrast, Wright and Silverstein reported neither the CR ligands C3b nor C3bi to release ROS species, even in conditions in which phagocytosis was strongly promoted (Wright and Silverstein, 1983). Our data fit the latter finding, as under these circumstances an increased parasite survival would occur.

Also the host's gene expression profile was analyzed. After blocking of CR1 on pro-inflammatory macrophages, we observed an increase in the gene expression of molecules related with cell activation such as Synaptotagmin XI, LL-37 and ULK1. First we analyzed Synaptotagmins, a group of membrane-associated proteins that regulate vesicle-associated processes (Pang and Südhof, 2010). In mouse macrophages, the recruitment of Synaptotagmin V to the nascent phagosome

Discussion

was impaired by *Leishmania* LPG, resulting in a reduction in the phagocytic capacity of host macrophages (Vinet et al., 2011). The work of Duque et al. showed Synaptotagmin XI to be excluded from the parasitophorous vacuole. Subsequently Synaptotagmin XI was degraded in a GP63-dependent manner, followed by an increased secretion of TNF and IL6. The authors also showed that the intracellular survival of *E. coli* is increased after knockdown of Synaptotagmin XI (Arango Duque et al., 2014). Recent literature, describes Synaptotagmin XI to play a predominantly pro-inflammatory role. During blocking of CR1 however, we observed an increased parasite survival, and against our expectations an increased Synaptotagmin XI expression. In a next step, an increased protein expression should be assessed, by e.g. western blot analysis. Of note, mRNA levels were significantly increased, but not in strong amounts, which may indicate that Synaptotagmin XI is not playing such a crucial role in parasite elimination in our experimental setup. Our next target, ULK1, also known as ATG1, plays a central role in starvation induced autophagy (Wong et al., 2014). ULK1 was described as being responsible for phosphorylation of beclin-1 and activation of vsp34 which leads to the induction of the autophagy process (Russell et al., 2013). Host cell autophagy machinery has been used by intracellular pathogens in order to increase their intracellular survival and long term infection (Skendros and Mitroulis, 2012). Crauwels et al. showed that the autophagy machinery is able to enhance *Leishmania* survival in human macrophages (Crauwels et al., 2015). Our data are in concordance, as the *Leishmania* parasites take advantage of the host's autophagy machinery to increase their survival and by the fact that the blocking of CR1 increase ULK1 gene expression in pro-inflammatory macrophages. Both phagosomes and autophagosomes and their dynamics are of great importance during *Leishmania* development. We also investigated the expression of cathelicidins, which may remain inside these compartments. Cathelicidins are suggested to be an effective anti-Leishmaniasis therapeutic approach by reducing parasite viability within a macrophage infection model (Lynn et al., 2011). Rivas-Santiago et al. showed a high expression of LL-37 in alveolar macrophages after TLR-9 activation with *Mycobacterium tuberculosis* (Rivas-Santiago et al., 2008). Moreover, LL-37 was showed to specifically kill *Leishmania* promastigotes and to negatively regulate parasite survival in pro-inflammatory macrophages (Bank, unpublished). After blocking CR1, also LL-37 was found to be upregulated 7 days after infection.

Discussion

As for Synaptotagmin XI, LL-37 was significantly upregulated on mRNA level, but also present in small absolute numbers, after which one could ask the question, are these differences biologically relevant. A next step would be to first check the protein amount, to make certain that the targets are of biological relevance. Furthermore, it may be speculated that the upregulation of these pro-inflammatory molecules is due to the amastigote re-infection which also may occur 7 days post infection. The amastigote development was verified by the upregulation of the amastigote stage specific genes, ABC, GP63 and Cysteine Peptidase.

7. CONCLUDING REMARKS

In this PhD work we aimed to elucidate on the fact why distinct species are responsible for different clinical manifestations. We could demonstrate that the responsible *Leishmania* species have their own unique growth characteristics and are able to infect human primary macrophages. Nevertheless, the degree of infectivity, as also the sustainment of infection is different between *Leishmania* species which cause visceral or cutaneous Leishmaniasis.

Focusing on the human host cell, the macrophage, we could identify CR1 as a marker of pro-inflammatory macrophages. The CR3 was found on both pro- and anti-inflammatory macrophages. The anti-inflammatory macrophages were also more susceptible for infection, which phenotype repolarizes in some extent to a more pro-inflammatory phenotype upon infection. Independent of the macrophage phenotype, *Lm* was able to sustain infection, whereas both *Lae* and *Ld* infection rates decreased over time.

With regard to hMDM I and *Lm*, we demonstrated CR1-mediated phagocytosis to be disadvantageous for parasite survival. Upon blocking CR1-mediated uptake, fewer parasites were internalized; however, parasite survival was dramatically increased over time. Of note, the pro-inflammatory status, focusing on the gene expression of ULK1, LL-37 and Synaptotagmin XI, was increased.

Future research will help us to increase our knowledge and to further elucidate on host pathogen interactions, focusing on (a) interspecies differences, causing distinct clinical manifestations and (b) how CR1-mediated phagocytosis of *Leishmania*, lead to parasite elimination.

8. FIGURE AND TABLE LIST

| | | |
|-------------------|---|------|
| Figure 1: | Distribution of cutaneous Leishmaniasis worldwide according to WHO report of 2015 | p 20 |
| Figure 2: | Distribution of mucocutaneous Leishmaniasis in the New World according to WHO report | p 21 |
| Figure 3: | Distribution of visceral Leishmaniasis worldwide according to WHO report of 2015 | p 22 |
| Figure 4: | Life cycle of <i>Leishmania</i> parasite | p 24 |
| Figure 5: | Fluorescent staining of a pro-inflammatory type 1 macrophage (left) and an anti-inflammatory type 2 macrophage (right) | p 25 |
| Figure 6: | Representation of <i>Leishmania</i> parasite uptake by macrophage based on the set of expressed receptors | p 28 |
| Figure 7: | Phenotypical characterization of human macrophages | p 62 |
| Figure 8: | Assessment of the expression levels of CR1 and CR3 on hMDM I and hMDM II | p 64 |
| Figure 9: | Restriction fragment length polymorphism of different <i>Leishmania</i> species | p 65 |
| Figure 10: | Growth kinetics and morphology profile of distinct <i>Leishmania</i> promastigote species | p 67 |
| Figure 11: | Growth kinetics and morphology analysis of the amastigote stage of different <i>Leishmania</i> species | p 69 |
| Figure 12: | <i>Leishmania</i> promastigote stage specific gene expression | p 70 |
| Figure 13: | <i>Leishmania</i> amastigote stage specific gene expression | p 71 |
| Figure 14: | Relative gene expression of <i>Leishmania</i> stage specific genes after infection of hMDM I cells | p 73 |
| Figure 15: | Infection and development of different <i>Leishmania</i> promastigote species in pro- and anti-inflammatory human macrophages | p 76 |
| Figure 16: | Infection of <i>Lm</i> and <i>Lae</i> amastigotes and analysis of infection over | p 78 |

time in pro- and anti-inflammatory macrophages

- Figure 17:** Expression of surface markers on hMDM I and hMDM II after *Leishmania* infection p 79
- Figure 18:** Infection and development of different transgenic *Leishmania* promastigote species in pro- and anti-inflammatory human macrophages p 81
- Figure 19:** In contrast to *Lae*, *Lm* amastigotes establish a sustained infection in human primary macrophages p 83
- Figure 20:** High Throughput Screening in primary human macrophages p 86
- Figure 21:** Knockdown efficiency and expression levels of CR1 in hMDM I and hMDM II after siRNA treatment p 88
- Figure 22:** Knockdown efficiency and expression levels of CR3 in hMDM I and hMDM II after siRNA treatment p 89
- Figure 23:** Effect of the CR1 KD on the uptake of *Leishmania* parasites after infection of hMDM I and hMDM II p 90
- Figure 24:** Effect of the CR3 KD on the uptake of *Leishmania* parasites after infection of hMDM I and hMDM II p 91
- Figure 25:** CR1 and CR3-mediated phagocytosis of *Leishmania* is species-specific and macrophage phenotype dependent p 92
- Figure 26:** Phagocytosis of *Leishmania* is species/stage-specific and macrophage phenotype dependent after blocking of CR1 and CR3 p 93
- Figure 27:** CR1 and CR3-mediated phagocytosis of eGFP-expressing *Lm* and *Ld* is species-specific and macrophage phenotype dependent p 94
- Figure 28:** Uptake and intracellular survival of *Lm* DsRed after blocking of CR1 on hMDM I cells p 95
- Figure 29:** Effect of blocking CR1 on the uptake and intracellular survival of *Ld* eGFP in hMDM cells p 96
- Figure 30:** Assessing relative gene expression of *Leishmania* stage specific genes after CR1 blocking on hMDM I cells during infection p 98

- Figure 31:** Assessing lysosomal acidification/recruitment in infected hMDM I after blocking of CR1 using LysoTracker® Red DND-99 and LysoTracker® Green p 100
- Figure 32:** Relative gene expression host cell genes involved in the phagolysosome formation after CR1 blocking and *Leishmania* infection p 102
- Table 1:** Different conditions used in the attempt to generate *Ld* amastigotes p 46
- Table 2:** Representation of the siRNA library containing macrophage surface markers and molecules involved in cell trafficking p 85

9. REFERENCES

1. Akilov, O.E., Kasuboski, R.E., Carter, C.R., and McDowell, M.A. (2007). The role of mannose receptor during experimental leishmaniasis. *Journal of leukocyte biology* 81, 1188-1196.
2. Alvar, J., Aparicio, P., Aseffa, A., Den Boer, M., Cañavate, C., Dedet, J.-P., Gradoni, L., Ter Horst, R., López-Vélez, R., and Moreno, J. (2008). The relationship between leishmaniasis and AIDS: the second 10 years. *Clinical microbiology reviews* 21, 334-59, table of contents.
3. Arango Duque, G., and Descoteaux, A. (2015). Leishmania survival in the macrophage: where the ends justify the means. *Current opinion in microbiology* 26, 32-40.
4. Arango Duque, G., Fukuda, M., and Descoteaux, A. (2013). Synaptotagmin XI regulates phagocytosis and cytokine secretion in macrophages. *Journal of immunology (Baltimore, Md. : 1950)* 190, 1737-1745.
5. Arango Duque, G., Fukuda, M., Turco, S.J., Stäger, S., and Descoteaux, A. (2014). Leishmania promastigotes induce cytokine secretion in macrophages through the degradation of synaptotagmin XI. *Journal of immunology (Baltimore, Md. : 1950)* 193, 2363-2372.
6. Ashford, R.W. (2000). The leishmaniasis as emerging and reemerging zoonoses. *International journal for parasitology* 30, 1269-1281.
7. Attila Trájer, Ákos Bede-Fazekas, János Bobvos and Anna Páldy (2013). The effect of climate change on the potential distribution of the European Phlebotomus species and the parasite Leishmania infantum in 2011-2070. A climate env. Conference Abstract.
8. Bank, E. unpublished.
9. Bates, P.A. (2007). Transmission of Leishmania metacyclic promastigotes by phlebotomine sand flies. *International journal for parasitology* 37, 1097-1106.
10. Beetham, J.K., Donelson, J.E., and Dahlin, R.R. (2003). Surface glycoprotein PSA (GP46) expression during short- and long-term culture of Leishmania chagasi. *Molecular and biochemical parasitology* 131, 109-117.
11. Berton, G., and Lowell, C.A. (1999). Integrin signalling in neutrophils and macrophages. *Cellular signalling* 11, 621-635.
12. Bhattacharya, P., Dey, R., Dagur, P.K., Kruhlak, M., Ismail, N., Debrabant, A., Joshi, A.B., Akue, A., Kukuruga, M., and Takeda, K., et al. (2015). Genetically Modified Live Attenuated Leishmania donovani Parasites Induce Innate Immunity through Classical Activation of Macrophages That Direct the Th1 Response in Mice. *Infection and immunity* 83, 3800-3815.
13. Bogdan, C., and Röllinghoff, M. (1998). The immune response to Leishmania: mechanisms of parasite control and evasion. *International journal for parasitology* 28, 121-134.
14. Bogie, J.F.J., Jorissen, W., Mailleux, J., Nijland, P.G., Zelcer, N., Vanmierlo, T., van Horsen, J., Stinissen, P., Hellings, N., and Hendriks, J.J.A. (2013). Myelin alters the inflammatory phenotype of macrophages by activating PPARs. *Acta neuropathologica communications* 1, 43.
15. Cameron, P., McGachy, A., Anderson, M., Paul, A., Coombs, G.H., Mottram, J.C., Alexander, J., and Plevin, R. (2004). Inhibition of lipopolysaccharide-induced macrophage IL-12 production by Leishmania mexicana amastigotes: the role of cysteine peptidases and the

References

- NF-kappaB signaling pathway. *Journal of immunology* (Baltimore, Md. : 1950) 173, 3297-3304.
16. Caroselli, E.E., Assis, D.M., Barbiéri, C.L., Júdice, W.A.S., Juliano, M.A., Gazarini, M.L., and Juliano, L. (2012). *Leishmania* (L.) *amazonensis* peptidase activities inside the living cells and in their lysates. *Molecular and biochemical parasitology* 184, 82-89.
 17. Carrada, G., Cañeda, C., Salaiza, N., Delgado, J., Ruiz, A., Sanchez, B., Gutiérrez-Kobeh, L., Aguirre, M., and Becker, I. (2007). Monocyte cytokine and costimulatory molecule expression in patients infected with *Leishmania mexicana*. *Parasite immunology* 29, 117-126.
 18. Castes, M., Agnelli, A., Verde, O., and Rondón, A.J. (1983). Characterization of the cellular immune response in American cutaneous leishmaniasis. *Clinical immunology and immunopathology* 27, 176-186.
 19. Chávez-Galán, L., Olleros, M.L., Vesin, D., and Garcia, I. (2015). Much More than M1 and M2 Macrophages, There are also CD169(+) and TCR(+) Macrophages. *Frontiers in immunology* 6, 263.
 20. Crauwels, P., Bohn, R., Thomas, M., Gottwalt, S., Jäckel, F., Krämer, S., Bank, E., Tenzer, S., Walther, P., and Bastian, M., et al. (2015). Apoptotic-like *Leishmania* exploit the host's autophagy machinery to reduce T-cell-mediated parasite elimination. *Autophagy* 11, 285-297.
 21. Da Silva, R.P., Hall, B.F., Joiner, K.A., and Sacks, D.L. (1989). CR1, the C3b receptor, mediates binding of infective *Leishmania* major metacyclic promastigotes to human macrophages. *Journal of immunology* (Baltimore, Md. : 1950) 143, 617-622.
 22. Dasgupta, D., Chakraborty, P., and Basu, M.K. (2000). Ligation of Fc receptor of macrophages stimulates protein kinase C and anti-leishmanial activity. *Molecular and cellular biochemistry* 209, 1-8.
 23. Denise, H., Poot, J., Jiménez, M., Ambit, A., Herrmann, D.C., Vermeulen, A.N., Coombs, G.H., and Mottram, J.C. (2006). Studies on the CPA cysteine peptidase in the *Leishmania infantum* genome strain JPCM5. *BMC molecular biology* 7, 42.
 24. Devault, A., and Bañuls, A.-L. (2008). The promastigote surface antigen gene family of the *Leishmania* parasite: differential evolution by positive selection and recombination. *BMC evolutionary biology* 8, 292.
 25. Dunkelberger, J.R., and Song, W.-C. (2010). Complement and its role in innate and adaptive immune responses. *Cell research* 20, 34-50.
 26. Garg, R., Barat, C., Ouellet, M., Lodge, R., and Tremblay, M.J. (2009). *Leishmania infantum* amastigotes enhance HIV-1 production in cocultures of human dendritic cells and CD4 T cells by inducing secretion of IL-6 and TNF-alpha. *PLoS neglected tropical diseases* 3, e441.
 27. Garg, R., Lodge, R., Descoteaux, A., and Tremblay, M.J. (2008). *Leishmania infantum* promastigotes reduce entry of HIV-1 into macrophages through a lipophosphoglycan-mediated disruption of lipid rafts. *The Journal of infectious diseases* 197, 1701-1708.
 28. Ginger, M.L., Ngazoa, E.S., Pereira, C.A., Pullen, T.J., Kabiri, M., Becker, K., Gull, K., and Steverding, D. (2005). Intracellular positioning of isoforms explains an unusually large adenylate kinase gene family in the parasite *Trypanosoma brucei*. *The Journal of biological chemistry* 280, 11781-11789.

References

29. He, J.Q., Wiesmann, C., and van Lookeren Campagne, M. (2008). A role of macrophage complement receptor CR1g in immune clearance and inflammation. *Molecular immunology* 45, 4041-4047.
30. Helmy, K.Y., Katschke, K.J., Gorgani, N.N., Kljavin, N.M., Elliott, J.M., Diehl, L., Scales, S.J., Ghilardi, N., and van Lookeren Campagne, M. (2006). CR1g: a macrophage complement receptor required for phagocytosis of circulating pathogens. *Cell* 124, 915-927.
31. Henry, R.M., Hoppe, A.D., Joshi, N., and Swanson, J.A. (2004). The uniformity of phagosome maturation in macrophages. *The Journal of cell biology* 164, 185-194.
32. Isnard, A., Shio, M.T., and Olivier, M. (2012). Impact of *Leishmania* metalloprotease GP63 on macrophage signaling. *Frontiers in cellular and infection microbiology* 2, 72.
33. Kaye, P., and Scott, P. (2011). Leishmaniasis: complexity at the host-pathogen interface. *Nature reviews. Microbiology* 9, 604-615.
34. Kemp, M., Handman, E., Kemp, K., Ismail, A., Mustafa, M.D., Kordofani, A.Y., Bendtzen, K., Kharazmi, A., and Theander, T.G. (1998). The *Leishmania* promastigote surface antigen-2 (PSA-2) is specifically recognised by Th1 cells in humans with naturally acquired immunity to *L. major*. *FEMS immunology and medical microbiology* 20, 209-218.
35. Killick-Kendrick R. (1999). The Biology and Control of Phlebotomine Sand Flies.
36. Krych-Goldberg, M., and Atkinson, J.P. (2001). Structure-function relationships of complement receptor type 1. *Immunological reviews* 180, 112-122.
37. Labonte, A.C., Tosello-Trampont, A.-C., and Hahn, Y.S. (2014). The role of macrophage polarization in infectious and inflammatory diseases. *Molecules and cells* 37, 275-285.
38. Lainson, R. (1988). Ecological interactions in the transmission of the leishmaniasis. *Philosophical transactions of the Royal Society of London. Series B, Biological sciences* 321, 389-404.
39. Lambris, J.D., Ricklin, D., and Geisbrecht, B.V. (2008). Complement evasion by human pathogens. *Nature reviews. Microbiology* 6, 132-142.
40. Leprohon, P., Légaré, D., Girard, I., Papadopoulou, B., and Ouellette, M. (2006). Modulation of *Leishmania* ABC protein gene expression through life stages and among drug-resistant parasites. *Eukaryotic cell* 5, 1713-1725.
41. Lewis, D.J. (1971). Phlebotomid sandflies. *Bulletin of the World Health Organization* 44, 535-551.
42. Lima, A P C A, Reis, F.C.G., and Costa, T.F.R. (2013). Cysteine peptidase inhibitors in trypanosomatid parasites. *Current medicinal chemistry* 20, 3152-3173.
43. Lynn, M.A., Kindrachuk, J., Marr, A.K., Jenssen, H., Panté, N., Elliott, M.R., Napper, S., Hancock, R.E., McMaster, W.R., and Bates, P.A. (2011). Effect of BMAP-28 Antimicrobial Peptides on *Leishmania major* Promastigote and Amastigote Growth. Role of Leishmanolysin in Parasite Survival. *PLoS Negl Trop Dis* 5, e1141.
44. Martinez, F.O., and Gordon, S. (2014). The M1 and M2 paradigm of macrophage activation: time for reassessment. *F1000prime reports* 6, 13.
45. Martinez, F.O., Gordon, S., Locati, M., and Mantovani, A. (2006). Transcriptional profiling of the human monocyte-to-macrophage differentiation and polarization: new molecules and patterns of gene expression. *Journal of immunology (Baltimore, Md. : 1950)* 177, 7303-7311.

References

46. Mia, S., Warnecke, A., Zhang, X.-M., Malmström, V., and Harris, R.A. (2014). An optimized protocol for human M2 macrophages using M-CSF and IL-4/IL-10/TGF- β yields a dominant immunosuppressive phenotype. *Scandinavian journal of immunology* 79, 305-314.
47. Mosser, D.M., and Edwards, J.P. (2008). Exploring the full spectrum of macrophage activation. *Nature reviews. Immunology* 8, 958-969.
48. Mosser, D.M., and Karp, C.L. (1999). Receptor mediated subversion of macrophage cytokine production by intracellular pathogens. *Current opinion in immunology* 11, 406-411.
49. Neu, C., Sedlag, A., Bayer, C., Förster, S., Crauwels, P., Niess, J.-H., van Zandbergen, G., Frascaroli, G., and Riedel, C.U. (2013). CD14-dependent monocyte isolation enhances phagocytosis of *listeria monocytogenes* by proinflammatory, GM-CSF-derived macrophages. *PloS one* 8, e66898.
50. Oliveira, E.F. de, dos Santos Fernandes, Carlos Eurico, Araújo e Silva, E., Brazil, R.P., and Oliveira, A.G. de (2013). Climatic factors and population density of *Lutzomyia longipalpis* (Lutz & Neiva, 1912) in an urban endemic area of visceral leishmaniasis in midwest Brazil. *Journal of vector ecology : journal of the Society for Vector Ecology* 38, 224-228.
51. Pang, Z.P., and Südhof, T.C. (2010). Cell biology of Ca²⁺-triggered exocytosis. *Current opinion in cell biology* 22, 496-505.
52. Pescher, P., Blisnick, T., Bastin, P., and Späth, G.F. (2011). Quantitative proteome profiling informs on phenotypic traits that adapt *Leishmania donovani* for axenic and intracellular proliferation. *Cellular microbiology* 13, 978-991.
53. Piscopo, T.V., and Mallia, A.C. (2006). Leishmaniasis. *Postgraduate medical journal* 82, 649-657.
54. Polando, R., Dixit, U.G., Carter, C.R., Jones, B., Whitcomb, J.P., Ballhorn, W., Harintho, M., Jerde, C.L., Wilson, M.E., and McDowell, M.A. (2013). The roles of complement receptor 3 and Fc γ receptors during *Leishmania* phagosome maturation. *Journal of leukocyte biology* 93, 921-932.
55. Ramírez, J.L., and Guevara, P. (1997). Persistent infections by *Leishmania* (*Viannia*) *braziliensis*. *Memórias do Instituto Oswaldo Cruz* 92, 333-338.
56. Ritter, U., Frischknecht, F., and van Zandbergen, G. (2009). Are neutrophils important host cells for *Leishmania* parasites? *Trends in parasitology* 25, 505-510.
57. Rivas-Santiago, B., Hernandez-Pando, R., Carranza, C., Juarez, E., Contreras, J.L., Aguilar-Leon, D., Torres, M., and Sada, E. (2008). Expression of cathelicidin LL-37 during *Mycobacterium tuberculosis* infection in human alveolar macrophages, monocytes, neutrophils, and epithelial cells. *Infection and immunity* 76, 935-941.
58. Rodríguez, N.E., Gaur, U., and Wilson, M.E. (2006). Role of caveolae in *Leishmania chagasi* phagocytosis and intracellular survival in macrophages. *Cellular microbiology* 8, 1106-1120.
59. Rosenthal, L.A., Sutterwala, F.S., Kehrl, M.E., and Mosser, D.M. (1996). *Leishmania* major-human macrophage interactions: cooperation between Mac-1 (CD11b/CD18) and complement receptor type 1 (CD35) in promastigote adhesion. *Infection and immunity* 64, 2206-2215.
60. Russell, D.G. (1987). The macrophage-attachment glycoprotein gp63 is the predominant C3-acceptor site on *Leishmania mexicana* promastigotes. *European journal of biochemistry / FEBS* 164, 213-221.

References

61. Russell, R.C., Tian, Y., Yuan, H., Park, H.W., Chang, Y.-Y., Kim, J., Kim, H., Neufeld, T.P., Dillin, A., and Guan, K.-L. (2013). ULK1 induces autophagy by phosphorylating Beclin-1 and activating VPS34 lipid kinase. *Nat Cell Biol* 15, 741-750.
62. Sacks, D.L. (1989). Metacyclogenesis in *Leishmania* promastigotes. *Experimental parasitology* 69, 100-103.
63. Sádlová, J., Price, H.P., Smith, B.A., Votýpka, J., Volf, P., and Smith, D.F. (2010). The stage-regulated HASPB and SHERP proteins are essential for differentiation of the protozoan parasite *Leishmania major* in its sand fly vector, *Phlebotomus papatasi*. *Cellular microbiology* 12, 1765-1779.
64. Schönian, G., Akuffo, H., Lewin, S., Maasho, K., Nylén, S., Pratlong, F., Eisenberger, C.L., Schnur, L.F., and Presber, W. (2000). Genetic variability within the species *Leishmania aethiopica* does not correlate with clinical variations of cutaneous leishmaniasis. *Molecular and biochemical parasitology* 106, 239-248.
65. Scott, M.G., Davidson, D.J., Gold, M.R., Bowdish, D., and Hancock, R.E.W. (2002). The human antimicrobial peptide LL-37 is a multifunctional modulator of innate immune responses. *Journal of immunology (Baltimore, Md. : 1950)* 169, 3883-3891.
66. Skendros, P., and Mitroulis, I. (2012). Host Cell Autophagy in Immune Response to Zoonotic Infections. *Clinical and Developmental Immunology* 2012, 1-9.
67. Smith, B.O., Mallin, R.L., Krych-Goldberg, M., Wang, X., Hauhart, R.E., Bromek, K., Uhrin, D., Atkinson, J.P., and Barlow, P.N. (2002). Structure of the C3b binding site of CR1 (CD35), the immune adherence receptor. *Cell* 108, 769-780.
68. Stenger, S., and van Zandbergen, G. (2011). Measuring the killing of intracellular pathogens: *Leishmania*. *Current protocols in immunology / edited by John E. Coligan ... [et al.] Chapter 14, Unit14.23.*
69. Stout, R.D. (2010). Editorial: macrophage functional phenotypes: no alternatives in dermal wound healing? *Journal of leukocyte biology* 87, 19-21.
70. Stout, R.D., Jiang, C., Matta, B., Tietzel, I., Watkins, S.K., and Suttles, J. (2005). Macrophages sequentially change their functional phenotype in response to changes in microenvironmental influences. *Journal of immunology (Baltimore, Md. : 1950)* 175, 342-349.
71. Thi, E.P., and Reiner, N.E. (2012). Phosphatidylinositol 3-kinases and their roles in phagosome maturation. *Journal of leukocyte biology* 92, 553-566.
72. Ueno, N., and Wilson, M.E. (2012). Receptor-mediated phagocytosis of *Leishmania*: implications for intracellular survival. *Trends in parasitology* 28, 335-344.
73. van Lookeren Campagne, M., Wiesmann, C., and Brown, E.J. (2007). Macrophage complement receptors and pathogen clearance. *Cellular microbiology* 9, 2095-2102.
74. van Zandbergen, G., Bollinger, A., Wenzel, A., Kamhawi, S., Voll, R., Klinger, M., Müller, A., Hölscher, C., Herrmann, M., and Sacks, D., et al. (2006). *Leishmania* disease development depends on the presence of apoptotic promastigotes in the virulent inoculum. *Proceedings of the National Academy of Sciences of the United States of America* 103, 13837-13842.
75. van Zandbergen, G., Solbach, W., and Laskay, T. (2007). Apoptosis driven infection. *Autoimmunity* 40, 349-352.
76. Villa, H., Pérez-Pertejo, Y., García-Estrada, C., Reguera, R.M., Requena, J.M., Tekwani, B.L., Balaña-Fouce, R., and Ordóñez, D. (2003). Molecular and functional characterization of

References

- adenylate kinase 2 gene from *Leishmania donovani*. *European journal of biochemistry / FEBS* 270, 4339-4347.
77. Vinet, A.F., Jananji, S., Turco, S.J., Fukuda, M., and Descoteaux, A. (2011). Exclusion of synaptotagmin V at the phagocytic cup by *Leishmania donovani* lipophosphoglycan results in decreased promastigote internalization. *Microbiology (Reading, England)* 157, 2619-2628.
78. Vural, A., and Kehrl, J.H. (2014). Autophagy in macrophages: impacting inflammation and bacterial infection. *Scientifica* 2014, 825463.
79. Wenzel, U.A., Bank, E., Florian, C., Förster, S., Zimara, N., Steinacker, J., Klinger, M., Reiling, N., Ritter, U., and van Zandbergen, G. (2012). *Leishmania major* parasite stage-dependent host cell invasion and immune evasion. *FASEB journal : official publication of the Federation of American Societies for Experimental Biology* 26, 29-39.
80. WHO (2015). Investing to overcome the global impact of neglected tropical diseases.
81. Wilson, M.E., Hardin, K.K., and Donelson, J.E. (1989). Expression of the major surface glycoprotein of *Leishmania donovani* chagasi in virulent and attenuated promastigotes. *Journal of immunology (Baltimore, Md. : 1950)* 143, 678-684.
82. Wong, P.-M., Puente, C., Ganley, I.G., and Jiang, X. (2014). The ULK1 complex. *Autophagy* 9, 124-137.
83. Wright, S.D., and Silverstein, S.C. (1983). Receptors for C3b and C3bi promote phagocytosis but not the release of toxic oxygen from human phagocytes. *The Journal of experimental medicine* 158, 2016-2023.
84. Zufferey, R., Allen, S., Barron, T., Sullivan, D.R., Denny, P.W., Almeida, I.C., Smith, D.F., Turco, S.J., Ferguson, M.A.J., and Beverley, S.M. (2003). Ether phospholipids and glycosylinositolphospholipids are not required for amastigote virulence or for inhibition of macrophage activation by *Leishmania major*. *The Journal of biological chemistry* 278, 44708-44718.

10. ACKNOWLEDGMENTS

Acknowledgments

11. DECLARATION OF AUTHORSHIP

I hereby declare that I have written the present dissertation with the topic:

“Complement Receptor 1 mediated control of *Leishmania* infection in inflammatory human macrophages”

The work was written independently, using no other assistances then those I have cited. All sources used to support the statements were clearly mentioned.

Stephan Alberto Machado de Oliveira

Mainz, 31 March 2016

12. CURRICULUM VITAE

13. Publications

Only the manuscript, which is submitted, is attached.

Stephan A. M. de Oliveira, Sabine Förster, Elena Bank, Menberework Chanyalew, Peter Crauwels, Ger van Zandbergen. Distinct *Leishmania* species, causing cutaneous or visceral Leishmaniasis, interact differently with human primary macrophages. **PLoS ONE, submitted**